RDD:84:5303-04:02

Babcock & Wilcox
a McDermott company

EXAMINATION OF OTSG TUBES B73-8 AND B112-19 FROM ANO-1

– FINAL REPORT –

RESEARCH AND DEVELOPMENT DIVISION
LYNCHBURG RESEARCH CENTER

SPONSORED BY
ARKANSAS POWER AND LIGHT

JUNE 1983

B&W makes no warranty or representation, expressed or implied:

- with respect to the accuracy, completeness, or usefulness of the information contained in this report
- that the use of any information, apparatus, method, or process disclosed in this report may infringe privately owned rights.

B&W assumes no liability with respect to the use of, or for damages resulting from the use of:

- any information, apparatus, method, or process disclosed in this report
- experimental apparatus furnished with this report.

EXAMINATION OF OTSG TUBES B73-8 AND B112-19 FROM ANO-1

- Final Report -

RDD:84:5303-04:02

BY

S. C. Inman
Nuclear Materials

June 10, 1983

Sponsored by: AP&L

BABCOCK & WILCOX COMPANY
Research & Development Division
Lynchburg Research Center
P. O. Box 239
Lynchburg, Virginia 24505

TABLE OF CONTENTS

List of Tables

List of Figures

List of Figures (Cont'd)

ACKNOWLEDGMENTS

The author would like to acknowledge those persons who contributed to the completion of this report.

Gary Bain Dave Kimmel Macon Hensley Bill Shield Bill Machin Wayne Dalton Jimmy Seagle Carlton Stinnett	-	General support and help whenever it was required.
Bobby Dudley	-	Tube sectioning and machining operations.
Woody White	-	Scanning electron microscopy and energy dispersive x-ray analysis.
Don Harris Scott Pennington	-	Health Physics support.
Larry Sarver Phil Daniel Mike Rigdon Norm Jacob	-	Consultation and project support.
Bernard Parham	-	Metallography.
John Bullard	-	Chemical analyses.
Wayne Latham Sam Lester	-	Eddy current examinations.
Susan Haghi	-	Typing of reports.

SUMMARY

The upper portion of two steam generator tubes was removed from service and sent to the LRC for metallurgical examinations. Tube B73-8 had in-service eddy current defect indications within the upper tubesheet (UTS) and B112-19 had an indication near the 15th tube support plate. Laboratory examination techniques used were eddy current, stereomacroscopy, scanning electron microscopy, bend tests, chemical analyses, and metallography. Circumferentially oriented through-wall intergranular cracking was found within the UTS region of tube B73-8. A region of 20% through-wall intergranular attack (IGA) was found in tube B112-19 in the eddy current indication area. Sampled areas of both tubes showed surface IGA less than 10% through-wall. The attack on the tubes initiated on the outside surface.

1. INTRODUCTION

An eddy current inspection was performed in both ANO-1 OTSGs during the November 1982 outage. A large number of eddy current indications were identified during the inspection. In order to verify the type of indication and determine the damage extent and mechanism, the upper portion of tubes 73-8 and 112-19 containing the defect indication areas were removed from the B-OTSG and sent to the Lynchburg Research Center (LRC) for metallurgical examination. Tube 73-8 contained multiple defect indication signatures within the UTS and tube 112-19 contained a signature typical of those seen below the UTS.

This laboratory examination was performed in four phases: Phase I - Receipt Inspection and Nondestructive Examinations, Phase II - Destructive Examinations, Phase III - Bend Testing, and Phase IV - Additional Tube Surface Characterization. The activities performed during this examination are shown below. The results of these activities are presented in this report.

ANO-1 OTSG Tube Examination Activities

- Radiation level measurement
- Tube length measurement
- Tube orientation determination
- X-ray radiography
- Diameter measurement
- Eddy current inspection
- Macro- and microvisual examinations
- Tube sectioning
- Bend testing
- Chemical cleaning
- Scanning electron microscopy and energy dispersive x-ray analyses (SEM/EDX)

- X-ray diffraction (XRD) and emission spectroscopy
- Electron microprobe analyses (EMP)
- Electron spectroscopy for compound analysis (ESCA)
- Metallography

2. METHODS AND RESULTS

2.1 Phase I - Receipt Inspection and Nondestructive Examinations

2.1.1 Receipt Inspection

The tube sections were packaged in "lay-flat" plastic tubing and labeled prior to shipment from the ANO-1 site. A 55-gallon drum with an inner six-inch diameter tube holder was used to ship the tube sections. The drum was received at the LRC on January 31, 1983 and read 250 millirem radiation on contact and approximately 13 millirem at a distance of three feet. Individual tube sections were removed from the drum and read between 250 and 400 millirem radiation on contact and 50 millirem at one foot.

The length of each tube section was measured and is listed in Table 2-1. Tube B73-8 was first cut during the removal operation at 69-3/16 inches, the location just above the 15th tube support plate (TSP), and removed from the OTSG in four sections. Tube B112-19 was cut at 105 inches, the location of the 14th TSP, and removed in five sections. Schematics of the two removed tubes with respect to the OTSG are shown in Figures 2-1 and 2-2. The orientation of each tube section with respect to the OTSG was then determined by locating an axial scribe near the top of the tube which corresponded to the X-axis of the OTSG. Each tube section was marked as to piece number and location of X-axis.

2.1.2 Macrovisual Inspection and Photography

The full length of each tube section was photographed at four 90° intervals using 35mm color photography. Tables 2-2 and 2-3 list the results of the visual inspection of tubes B73-8 and B112-19, respectively. Observations made on these tubes were typical of those made on tubes removed from other plants and include dry-out stains, removal and handling markings, and color variations along their length. Figure 2-3 shows photographs of some typical observations seen on tubes B73-8 and B112-19.

Both tubes had unusually heavy black deposits near the UTS secondary face. Tube B73-8 had deposits extending from three inches within the UTS to a maximum of nine inches below the UTS secondary face. Figure 2-4 shows these deposits in different orientations. A through-wall hole is visible just above the UTS face on the Y-axis. It appears that the UTS crevice may have been tightly packed with deposits at the secondary face and were spalled during tube removal. This would help explain why the B73-8 required a breakaway force of 2,748 pounds during removal and why the through-wall cracks within the UTS (discussed later) did not leak during service.

The deposits on tube B112-19 were within four inches above the UTS secondary face and are shown in Figure 2-5. These deposits appeared relatively uniform in thickness and were not as heavy or spalled as were those on tube B73-8. The 15th tube support plate (TSP) region of tube B112-19 also appeared to have black deposits where the lands contacted the tube. These deposits are shown in Figure 2-6, and were not as heavy as those seen near the UTS face.

The most defined dry-out stains on both tubes were located at approximately midspan 16 and above. Very light and spotted stains were seen along the full lengths. The dry-out stains are thought to be due to the auxiliary feedwater flow, which enters the OTSG at an elevation near midspan 16. This is supported by the fact that the heaviest stained areas of these tubes were on surfaces in the direction of the auxiliary feedwater inlet nozzles.

No consistent trends in color variations on these tubes could be determined. The color of the tubes varied with axial location, being light brown within the UTS and a mixture of greenish-blue brown and purple further down the tubes.

2.1.3 X-Ray Radiography

Each tube section was radiographed at two orientations, 90° apart. Table 2-4 lists the comments made while inspecting the radiograph prints shown in

Appendix A. The circumferential and vertical scribes near the top of the tube are made during the site removal operation to maintain proper OTSG orientation. Small dark specks were occasionally seen and correspond to areas of greater mass, thus decreasing the amount of X-rays to expose the film. These dark specks are probably chips and fines produced during the tube removal operation. Light marks, on the other hand, indicate lower mass areas, i.e., tubewall defects.

Tube B73-8

Piece 2 contained circumferentially-oriented indications typical of tubewall defects. A total of six defect indications were visible in the 0° orientaion, with four visible when rotated 90°. The indication at 12 inches from the top of Piece 2 was the most well defined and corresponded to a through-wall hole which was visible on the OD surface of the tube section (discussed in Section 2.1.2). Piece 3 contained the most tube removal damage, with OD fluctuations at 3-1/2 inches and a slight bend at 1-1/2 inches from the top. The diameter fluctuations near the bottom of Piece 4 appear to have been caused by the ID cutting device used during the tube removal operation.

Tube B112-19

Other than the previously mentioned dark specks, this tube was relatively free of indications. There were, however, areas of mechanical damage in the form of mandrel marks in Piece 3 and OD fluctuations in Piece 4. A very uniform circumferential band was near the area of OD fluctuations in Piece 4. It was later determined during the visual inspections that the presence of mechanical damage on the outside surface resulted in the circumferential band.

2.1.4 Eddy Current Inspection

Prior to the laboratory eddy current (EC) inspection, the ends of each tube section were "faced" lightly on a lathe to remove the crimp caused by the tubing cutter used during the site removal operation. This permitted easy insertion of the EC probes.

In attempts to simulate the site (ANO-1) EC responses, a carbon steel UTS mock-up was placed over the UTS region of the tube when inspected. The laboratory inspections used a 0.500-inch diameter annular differential probe with 600 kHz and a 400/200 kHz mix for suppression of tube support plate (TSP) response.

Table 2-5 lists the defect indications seen during the site (ANO-1) and laboratory EC inspections. Figure 2-7 shows the locations of the EC indications with respect to the OTSG axes. A total of six laboratory defect indications were seen in tube B73-8 and were contained within a 6-inch region above the UTS secondary face. In all cases, the laboratory depth estimates were greater than those made at the site. This is commonly the case and has occurred with the UTS indications in other tube examinations. No depth estimate of the indication at 20.5 inches could be made in the laboratory due to a distorted signal (later determined to have been caused by two adjacent defects). The location of each defect indication was verified on the OD surface using a surface scanning absolute "pencil" probe. As listed in Table 2-5, each defect indication was designated as an examination area, with Area 1 being the uppermost indication.

A 63% through-wall defect indication was detected during the site inspection of tube B112-19 just below the 15th TSP (approximately 73 inches). Several techniques were used in the laboratory to examine this region of the tube. In addition to using the 0.500-inch probe with TSP mix, a dent mix was also used in attempts to simulate the site inspection signal. An absolute OD surface scanning "pencil" probe was used to inspect the 15 TSP region. A 0.540-inch differential probe with increased defect sensitivity was also used, but a small dent just below the 15 TSP region prevented it from passing the suspect area. No defect indications were seen during the laboratory EC inspections of tube B112-19. The presence of OD mechanical damage near the 15 TSP (shown in Figure 2-6) could have possibly "masked" or obscured any defect information. Other areas of minor mechanical damage were detected during the laboratory inspection in tube B112-19 which appear

to have been caused by the gripping tools used during the tube removal operations.

Additional details of the eddy current inspections are given in Reference 1, which is contained in Appendix B.

2.1.5 Diameter Measurements

Outside and inside diameter (OD and ID) measurements were made at 1/2-inch increments and two 90° orientaions along the entire length of each tube section. The OD measurements were made using a Zygo Laser Telemetric System with an accuracy of 0.00001-inch. A Brown and Sharpe Intrimik with an accuracy of 0.0002 was used to measure the ID. The two orientation measurements for both the ID and OD taken at each increment were averaged, from which the tubewall thickness was calculated. These data are listed in Appendix C. Variations in tube diameters correlated well with anomalies identified during the macrovisual, X-ray radiography, and eddy current inspections.

Tube B73-8

Figure 2-8 shows the diameter data plotted versus tube axial position, with areas of previously observed anomalies noted. Areas of tube removal damage, surface deposits and eddy current indications corresponded to variations in tube diameters ranging from approximately 0.0005- to 0.020-inch. The most abrupt change occurred at approximately 32 to 35 inches from the top, where the OD and ID decreased from nominal 0.625- and 0.550-inch, respectively, to 0.615- and 0.540-inch. There is no apparent service-related explanation for this sudden 0.010-inch decrease in diameter. Althougn this tube required a very large tensile load to remove from the OTSG, the diameter uniformity of the lower portion implies that the diameter decrease may be a manufacturing artifact and not caused during tube removal.

Tube B112-19

The tube diameters were relatively uniform along the length as Figure 2-9 indicates. Small dent indications were observed during the laboratory EC inspection just below the UTS secondary face and near the 15th TSP. These locations corresponded to small irregularities in the diameter plots. In addition, a defect indication was observed during the site EC inspection and mechanical damage was visible during the macrovisual inspection just below the 15th TSP. The small diameter increases at 38 inches from the top were visible on the radiographs and appeared to be caused by the tube gripping tools used during the removal operation.

2.2 Phase II - Destructive Examinations

2.2.1 Tube Sectioning

The tube sectioning diagrams in Appendix D show the areas sampled for further examinations. All cuts were made using either a Leco slow speed diamond saw or a jeweler's hand saw, both with a 0.020-inch blade width. Coolant was occasionally used with the diamond saw. No allowances were made on the diagrams for saw kerfs.

Initially, only those areas containing eddy current indications were sectioned from the tubes. These were Areas 1 to 6 from tube B73-8 and Area 1 from tube B112-19. Additional areas of both tubes were later sampled and are Areas 7 to 13 from B73-8 and Areas 2 to 7 from B112-19. The length of the sectioned samples was between 1/2 and 1-1/2 inch. Figure 2-10 shows the technique used to longitudinally split the samples in half to permit visual inspection of the ID surfaces. Bend test and metallography samples were obtained by sectioning each half into two longitudinal strips each.

2.2.2 Visual Inspections

2.2.2.1 Stereoscopic Low Power Inspection

A Nikon stereo macroscope was used with magnifications up to 32X to visually inspect the tube ID and OD surfaces. In general, the ID surface appearance

of all samples examined was light brown in color and typical of OTSG tubing removed from service.

Tube B73-8

OD surface micrographs of defect indication areas are shown in Figures 2-11 through 2-14. The approximate extent of the indications was circled with black ink during the EC inspection. Heavy black OD surface deposits in these areas prevented an accurate confirmation of defect presence during the visual inspections. Areas 1, 2, and 3 did have circumferential crack-like features, but nothing anomalous was visible in Areas 4 and 5. A 100% through-wall hole was visible in Area 6, with unusually large axial extent on the OD surface, and is shown in Figure 2-14. Areas 7 to 12 were inspected using other techniques and not examined by stereo macroscopy.

Inspection of the ID surfaces revealed a circumferential crack in Areas 2 and 3. Figure 2-15 shows these cracks, which appear to have been "stretched" at the crack tips, thus opening them slightly in the axial direction. This probably occurred during tube removal, since large (approximately 2,700 pounds) axial forces were applied, and may have contributed to the larger depth estimates of the laboratory EC indications. The ID surface of the sample removed from Areas 4 and 5 appeared normal with no defects visible. The axial scrapes visible on the ID surface were caused by the insertion and removal of EC probes and tube removal devices and are typical for OTSG tubes removed from service.

Tube B112-19

The OD surface of Area 1 revealed a substantial amount of mechanical damage. This damage consisted of axially oriented scrapes and "plowed-up" metal and is shown in Figure 2-16. Since the overall OD surface was dark in this region and the damage was shiny, this implies that the damage was not service related. No obvious defects or cracks were visible on either the ID or OD surfaces of Area 1 which could be attributed to the site EC defect

indication. The other sampled areas of tube B112-19 were not examined by stereo macroscopy.

2.2.2.2 Scanning Electron Microscopy/Energy Dispersive X-Ray Analysis (SEM and EDX)

An ETEC Autoscan microscope* was used to perform high magnification inspections of the tube samples. An EDX spectrum was obtained on selected areas of some samples while in the SEM to qualitatively determine the chemical species present in concentrations $\geq$2 weight percent (detectability limit).

- - - -

*The ETEC Autoscan microscope automatically records pertinent data on the micrographs:

Example:

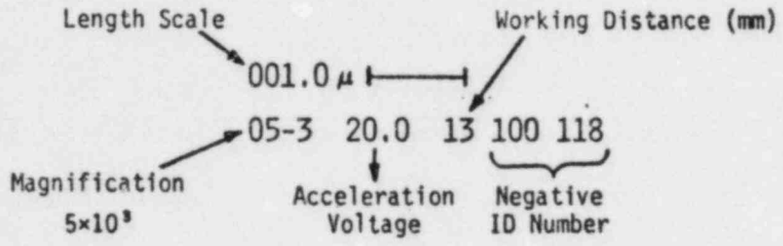

Tube B73-8

Micrographs of the OD surfaces of the samples from Areas 2 and 3 of tube B73-8 are shown in Figures 2-17 through 2-19. No cracks were visible in either area, but heavy surface deposits were present which would have covered any cracks. An EDX spectrum from the surface deposit in Area 3 shown in Figure 2-19 on which significant peaks ($\geq$2 wt. %) of magnesium (Mg), silicon (Si), sulfur (S), and zinc (Zn) were visible. These elements are in addition to chromium (Cr), iron (Fe), and nickel (Ni), the major alloying constituents of Inconel 600.

While examining the ID surfaces of Areas 2 and 3, the circumferential cracks seen during the macroscopic inspection were studied. Both cracks were intergranular in nature and relatively free of heavy deposits on the portion of the crack surfaces nearest the ID. Figures 2-20 and 2-21 show micrographs of these two cracks. Observations made during the macroscopic inspection were confirmed, in that the crack tips appear to have been "stretched". These observations support the theory that the cracks were "stretched" during the tube removal operation and, thus, may be a partial explanation as to why the laboratory defect indication depth estimates are slightly greater than those made from the site EC data.

The OD surface of Areas 4 and 5 appeared very similar, with heavy deposits in both areas. A typical micrograph of deposits, which contained detectable sulfur using EDX, is shown in Figure 2-22. Area 5 did, however, have a circumferential crack-like feature visible under high magnification and is shown in Figure 2-23. An accurate depth estimate could not be made using the SEM, therefore it was not determined whether or not the cracking was limited to the surface deposits. The EDX spectrum in Figure 2-23 showed silicon and sulfur to be present in the deposit cracking in Area 5. The ID surface of Areas 4 and 5 appeared typical of OTSG tubes removed from service and a micrograph is also shown in Figure 2-23.

Area 6 of B73-8 contained the 100% through-wall circumferential hole seen during the macrovisual inspection. Micrographs of the OD surface are shown in Figures 2-24, which identify its intergranular nature. The IGA was rather extensive on the OD surface, which produced its hole-like appearance. The entire crack surface was covered with deposits, which indicates its exposure to a corrosive environment during OTSG service. The EDX spectrum from a portion of the crack surface revealed a trace amount of sulfur and large quantities of silicon, and is shown in Figure 2-24.

Tube B112-19

The area of tube B112-19 with the 63% site EC indication (Area 1) was examined using SEM to try to determine the cause of the indication. Figure 2-25 shows micrographs of areas of mechanical damage on the OD surface of the sample (also visible during the macroscopic inspection). Nearly all of the scrapes and scratches were into the base metal and axially oriented, indicating axial forces resulted in the metal being pushed and "plowed-up." In attempts to further characterize this damage, the sample was cleaned in an ultrasonic bath of inhibited HCl solution (500 ml 6N hydrochloric acid plus 1g hexamethylene tetramine) at ambient temperature to remove the OD surface deposits. The sample was re-examined using SEM and the micrographs are shown in Figure 2-26. As is clearly evident at higher magnifications, the base metal was "smeared" in the axial direction, indicating that this may have occurred during the site tube removal operation.

2.2.3 Chemical Analyses

In order to determine the elements and compounds present on the ID, OD and crack surfaces, samples were analyzed using several chemical analysis techniques. An OD scrape sample was taken from the heavily deposited region of tube B73-8 at 24 to 32 inches and analyzed using x-ray diffraction, x-ray emission spectroscopy, and wet chemistry. An ID powder sample was removed from the same tube section with a silicon carbide hone and drill motor. X-ray diffraction was used to analyze this sample. The x-ray diffraction work was performed at Battelle Columbus Laboratories.

Two surface analysis methods were used to chemically characterize the intergranular crack surface from Area 1 of tube B73-8. These methods were Electron Spectroscopy for Compound Analyses (ESCA) and Electron Microprobe (EMP) analysis and were also performed at Battelle.

2.2.3.1 X-Ray Diffraction and Emission Spectroscopy

A Phillips X-ray diffractometer with a Debye-Scherrer powder camera was used to analyze the ID powder sample and the OD scrape sample. Table 2-6 lists the elements and compounds identified by studying the diffraction line intensitites. The suspected origination of the species found is also listed, along with the relative strengths of the diffraction lines. Intensity data should only be used as a rough indication of relative concentration. The unknown species listed are due to very weak diffraction lines, from which the compound(s) could not be identified. No anomalous species were observed from the results of the ID powder sample. The OD scrape sample consisted mainly of ferroan trevorite and nickel. A nickel sulfide specie and sobotkite were identified by barely detectable diffraction lines, indicating their presence in very low concentrations.

Table 2-7 lists the compounds and their concentrations detected in the OD scrape sample when analyzed using X-ray emission spectroscopy. The compounds listed are based on the calibration standards used and may not be the actual form of the elements in the sample. The bulk of the sample was comprised of iron and nickel oxides, while oxides of Cu, Cr, Si, and Mn were present in concentrations greater than their nominal alloying compositions. Approximately 6 wt. % of copper oxide was detected using emission spectroscopy and was not detected using diffraction. Other discrepancies also exist and may be attributed to an inhomogeneous scrape sample or that the X-ray beam was not bombarding the entire sample.

2.2.3.2 Wet Chemistry

A wet chemistry test was performed on the OD scrape sample to determine the total sulfur content. The sample was dissolved in acid and a turbidimeter used to compare its turbidity to a known standard. The total sulfur detected as sulfate was 0.13%, with ±10% accuracy.

2.2.3.3 Electron Microprobe (EMP) Analyses

The EMP method uses the principle of wavelength dispersive analysis of electron beam-induced X-rays to detect elements with atomic number >4. Table 2-8 lists the elements analyzed for and the respective weight percent concentrations. Battelle personnel performed these analyses using a Materials Analysis Corporation electron microprobe system. Figure 2-27 shows SEM micrographs of the intergranular crack surface from Area 1 of tube B73-8 and the region analyzed with EMP. Starting nearest the OD, the crack surface was traversed in three adjacent regions and analyzed in each region for the elements listed.

The first round results listed in Table 2-8 were obtained using a 200X magnification and 10 second sweep speed to scan an area of 0.016 inch^2. This was thought to have analyzed a representative area of the crack surface, i.e., deposited and clean regions. After the first round data analysis, it was noticed that the totals of the weight percentages were too low to accurately determine surface deposit chemistry. Therefore, a higher magnification (500X) and slower sweep speed (20 seconds) was used to analyze only an area of crack surface deposits. The results of this analysis were within the expected range of weight percentages and correlate well with the XRD and EDX results. Much more accuracy is placed on the Round 2 data in which the weight percentage total is 99.9.

2.2.3.4 Electron Spectroscopy for Compound Analyses (ESCA)

ESCA was performed on crack surface sample at Battelle using a Leybold-Heraeus LHS 10 System. Quantitative and chemical shift measurements are made at various angstrom distances by the analysis of X-ray induced photoelectrons. Various depths are obtained by sputtering the sample surface with an argon beam in high vacuum. Table 2-9 lists the ESCA results from the analysis of the 100% through-wall intergranular fracture surface in Area 1 of tube B73-8. The adjacent ductile tear region was analyzed as a control. Approximately 50% of the oxygen concentration is a result of the oxides on the copper specimen holder and therefore affects the concentrations of the other elements present. Of significance is the fact that the Fe and Ni binding energies were of the atomic state at 10,000 and 5,000 angstroms within the crack surface. Since the binding energies of Cl and B on the crack surface indicate that they were in oxide form and the S in sulfide forms, the remaining O concentration is apparently due to Cl and B. B is present as boric acid (H_3BO_3) in primary coolant and thus, makes it the most likely candidate. The C concentrations follow what has typically been observed when analyzing other OTSG tube samples, in that it is high on the surface and drops off significantly with increasing sputtering depth. Handling contamination is thought to cause the high surface C. A partial explanation may be the fact that the sample is exposed to the atmosphere for a period of time before analysis.

2.2.3.5 Sodium Azide Test

This simple test is used to qualitatively determine the presence of sulfides, thiosulfates, and thiocyanates but is not sensitive to sulfur, sulfate, or sulfite.(4) The test is performed by placing a drop of test solution (3g NaN_3 in 100 cc 0.1 N iodine) on the surface of interest and observing the reaction through a stereomacroscope. If reduced forms of sulfur are present, the chemical reaction $2NaN_3 + I \rightleftarrows 2NaI + 3N_2$ will be catalyzed. Nitrogen gas will be evolved and the solution will bubble. If

reduced forms of sulfur are not present, the reaction does not proceed and no bubbles form.(4) The bent open crack surface in tube B73-8 Area 3 was tested using this technique. The bubbling reaction was termed moderate to slow, indicating the presence of a small amount of reduced sulfur.

2.3 Phase III - Bend Testing

Sectioning tube samples into longitudinal strips and bending the strips has proven to be very effective in opening tight intergranular cracks.(2,3) Figure 2-10 is a schematic of the two bend techniques used during this examination. Both the circumferential and longitudinal bend techniques place the surface of the tube in tension to open circumferentially or longitudinally oriented cracks, respectively. Since the EC inspection indicated that the tube defects were OD initiated, the tubes were bent with the OD surface in tension. Some of the tube samples were chemically cleaned either before or after bending to remove deposits and further evaluate the tube surface features.

2.3.1 Scanning Electron Microscopy/Energy Dispersive X-Ray Analysis (SEM/EDX)

Tube B73-8

Area 3

The tube sample with the crack visible on the ID surface was circumferentially bend tested with the OD in tension and opened a 100% through-wall intergranular crack. As Figure 2-28 shows, the main crack was circumferentially oriented with "branching" in essentially all directions. Secondary OD surface cracking also was present and was linked with the main crack via IGA and secondary cracking. For the most part, the crack surface itself was relatively free of deposits except near the OD surface, where the deposits extended into the crack surface. The EDX spectrum obtained from the crack surface deposit showed a substantial amount ($\geq$2 wt %) of sulfur in addition to traces of aluminum and silicon.

Area 8

A sample from midway into the UTS (12 inches from top) was circumferentially bend tested and examined. As shown in Figure 2-29, the surface deposit had parted along grain boundaries in mainly the circumferential direction. The deteriorated base metal grain boundaries were visible at higher magnifications where the deposit had parted. The actual depth of this surface IGA (SIGA) could not be determined using SEM and, therefore, this sample was examined using metallography (discussed in Section 2.3.2).

Area 9

Figure 2-30 shows micrographs of samples after circumferential bend testing, which confirmed the presence of SIGA at the elevation just below midspan 16 in the OTSG. A bend sample was cleaned for 30 seconds in an ultrasonic bath of inhibited HCl and reexamined. As Figure 2-31 shows, the cleaning was partially effective in removing the OD surface layer. In cleaned areas, the base metal grains became clearly visible due to the deteriorated grain boundaries.

Tube B112-19

Area 1

No obvious defect which could have produced the site eddy current indication at 73 inches was detected during the previous SEM examination in Phase II. Therefore, the 1-1/2 inch strip samples were circumferentially bent and reexamined. Figure 2-32 shows micrographs of the general OD surface IGA (SIGA) which opened due to bending. An axial band of IGA approximately one inch in height appeared deeper and more severe than other areas, where the SIGA was more uniform as Figure 2-33 shows. The depth of the penetrations could not be determined with SEM and subsequent metallography was therefore performed.

Area 2

A sample from just below Area 1 was sectioned into longitudinal strips to further investigate the cause of the EC indication at 73 inches from the top. Strip samples were circumferentially bend tested and revealed uniform OD SIGA very similar to that previously examined in Area 1. Figure 2-34 shows typical SEM micrographs taken in Area 2. Metallography was also performed to determine the depth of the SIGA penetrations.

Area 3

In order to try to quantify the extent of the SIGA seen on the Areas 1 and 2 samples, strip samples from the 15th TSP region were circumferentially bent and examined. Figure 2-35 shows the OD SIGA which opened due to bending. The SIGA seemed more prevalent in the axial scrape marks where the additional surface stresses apparently opened the small cracking. To determine the penetration depth, metallography was performed.

Area 4

Strip samples from midspan 16 were bend tested and examined, and similar SIGA was detected. Figure 2-36 shows typical micrographs of these samples, showing the larger openings in the axial scrapes. Metallography was subsequently performed.

Area 5

Similar SIGA was opened by bending strip samples from just above the UTS secondary face. Figure 2-37 shows micrographs of this area. Metallography was subsequently performed.

Area 6

SIGA was also detected at approximately 4 inches above the 14th TSP. The SIGA did not appear as uniform over the surface as in the previously examined areas, but there were localized openings which appeared deeper than the typical SIGA. Figure 2-38 shows two of these openings, in which the

deteriorated grain boundaries of the base metal were visible. Metallography was also performed in this area.

2.3.2 Metallography

The method of metallographic examination used successive longitudinal grind-and-polish steps of approximately 0.020-inch to characterize the areas of interest on the tube samples. Figure 2-39 shows a schematic of this method.

Tube B73-8

Area 2

Longitudinal metallography was used to examine the crack seen on the ID surface during the visual inspections. As Figure 2-40 shows, the crack was 100% through-wall OD initiated and intergranular, with extensive IGA adjacent to the main crack. The OD surface deposits "filled" the crack, preventing its detection during the OD surface visual inspections.

One region of localized OD-initiated IGA approximately 50% through-wall and two regions of localized OD pitting were detected. These defects were also "filled" with surface deposits and were not detected during the OD surface visual inspections. Figure 2-41 shows micrographs of these defects.

Areas 4 and 5

To determine the cause of the EC defect indications at 20.5 inches, a sample from this area was metallographically examined. 70% and 60% through-wall OD-initiated circumferential cracks were found in Areas 4 and 5, respectively. The extensive IGA adjacent to both main cracks made their axial extent larger than that previously seen in Area 2. As Figures 2-42 and 2-43 show, these cracks were also filled with surface deposits, where grains had either deteriorated and "fallen out" or were chemically transformed into deposits. Two individual cracks possibly originated in Area 5, and became linked together via IGA.

Area 7

To check for general IGA and undetected cracking, a sample from between Areas 5 and 6 was metallographically examined. No EC indication was seen in this area. The metallography revealed two areas of very small localized penetrations, which had the appearance of pits. As Figure 2-44 shows, these penetrations were approximately 0.002- to 0.003-inch deep.

Area 8

The longitudinal grind-and-polish technique was used to determine the depth of the SIGA opened by bending and previously observed using SEM. The maximum depth observed was approximately 0.004-inch (about 10%), and is shown in Figure 2-45.

Area 9

The same procedure was used to determine the depth of the SIGA found at midspan 16. As Figure 2-46 shows, the penetration depth was smaller, being approximately 0.001 to 0.002 inch.

Tube B112-19

Area 1

The bend samples on which SIGA was detected during the SEM examination were examined to quantify the depth and also check for undetected (subsurface) defects. Figure 2-47 shows micrographs which reveal the maximum observed depth of the penetrations in this area to be approximately 0.007-inch. The sections shown are polished longitudinal surfaces through the region of IGA in Figure 2-29 and represent the deepest SIGA penetrations detected during this examination.

Areas 2 and 3

Metallography was performed on the bend samples from below and above Area 1 to determine the depth of the penetrations seen using SEM. Figure 2-48 shows typical micrographs of the penetrations found in these areas.

Areas 4 and 5

The bend samples from these areas were also examined to determine the depth of the SIGA. As Figure 2-49 shows, the maximum depth of the penetrations was approximately 0.003-inch.

Area 6

The SIGA seen previously using SEM was metallographically examined. The maximum depth of the penetrations was approximately 0.002-inch and is shown in Figure 2-50.

2.4 Phase IV - Additional Tube Surface Characterization

To better characterize and quantify the SIGA detected previously, this phase was added to the examination plan. Additional areas were designated to be subjected to various cleaning techniques to remove the surface deposits, bend testing, and SEM examinations. These activities are discussed in detail below.

Tube B73-8

Area 6

The sample from just above the UTS secondary face containing the 100% through-wall hole was reexamined using SEM and revealed pitting attack which was covered with OD surface deposits. To remove those deposits, the sample was cleaned for two minutes in a UT bath of inhibited HCl at ambient temperature and reexamined. After cleaning, much more pitting was observed, along with minor etching or wastage attack. Figure 2-51 shows two individual pits just above the through-wall hole before and after cleaning. The cleaning was partially effective in removing the deposits on the tube surface and 100% effective within the pits. The lighter granular deposits appear to have attacked the base metal grain matrix more severely than the darker deposits and were associated with regions of grain boundary relief and preferential attack of slip lines. EDX data revealed the lighter deposits to be rich in Si and S before cleaning.

There were several regions of localized IGA surrounding the through-wall hole which were linked by secondary IGA cracking. Figure 2-52 shows two of those regions after the sample was cleaned to remove the surface deposits.

Area 7

The sample adjacent to Area 6 which was metallographically examined during Phase III was removed from the mounting material and longitudinally bend tested. After cleaning in a UT bath of inhibited HCl solution for two minutes, the OD surface of the sample was examined using SEM. The deposits were not removed from the surface so the sample was cleaned an additional five minutes (seven minutes total) and reexamined. Figure 2-53 shows micrographs which reveal pitting and SIGA, along with areas of more severe localized attack where grains had "fallen out." This pitting is similar to that seen previously in Area 6 after cleaning, and appears to be more severe in the region within two inches above the UTS secondary face.

Area 10

A sample was also removed from the midspan 16 location. After longitudinally sectioning the sample in half, a qualitative SEM examination was performed. In general, the OD surface appearance was typical to that previously noted. As Figure 2-54 shows, there were some areas where the surface deposits had spalled and base metal grains were clearly visible. This sample was then cleaned in a UT bath of inhibited HCl for five minutes and bent using the longitudinal technique. Reexamination of the cleaned and bent sample revealed the typical SIGA seen previously, while some deposits were still present. Therefore, the sample was cleaned an additional five minutes and reexamineed, revealing an axial scrape mark approximately half the length of the sample in which localized IGA was present. The localized IGA appeared deeper than the typical SIGA and is shown in Figure 2-55.

Area 11

The upper seal weld heat affected zone and hard rolled regions near the top of OTSG tubes have proven to be particularly susceptible to OD initiated IGA and cracking. Since these regions were "drilled out" during the ANO-1 tube removal operations (to permit tube removal), they were not available for examination. To determine if the corrosive specie(s) were present near this elevation, a sample was removed from the top of Piece 1 and examined. The preliminary SEM examination showed surface deposits typical of those seen previously. This sample was bent using the circumferential technique and reexamined using SEM. As Figure 2-56 shows, bending caused the deposits to open along the grain boundaries, prevalently in the circumferential direction. After cleaning the bend sample for five minutes in a UT bath of inhibited HCl, it was reexamined. The surface deposits were again only partially removed, but there were localized regions where individual grains had parted from the tube surface.

Area 12

A sample was taken from four inches below the UTS secondary face in the region of heavy black deposits. First the sample was viewed using SEM which showed that the OD surface deposits were, in general, extremely heavy. Other observations include pitting and spalling of surface deposits and are shown in Figure 2-57. The EDX spectrum showed the deposits to contain Mg, Al, Si, P, Ca, Mn, Fe, Ni, Cu, and possibly Zn. The sample was cleaned in a UT bath of inhibited HCl and then a UT bath of acetone. Reexamination of the sample showed that these solutions were not effective in removing the deposits. Therefore, the sample was cleaned in a UT bath of Endox 214 (commercial degreaser) for 20 minutes. This solution was only partially effective in removing the deposits and was limited to the pitted areas as shown in Figure 2-57. The sample was then bent in the circumferential direction and reexamined using SEM, revealing the typical SIGA seen on the previously examined samples. In attempts to remove more of the deposits, the sample was cleaned in a UT bath of inhibited HCl at 125°F for two

minutes. Many more areas of pitting were revealed when examined using SEM, but the surface deposits were not completely removed. A 125°F solution of 20% nitric acid and 2% hydrofluoric acid was then used to further clean the sample. As Figure 2-58 shows, this solution was 100% effective in removing the deposits. The grains were etched by the acid bath, making the attack appear more severe than the typical SIGA seen on previously examined samples.

Area 13

Longitudinal and circumferential bend samples were sectioned from the bottom of Piece 4, corresponding to the location just above the 15 TSP. The samples were bent, cleaned in a UT bath of inhibited HCl for two minutes and examined using SEM. The appearance of the OD surface was similar to that of the previous samples; i.e., SIGA visible in areas where the deposit had spalled.

B112-19

Area 7

A sample was taken from the top of Piece 1 to determine if the SIGA existed near the hard roll region. The preliminary SEM examination revealed the typical OD surface deposits. The sample was cleaned in a UT bath of Endox 214 for 20 minutes and then reexamined. The solution was partially effective in removing the deposits, but the SIGA was visible in cleaned areas. A very good estimate of deposit thickness can be taken from Figure 2-58 by using the micron bar in the legend. It appears that the surface deposit on this sample was approximately 2 to 3 microns thick. The sample was then bent in the circumferential direction which opened the deposits along the deteriorated grain boundaries, thus revealing the SIGA.

Table 2-1. Tube Section Lengths

Tube	Piece	Length, Inches	Axial Location of Top, Inches From Top of Tube
B73-8	1	10-5/16	1-5/8(1)
	2	21	11-15/16
	3	21-9/16	32-15/16
	4	14-11/16	54-1/2
	Total	67-9/16	69-3/16
B112-19	1	10-1/16	1-3/4(2)
	2	22-3/16	11-13/16
	3	22	34
	4	22	56
	5	27	78
	Total	103-1/4	105

(1) 1-5/8 inch drilled out during tube removal.
(2) 1-3/4 inch drilled out during tube removal.

Table 2-2. Microvisual Inspection Results for Tube B73-8

Axial Location, Inches From Top	W-Axis	X-Axis	Y-Axis	Z-Axis
0 - 10	Relatively clean, no stains or deposits.	Same as W-axis.	Relatively clean; darker in color.	Darkest in color. Dry-out stains, heavy stains at 7.5.
10 - 24 (UTS face)	Relatively clean at 10-18, darker in color near UTS face, dry-out stains at 18-24, heavy deposits 21-24.	Relatively clean at 10-15, darker in color near UTS face, dry-out stains at 15-24, heavy deposits 21-24.	Darker in color near UTS face, heavy deposits and dry-out stains at 18-24. Through-wall hole at 23.	Heavy deposits and dry-out stains.
24 (UTS face) - 33	Extra heavy build-up of deposits at 24-29.	Extra heavy build-up of deposits.	Same as X-axis.	Extra heavy build-up of deposits at 24-29.
33 to end	OD increase with scrapes and minor mechanical damage at 33 - 36.5 and at 64 - 67.5. Remainder of tube looked typical, i.e., handling scratches, stains, etc.	Same as W-axis.	Same as W-axis.	Same as W-axis.

General Observations

1. Heavy build-up of magnetic deposits extend from UTS secondary face down 8 inches.
2. Magnetic deposits at UTS secondary face appear to have been tightly packed in the crevice and some spalling occurred during tube removal.
3. Z-axis appears to be more heavily stained along the length of the tube.
4. Color of tube varies between brown and greenish-blue brown.

Table 2-3. Microvisual Inspection Results for Tube B112-19

Axial Location, Inches From Top	W-Axis	X-Axis	Y-Axis	Z-Axis
0-10	Very clean, no stains or deposits.	Very clean, minor dry-out stains at 0-1.	Longitudinal band of dry-out stains at 4 to 10, minor dry-out stains at 0-1.	Very clean, minor dry-out stains at 0-1 and 9-10.
10 - 24 (UTS face)	Dry-out stain at 16, deposits at 21-24.	Light dry-out stain at 18, deposits at 21-24.	Heavy dry-out stains, deposits at 21-24.	Dry-out stains, deposits at 21-24.
24 (UTS face) - 34	Longitudinal scratches just below UTS face, small spotted stains.	Same as W-axis.	Same as W-axis.	Same as W-axis.
34 to end	Small spotted stains at 34-52, purplish color at midspan 16, mechanical damage just below 15 TSP.	Small spotted stains at 34-56, purplish color at midspan 16, mechanical damage just below 15 TSP, green-blue color at span 15.	Same as X-axis.	Same as X-axis except very light stains.

General Observations

1. Magnetite deposits are heaviest within the UTS, 3 to 4 inches from secondary face.
2. Appears to be no heavy magnetite deposits just below UTS secondary face.
3. Magnetite deposits are relatively uniform and not spalled or flaked.
4. Dry-out stains within the UTS are mostly along the Y-axis.
5. No heavy dry-out stains were seen below midspan 16.
6. Light dry-out stains were seen below the 15 TSP.
7. Color of tube varies between light brown, greenish-blue brown, and purple, with purple mostly in span 16.

Table 2-4. X-Ray Radiography Results*

Tube	Piece	0° Orientation	90° Orientation
B112-19	1	Circumferential scribe at 1-1/2. Vertical scribe on X-axis.	Small dark speck at 6-7/8.
	2	Small dark specck at 5-5/8. Small dark spot at 21-11/16.	Nothing anomalous.
	3	Removal mandrel marks at 6-5/8.	Removal mandrel marks at 6-5/8.
	4	Circumferental dark band at 17.	Circumferential dark band at 17. OD fluctuations at 17.
	5	Small dark specks at 24, 25.	Small dark specks at 20-5/8, 24, 25.
B73-8	1	Circumferential scribe at 1-1/4. Vertical scribe on X-axis.	Small dark specks between 4-3/4 and 7-1/2.
	2	Circumferential defects at 6-3/4, 7-1/4, 7-3/4, 8-1/2, 8-3/4, 12. Small dark specks at 17-1/2.	Circumferential defects at 6-3/4, 7-1/4, 7-3/4, 12.
	3	OD fluctuations to 3-1/2. Slightly bent at 1-1/2.	Same as 0°.
	4	OD fluctuations from 13 to bottom. Small dark specks at 11, 12.	Same as 0°.

*Numerical locations are inches from top of piece.

Table 2-5. Eddy Current Inspection Results

		OD Defect Indications		
			% Through-Wall	
Tube	Piece	Axial Location, In. From Top	Site	Lab
B73-8	1	-	-	-
	2	18.3	84	92
		18.8	84	88
		19.3	60	83
		20.4	36	?(2)
		20.5		?(2)
		23.4	84	100
	3	-	-	-
	4	-	-	-
B112-19	1	-	-	-
	2	-	-	-
	3	-	-	-
	4	73.0	63	-(3)
	5	-	-	-

(1) Hypnen indicates no defect indications.

(2) Depth could not be determined due to distorted signals.

(3) Mechanical damage on OD surface may have altered response. Inspected with 0.540- and 0.500-inch differential probes and absolute OD surface scanning probe in laboratory.

Table 2-6. X-Ray Diffraction Results

ID Powder Sample

Species/ PDF Number	Relative Line Strength	Identification and Suspected Origin
Ni/4-850	Strong	Nickel, base metal
(α-SiC) 6H/ 29-1131	Medium	Moissanite-6H, hone
(SiC) 8H/ 29-1127	Medium to weak	Silicon carbide 8H, hone
δFeOOH/ 13-87	Very weak	Delta iron oxide hydroxide, base metal oxide
Unknowns	Very, very weak	--

OD Scrapings Sample

(Ni, Fe) Fe_2O_4/ 23-1119	Very strong	Ferroan Trevorite, surface deposit possibly formed by UTS interaction
Ni/4-850	Strong-medium	Nickel, base metal
$Ni_{3-X}S_2$/ 14-358	Very weak	Nickel sulfide, high temperature specie
Unknown	Very, very weak	--

Table 2-7. X-Ray Emission Spectroscopy Results

Compound	Concentration, Wt %
ZnO	0.6
CaO	0.07
Na_2O	<0.1
V_2O_5	<0.03
MoO_3	<0.03
ZrO_2	<0.03
TiO_2	0.09
CoO	0.04
SnO_2	0.06
NiO	11.0
MnO_2	1.4
Cr_2O_3	2.2
PbO	0.04
Fe_2O_3	>50.0
MgO	0.1
SiO_2	1.1
Al_2O_3	1.0
CuO	7.0

Table 2-8. Electron Microprobe Results

Region	Concentration, Weight Percent*										Round
	Ni	Fe	Cr	Mn	Cu	Si	S	Cl	P	Total	
Crack surface, near OD	42.9	33.0	16.4	0.52	--	0.13	0.005	--	-	93	
Crack surface, middle	36.2	23.1	17.4	0.28	--	-	0.001	--	-	77	(1)
Crack surface, near ID	42.0	15.8	18.2	0.25	--	0.03	0.0002	--	-	76	
Ductile tear	42.9	9.7	19.0	0.55	--	0.01	-	--	-	72	
Crack surface, near OD (region of deposit)	29.9	56.9	11.6	0.97	--	0.08	0.41	--	-	99.9	(2)

* Hyphen indicates not detectable.

(1) 200X
Sweep area: 0.016 in^2
Sweep speed: 10 seconds

(2) 500X
Sweep area: 0.006 in^2
Sweep speed: 20 seconds

Table 2-9. Electron Spectroscopy for Compound Analyses Results

Region	Sputtering Depth, Å	Concentration, Atomic Percent							
		Ni	Fe	Cr	O	C	Cl	B	S
Crack surface	50	7.2	8.8	3.3	23.4	56.4	0.4	-	0.5
	500	7.5	9.1	4.1	36.7	40.2	0.9	-	1.5
	1,000	7.7	9.5	2.6	43.9	24.4	0.4	8.0	3.5
	2,500	4.5	16.8	3.1	62.0	6.4	1.4	2.9	2.9
	5,000	12.9	11.9	3.1	51.1	8.4	3.1	6.6	2.3
	10,000	9.9	15.6	3.9	55.2	5.3	1.1	6.1	3.0

- Ni and Fe in atomic states at 10,000Å.
- O concentrations mainly due to oxides on copper specimen holder.
- Cl and B may be associated with oxygen (oxides).
- S probably in sulfide form.

Ductile tear	50	7.2	8.8	3.3	23.4	56.4	-	-	-
	500	2.7	5.5	2.0	46.1	43.7	-	-	-
	1,000	5.3	8.5	3.8	75.8	6.6	-	-	-
	5,000	9.3	28.0	2.4	50.7	9.7	-	-	-
	6,000	9.1	31.0	4.3	50.9	1.2	-	-	-

- Ni and Fe in atomic states at 5,000Å.
- O concentrations mainly due to oxides on copper specimen holder.

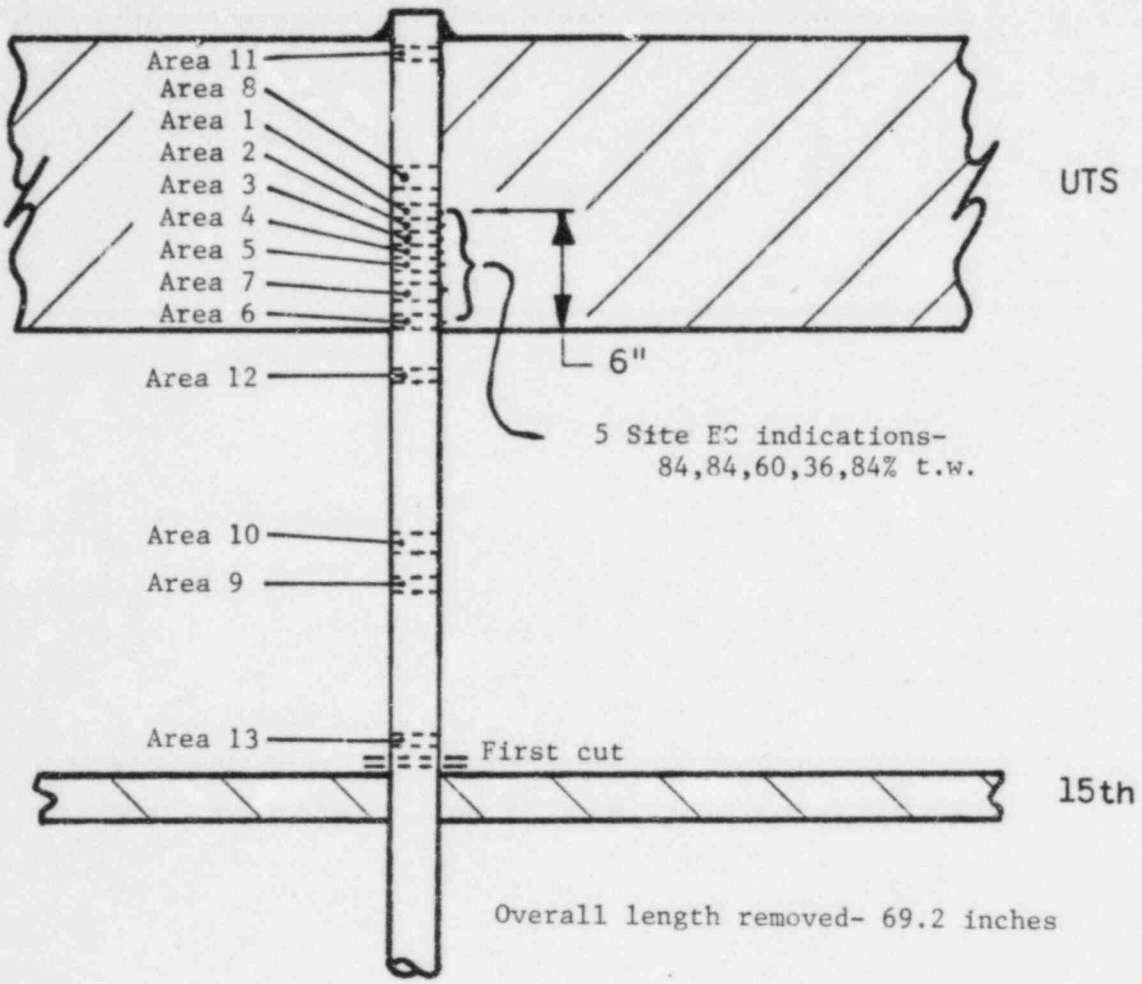

Figure 2-1. Tube B73-8 Schematic

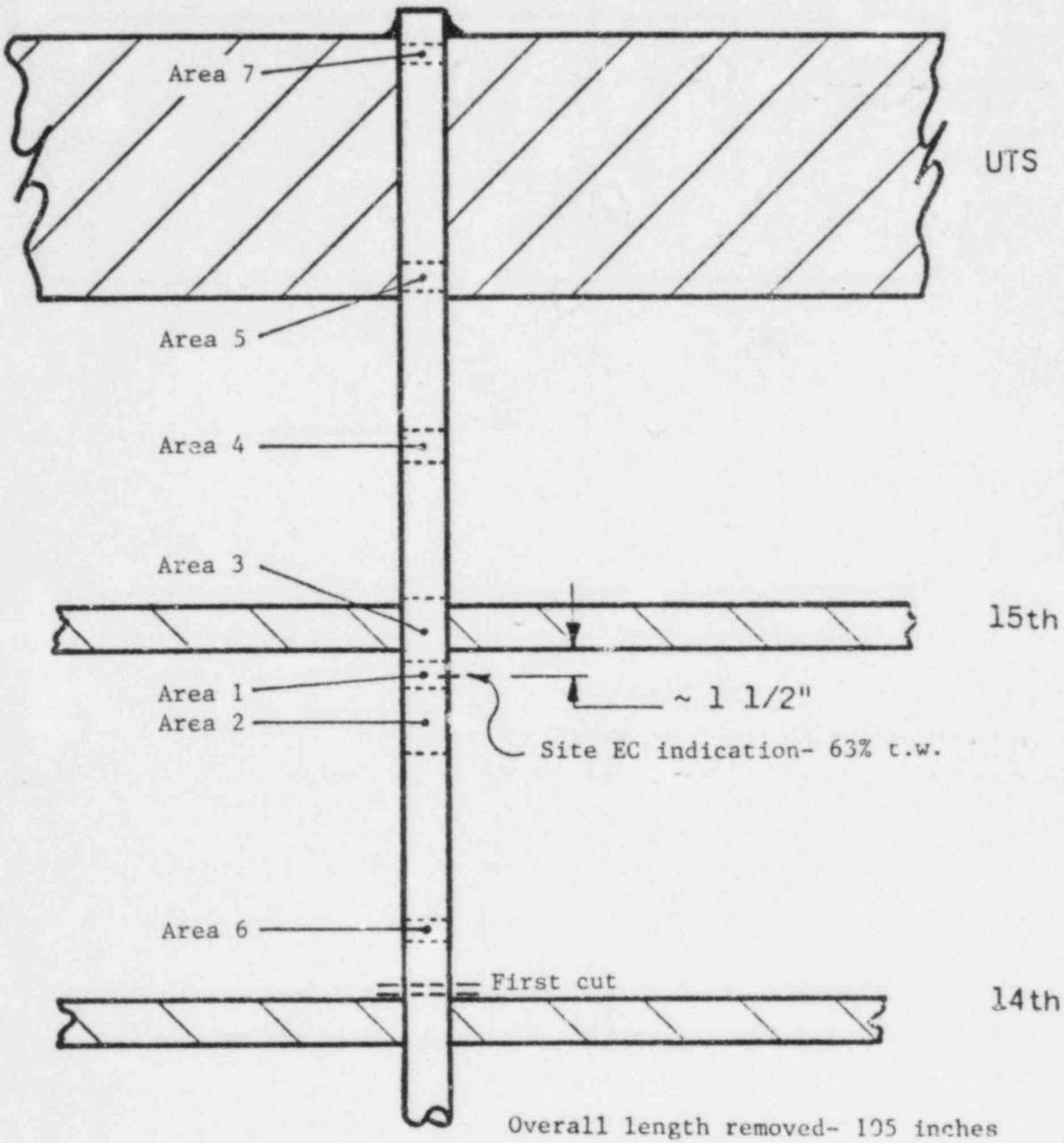

Figure 2-2. Tube B112-19 Schematic

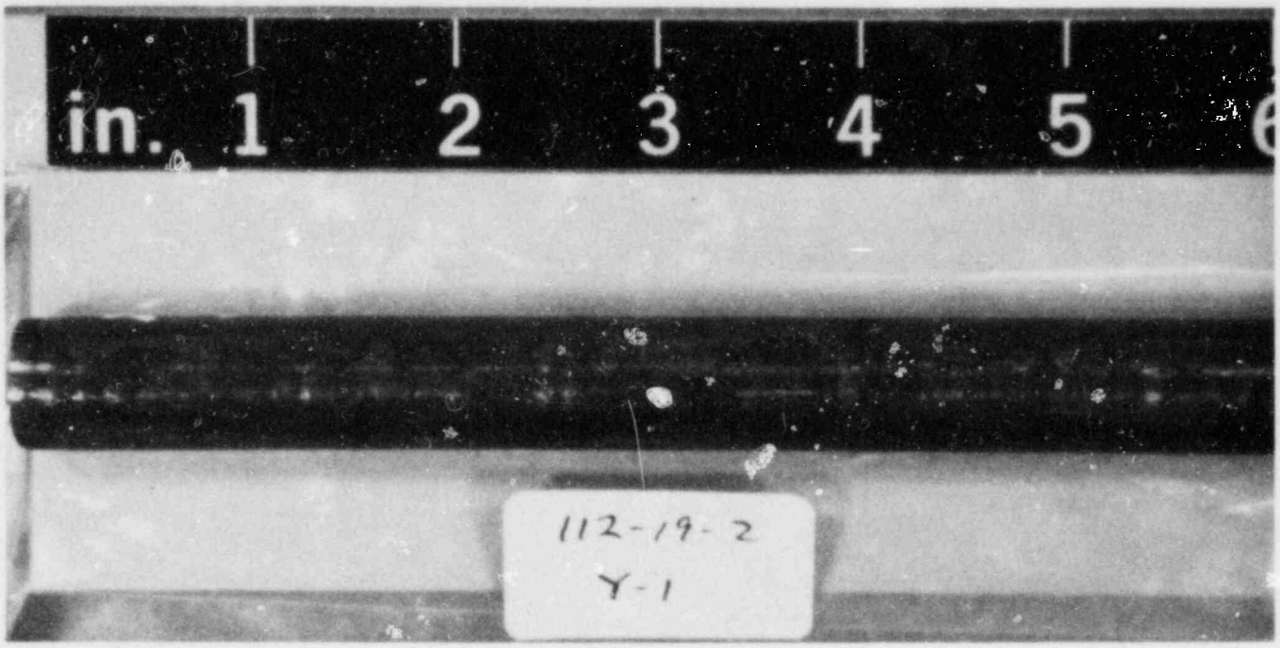

Piece 2 Y-Axis
Dry-out Stains

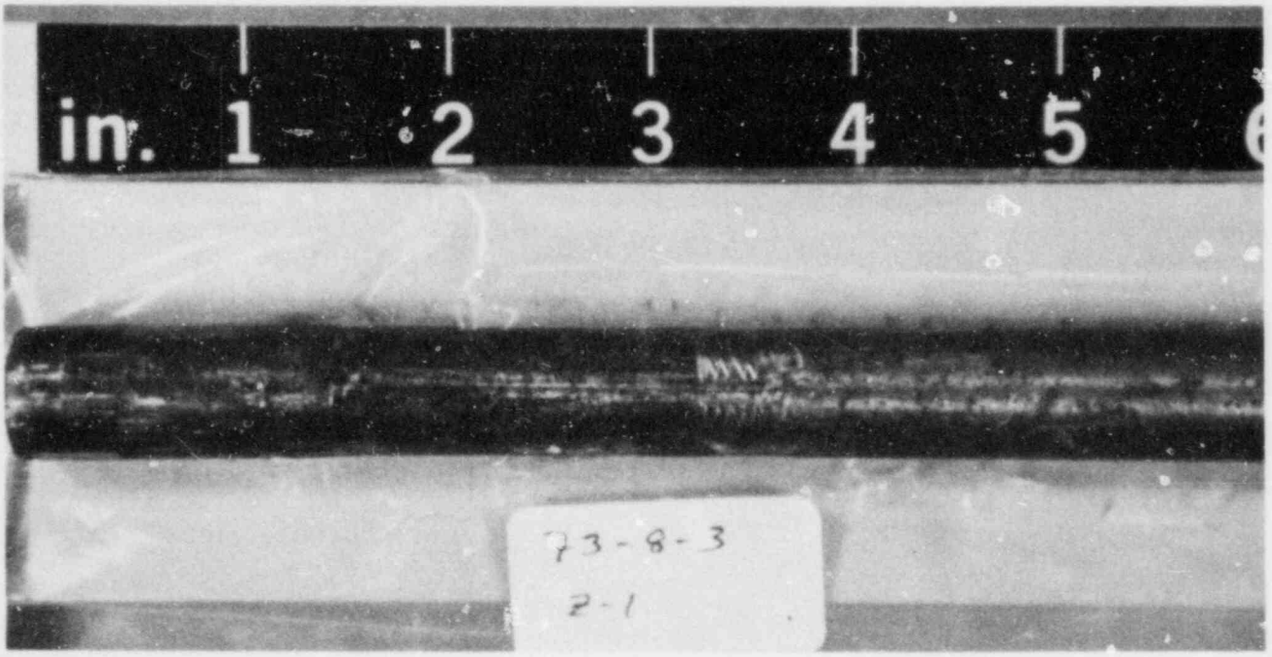

Piece 3 Z-Axis
Tube Removal Marks

Figure 2-3. Typical OTSG Tube Characteristics

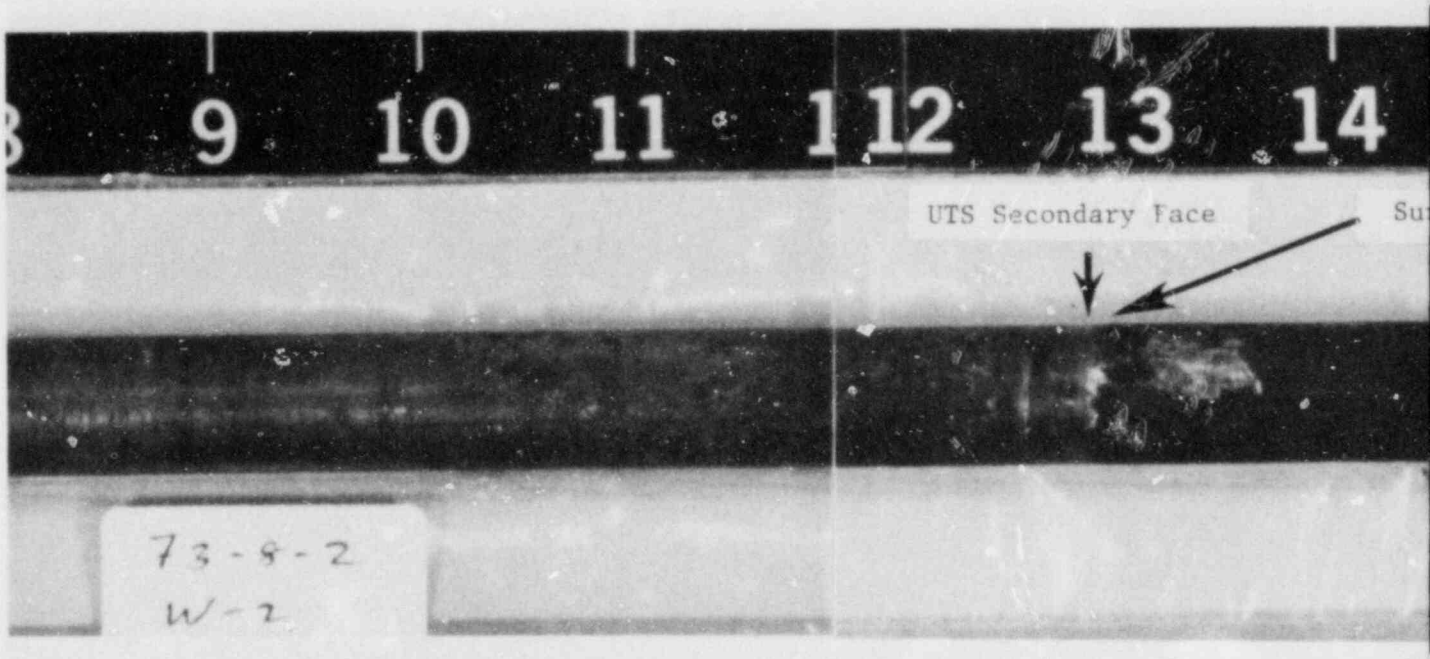

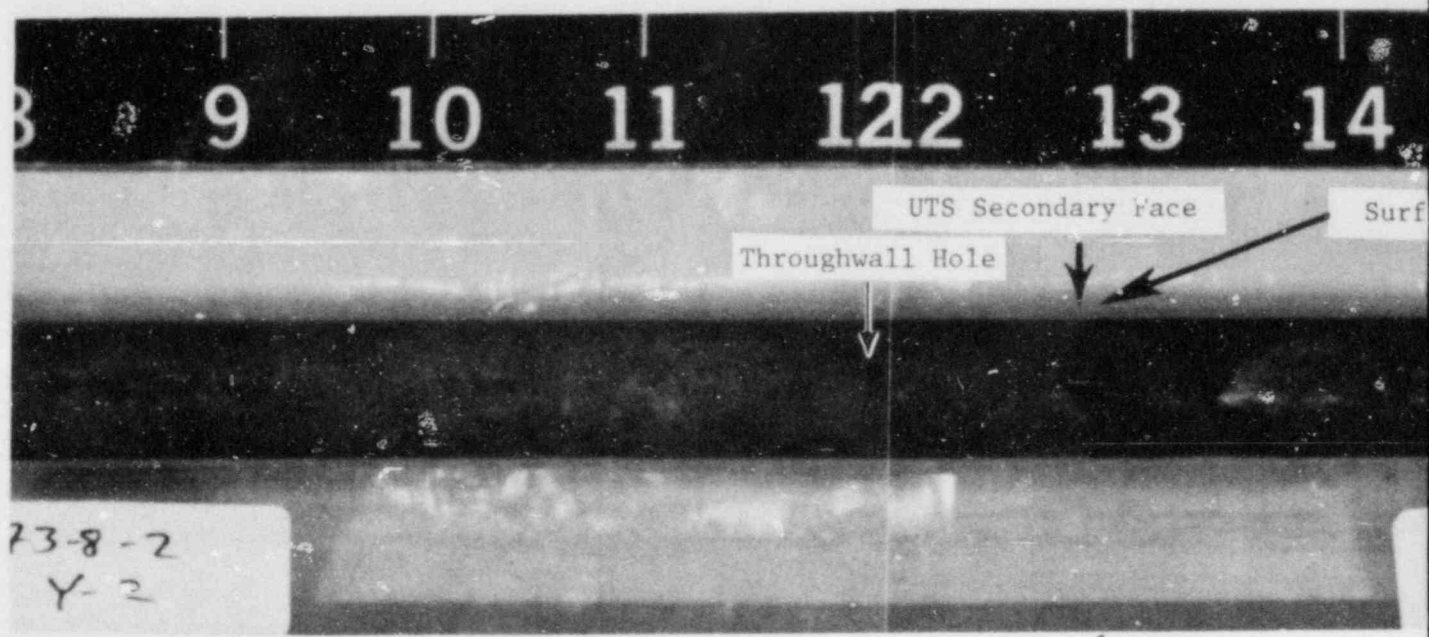

Figure 2-4. Tube B73-8 OD Surface Deposits Near UTS

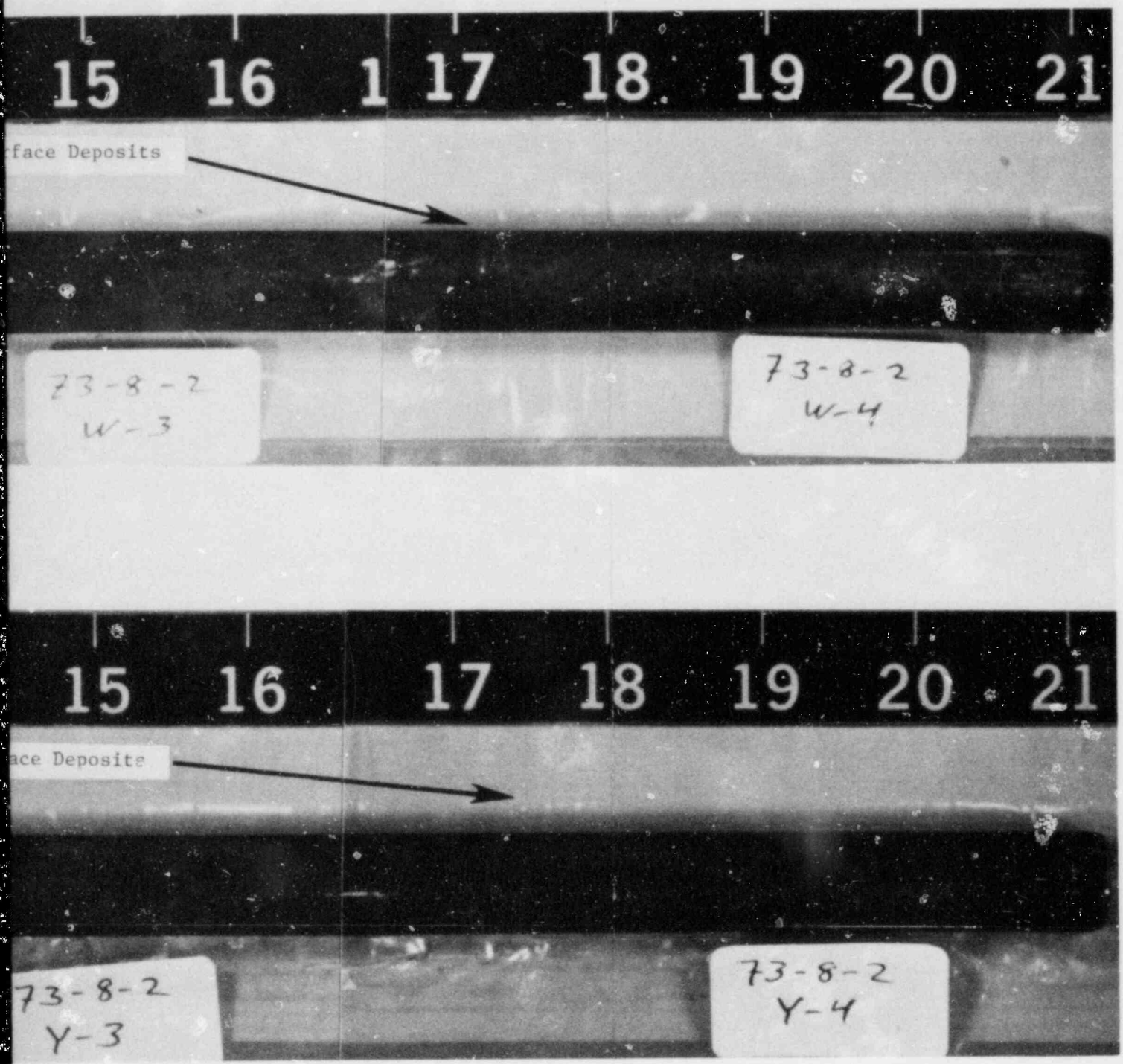

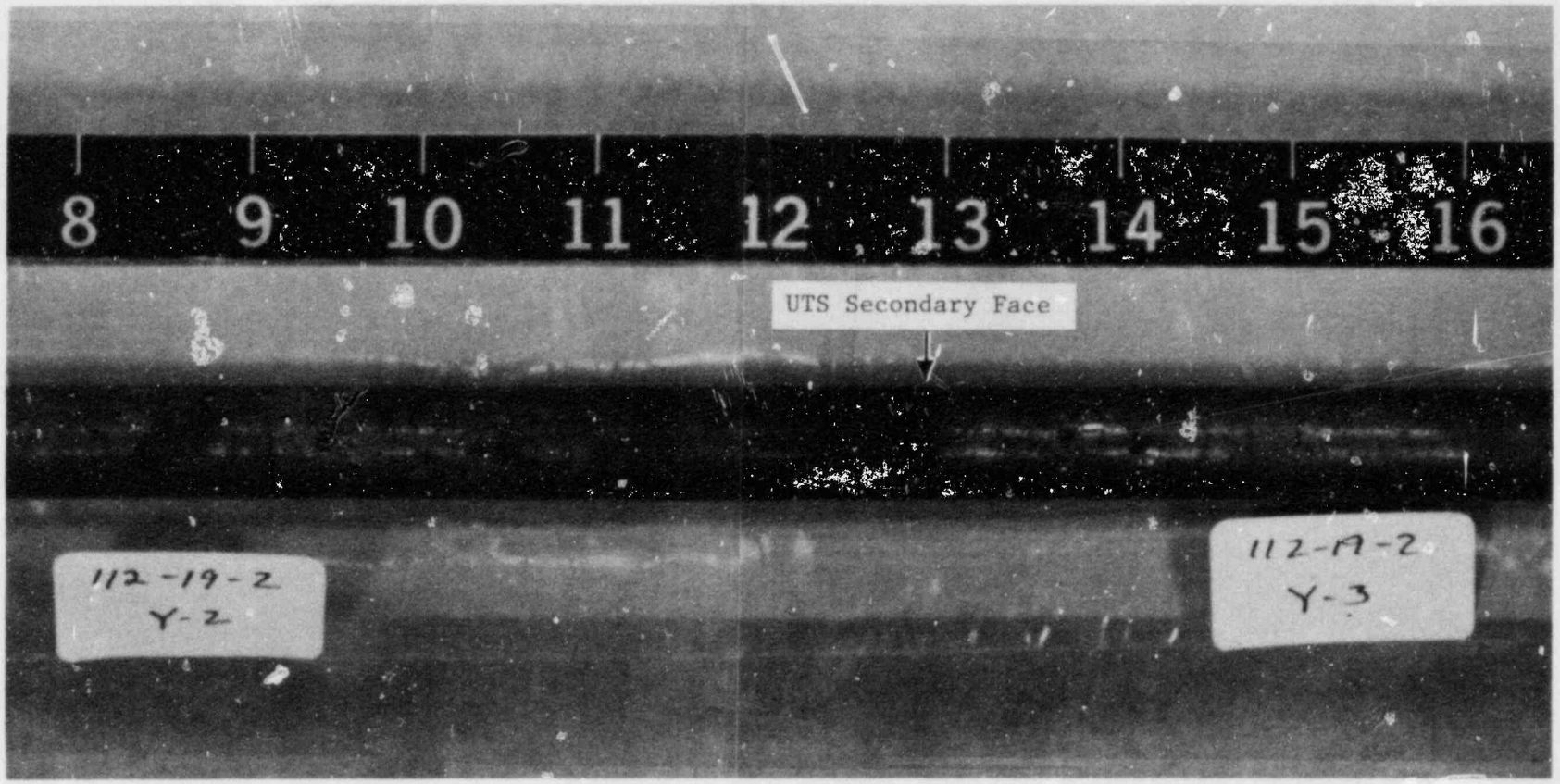

Piece 2 Y-axis

Figure 2-5. Tube B112-19 OD Surface Deposits Near UTS


12 13 14 15 16 17
15 TSP
Mechanic
TSP Land
112-19-4
W-3
Mechanic
TSP Land
112-19-4
Z-3

Figure 2-6. Tube B112-19 OD Surface Deposits Near 15th TSP

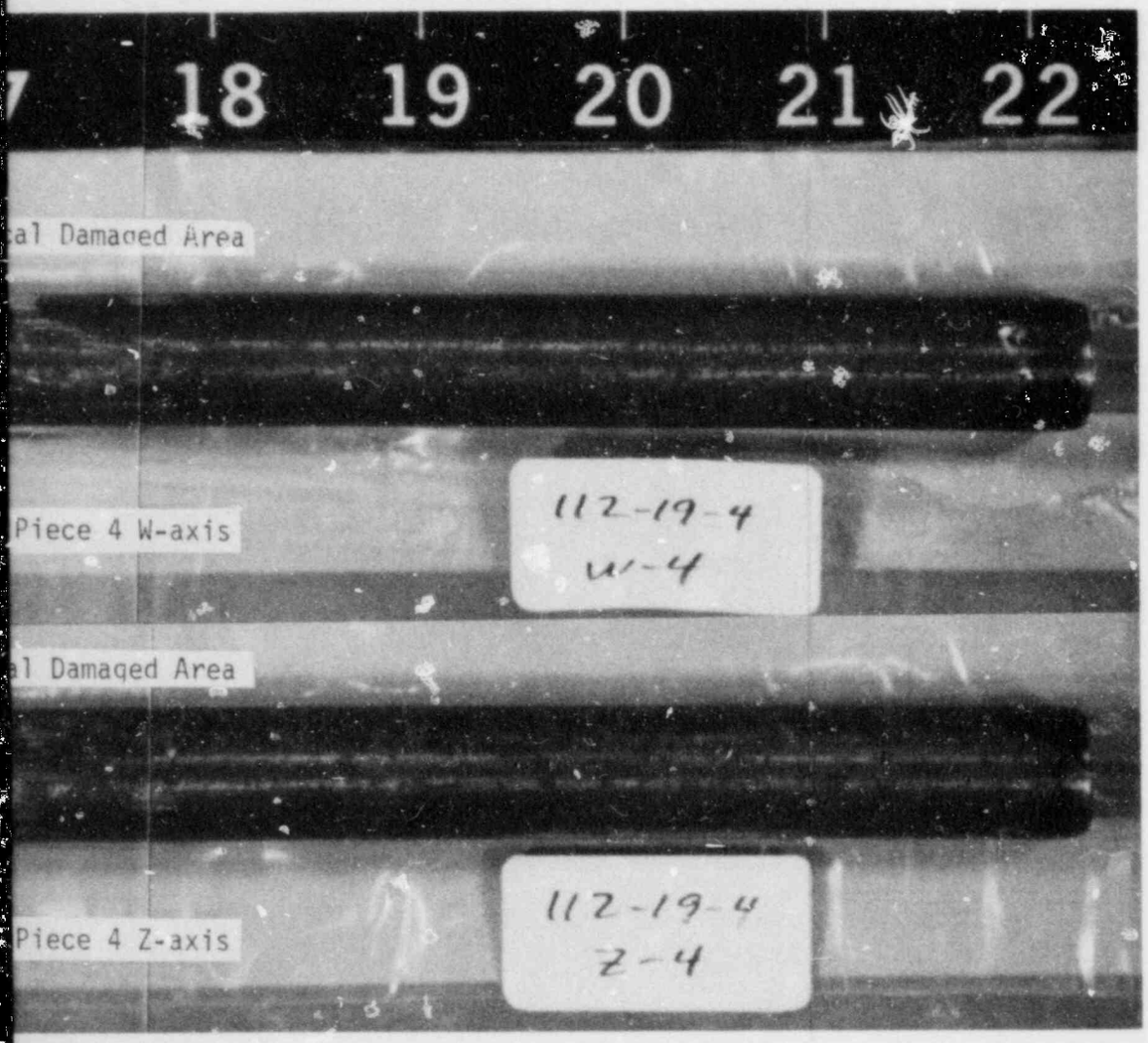

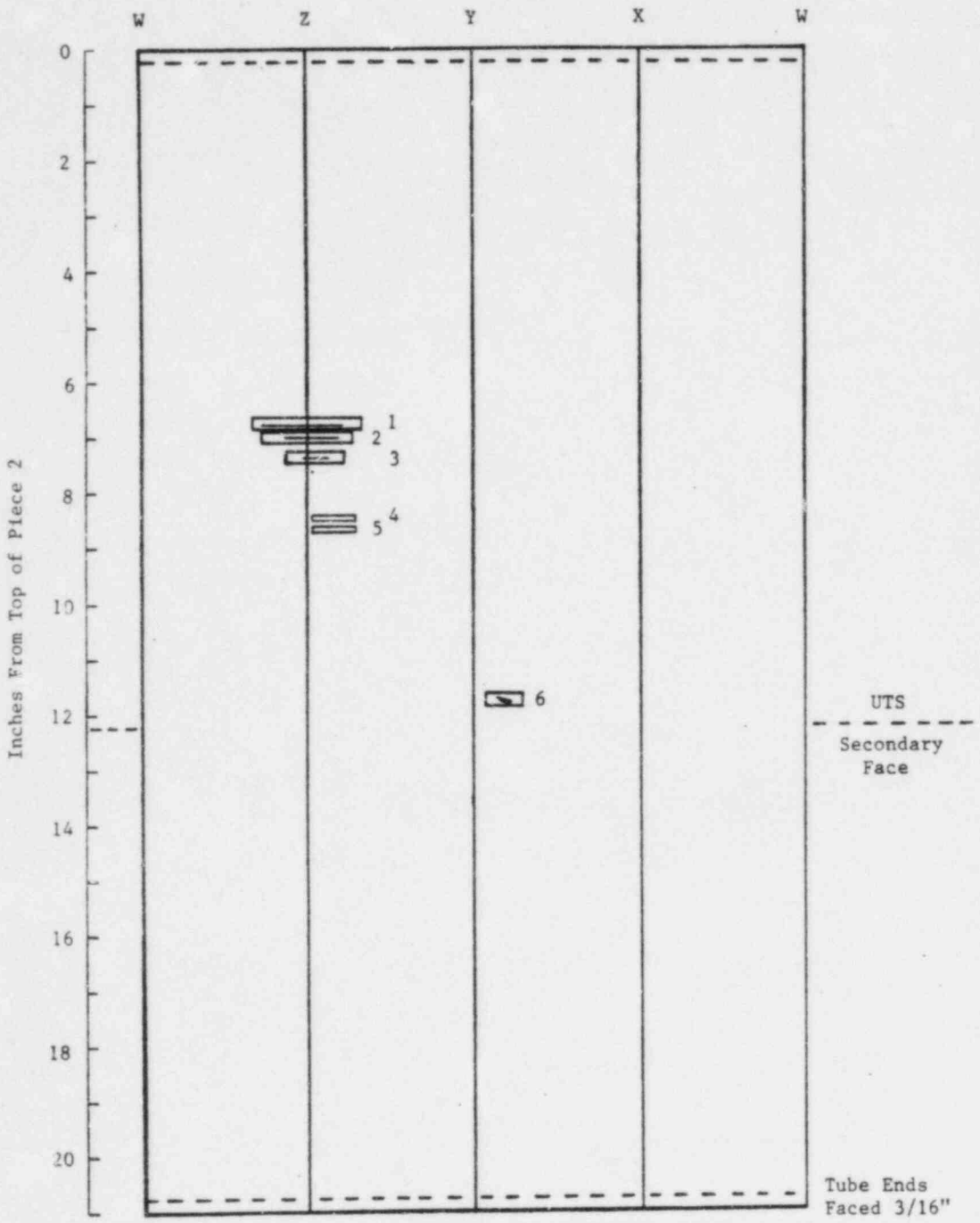

Figure 2-7. Location of Eddy Current Indications in Tube B73-8

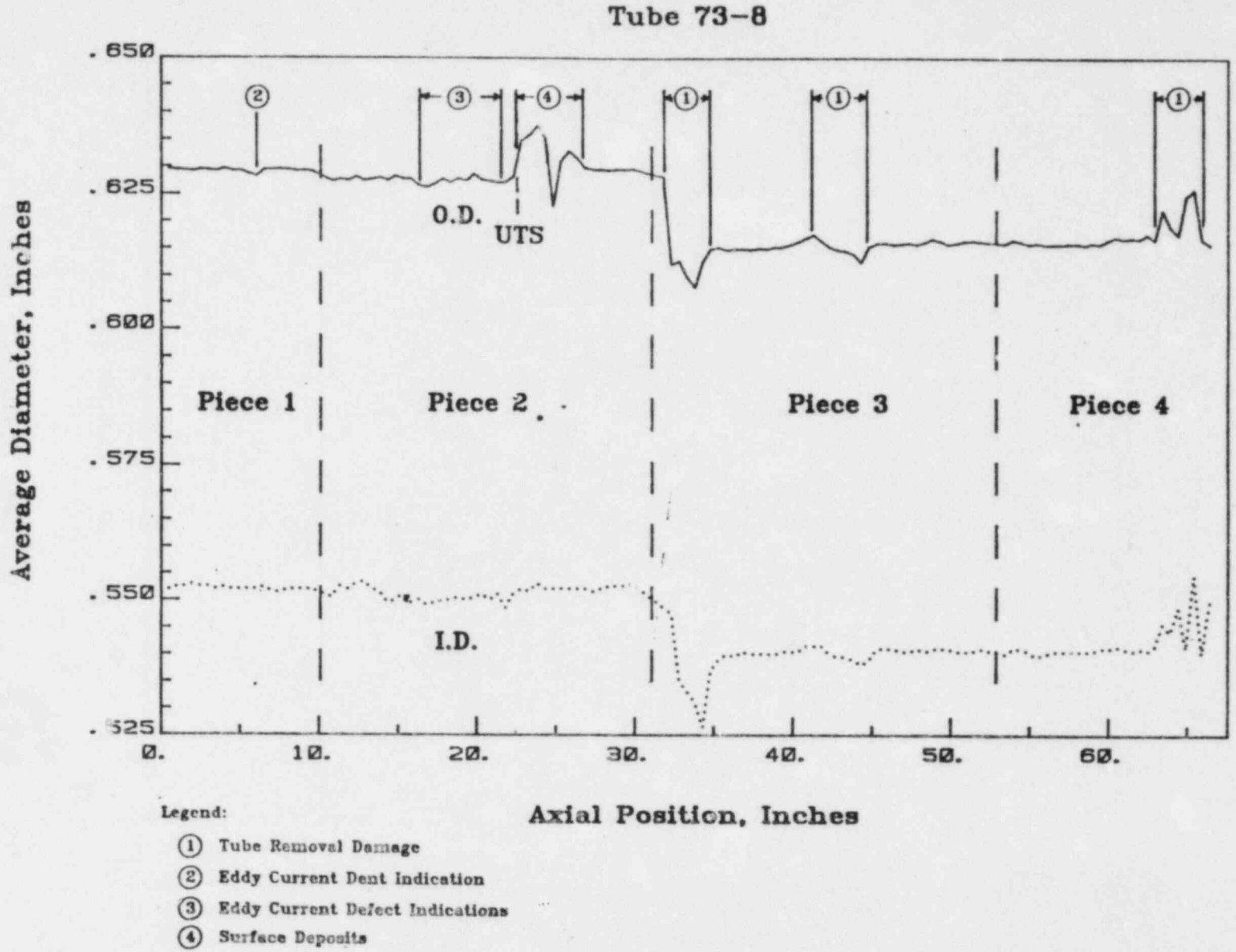

Figure 2-8. B73-8 Plot of Tube Diameter Versus Axial Position

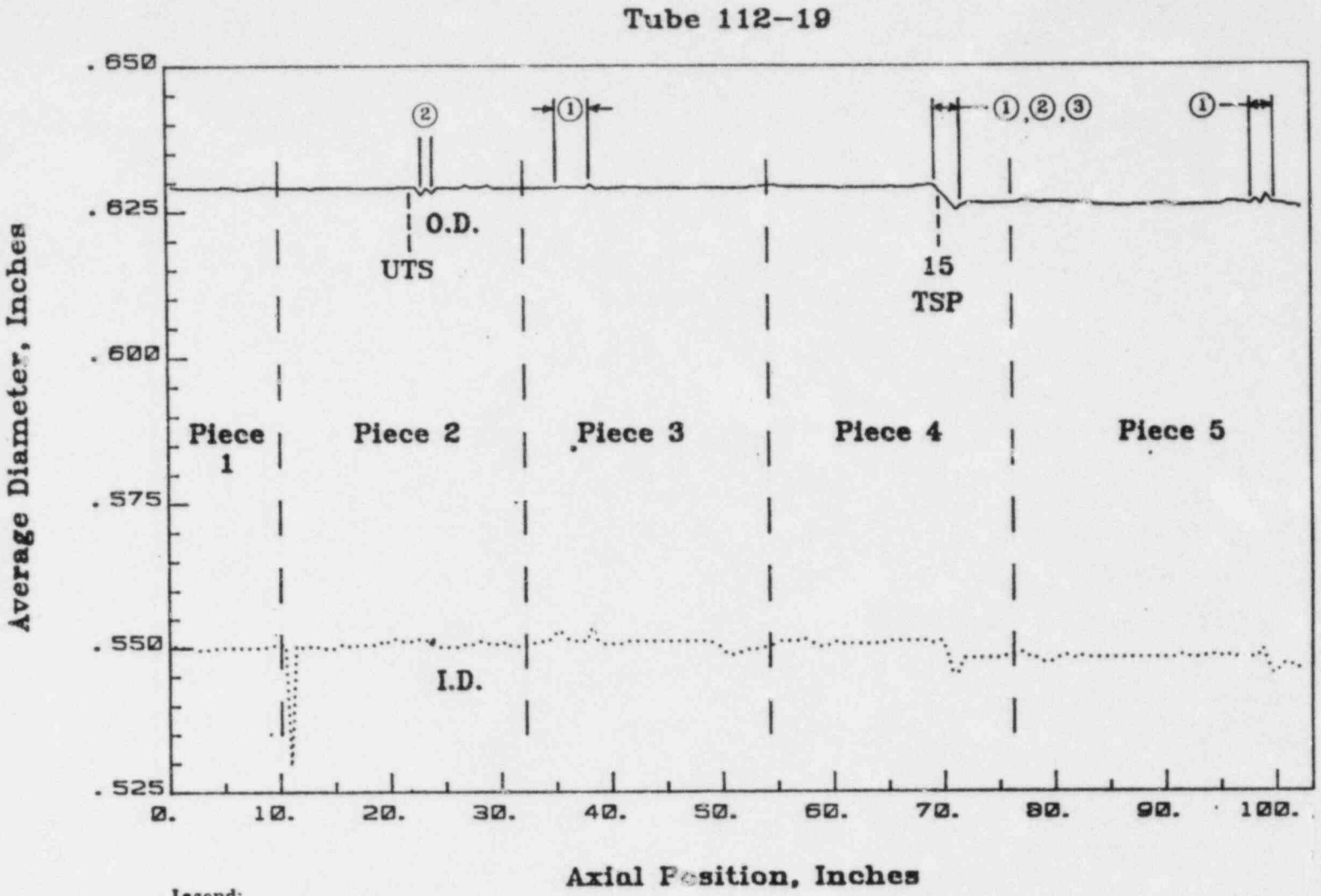

Figure 2-9. B112-19 Plot of Tube Diameter Versus Axial Position

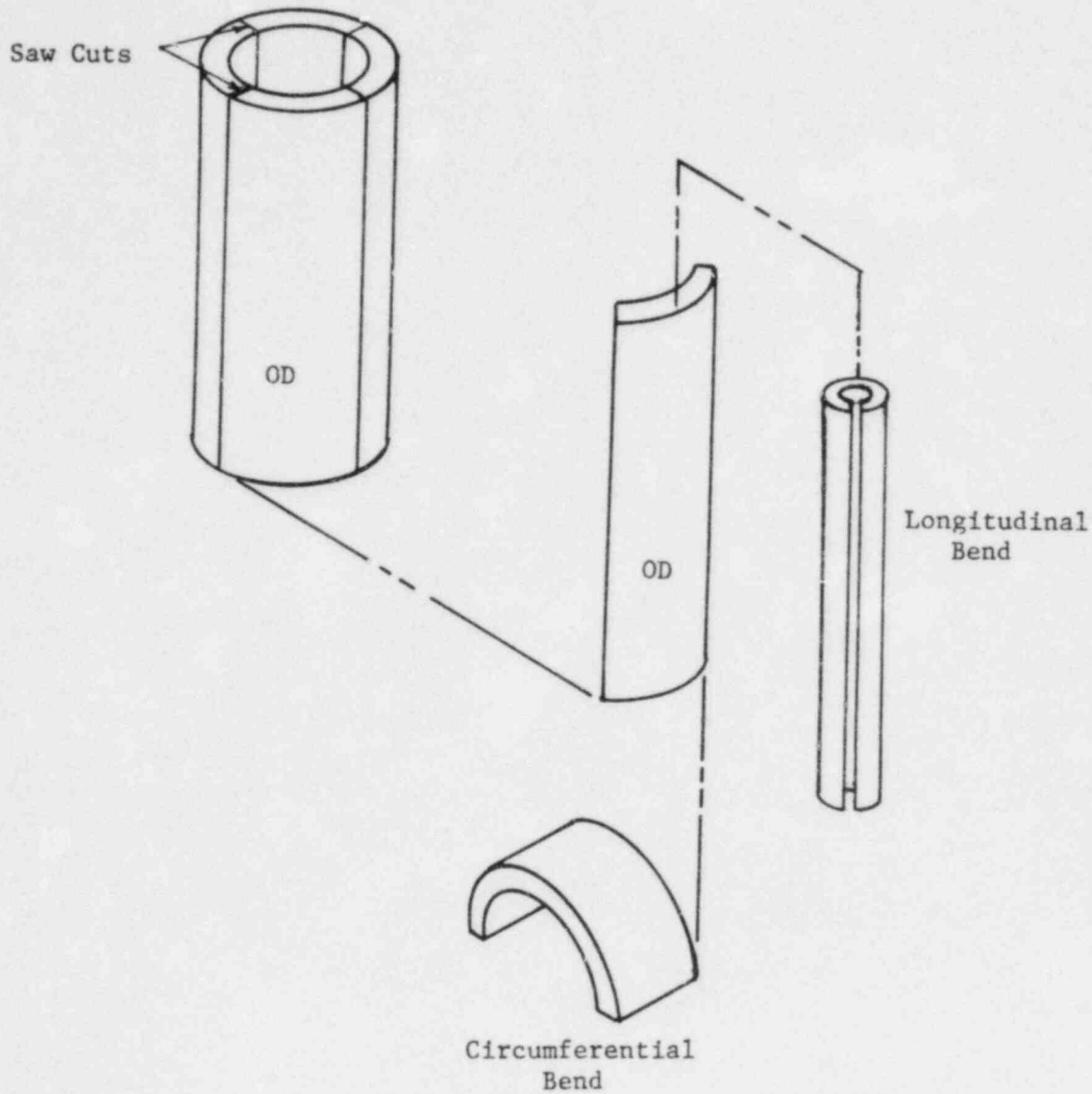

Figure 2-10. Tube Sectioning and Bending Technique

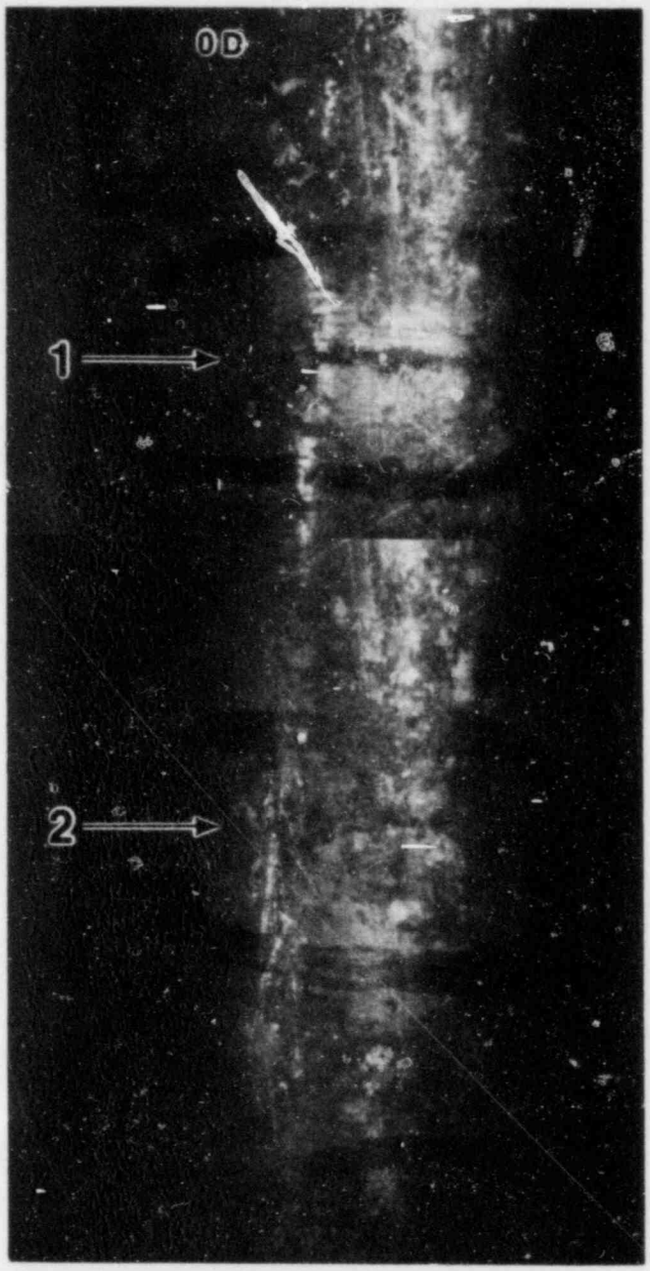

(5.6X)

Figure 2-11. OD Surface of Tube B73-8 Defect Indication Areas

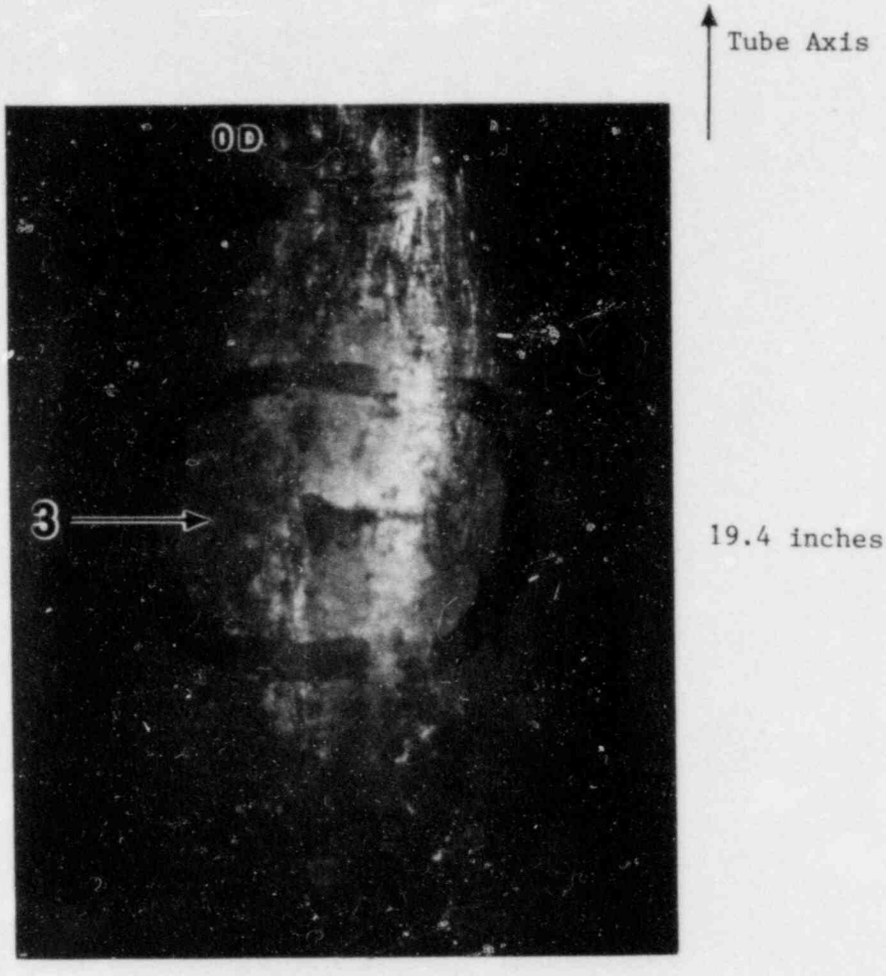

Figure 2-12. OD Surface of Tube B73-8 Defect Indication Areas

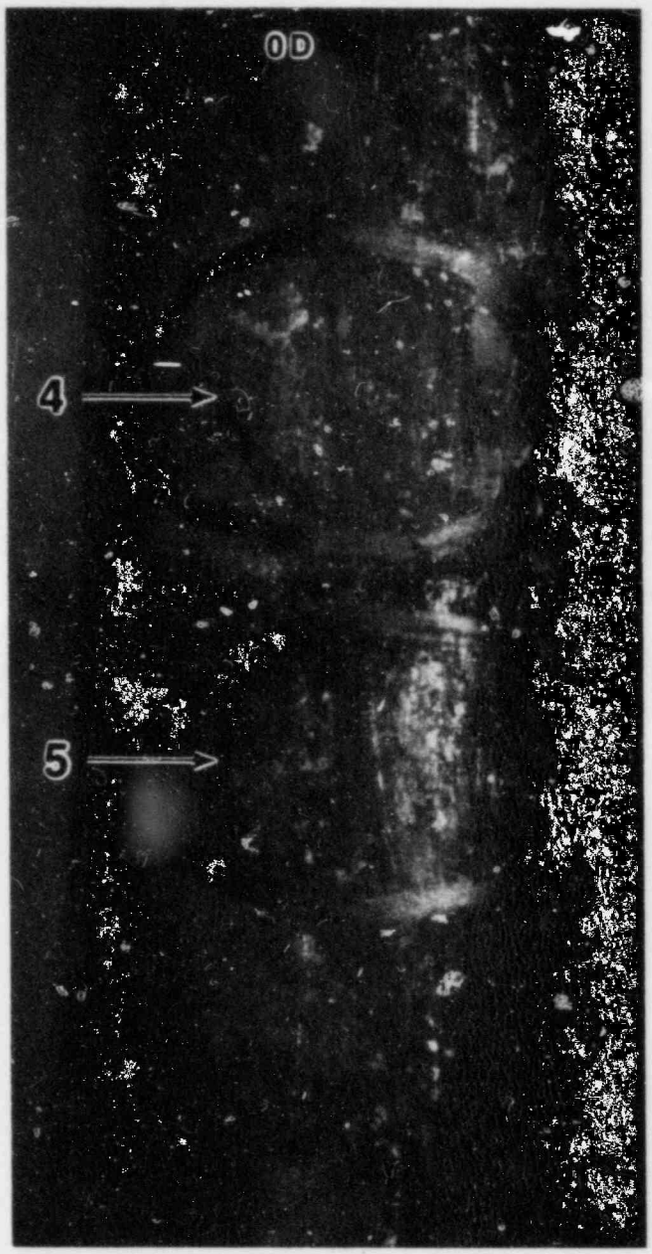

(5.6X)

Figure 2-13. OD Surface of Tube B73-8 Defect Indication Areas

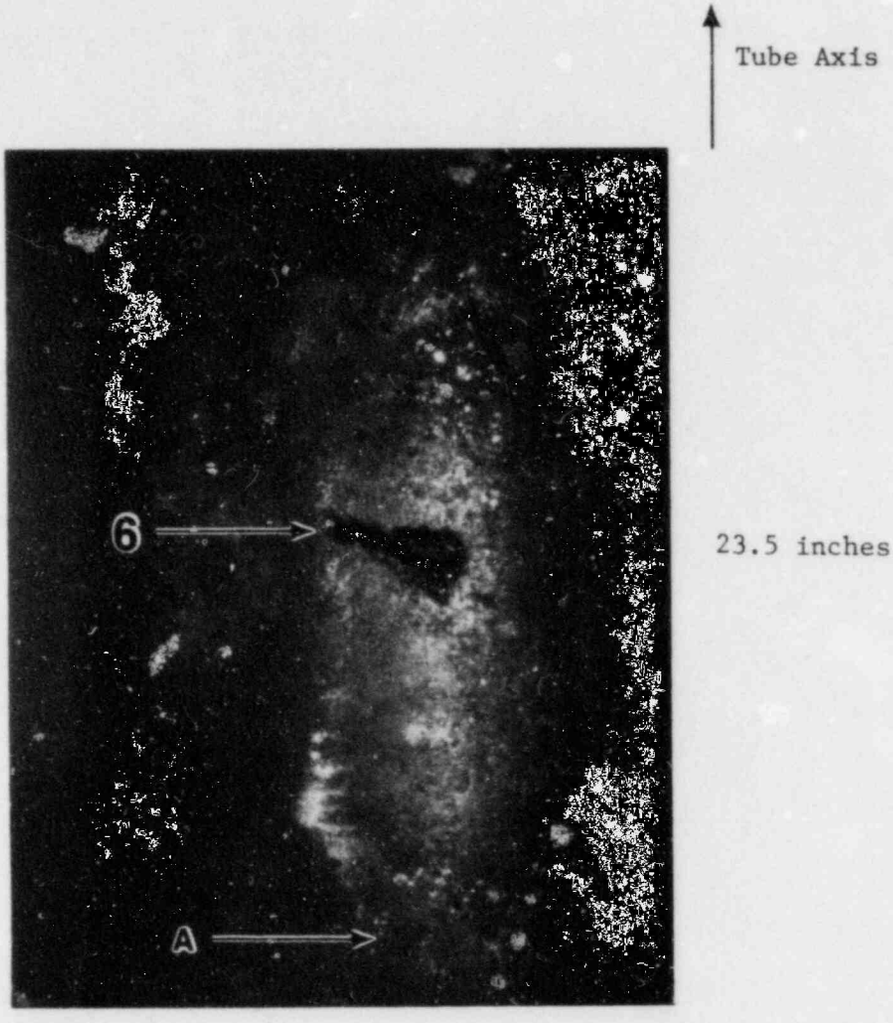

(5.6X)

A: Pitting and Wastage Attack

Figure 2-14. OD Surface of Tube B73-8 Defect Indication Areas

Tube Axis

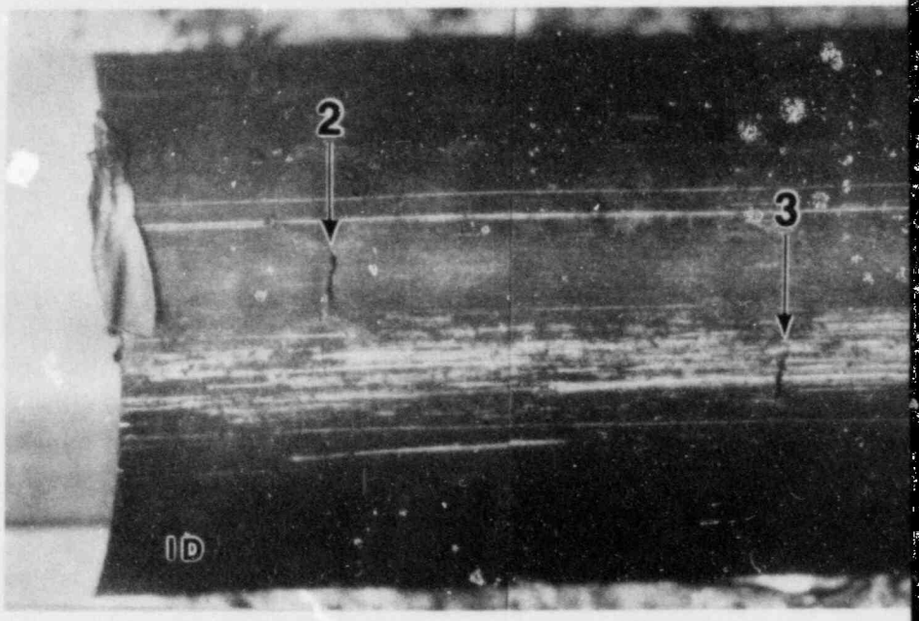

Areas 2 & 3 (3.6X)

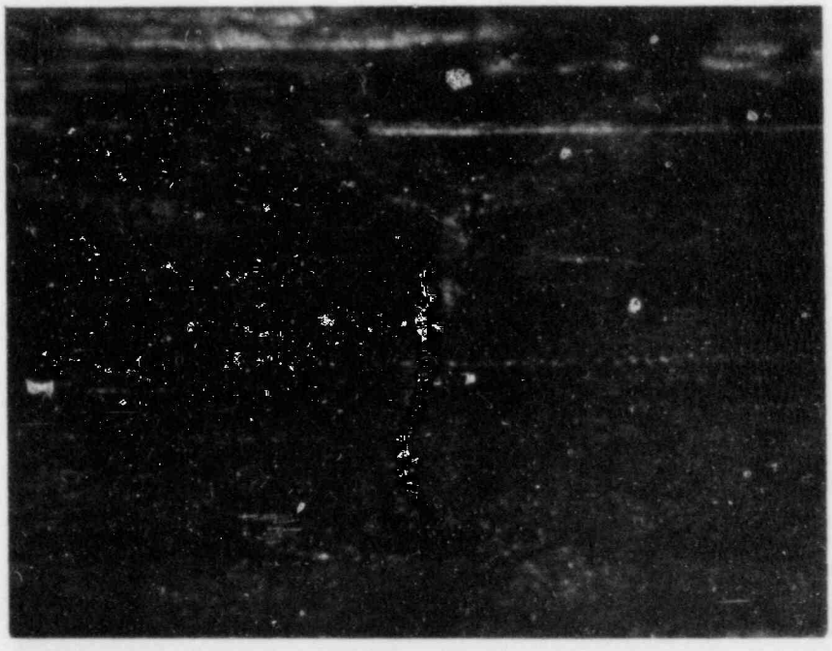

Area 2 (23X)

Figure 2-15. ID Surface of Tube B73-8 in Areas 2 and 3

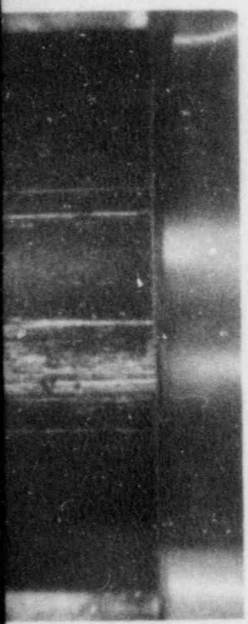

Area 3 (23X)

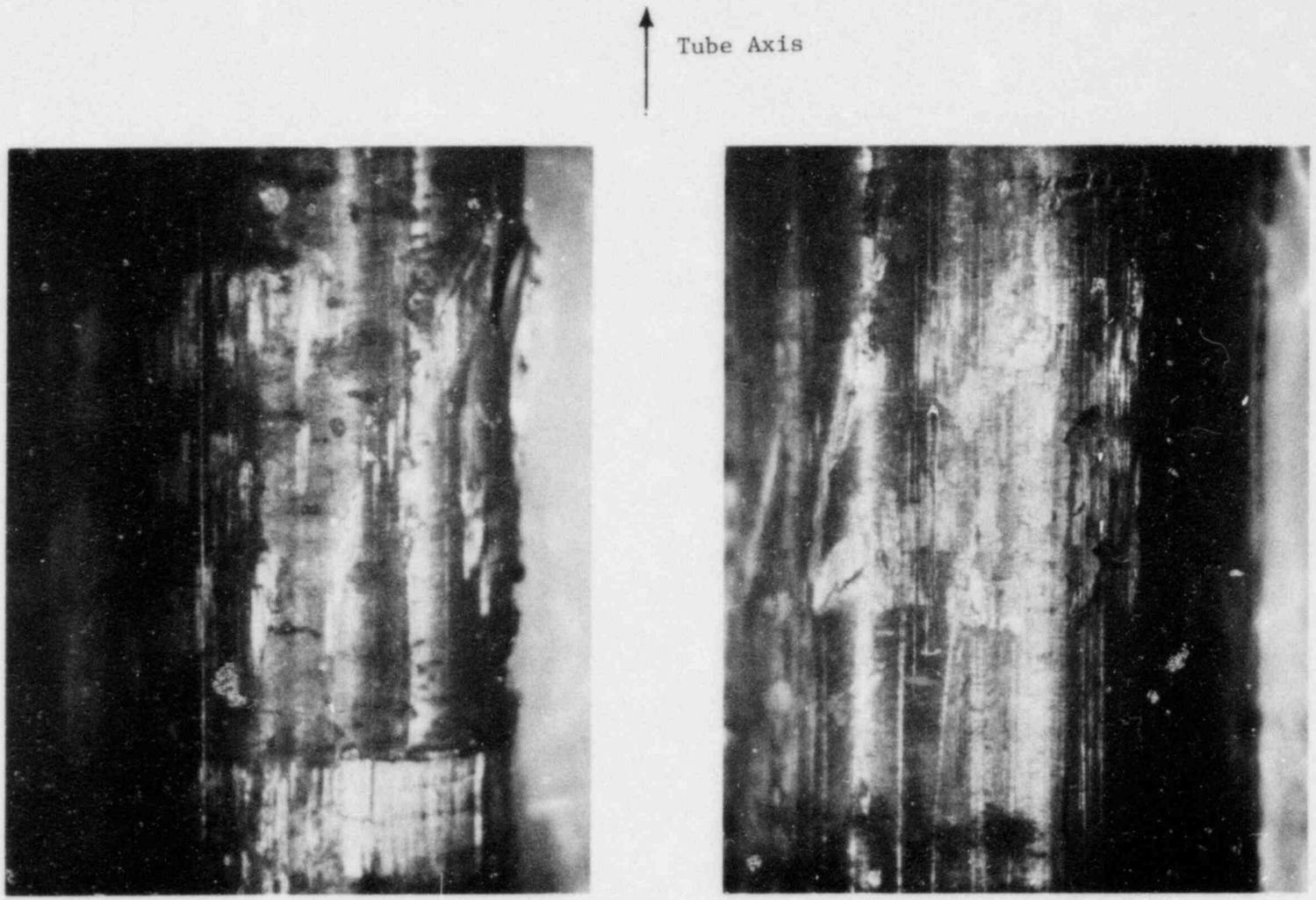

Figure 2-16. OD Surface of Tube B112-19 Defect Indication Area

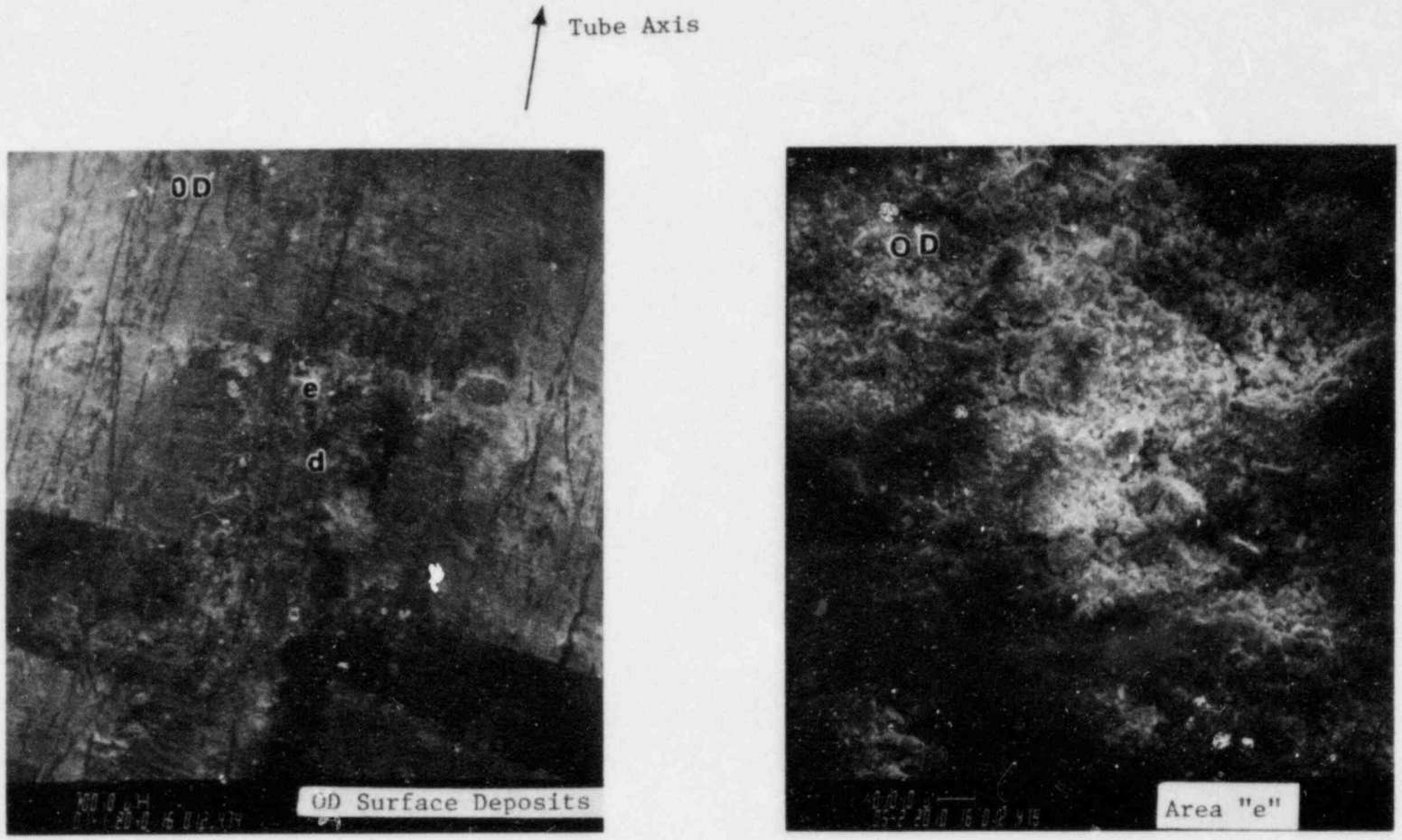

Figure 2-17. SEM Micrographs of Tube B73-8 Area 2

Tube Axis

OD Surface Deposits

Figure 2-18. SEM Micrographs of Tube B73-8 Area 3

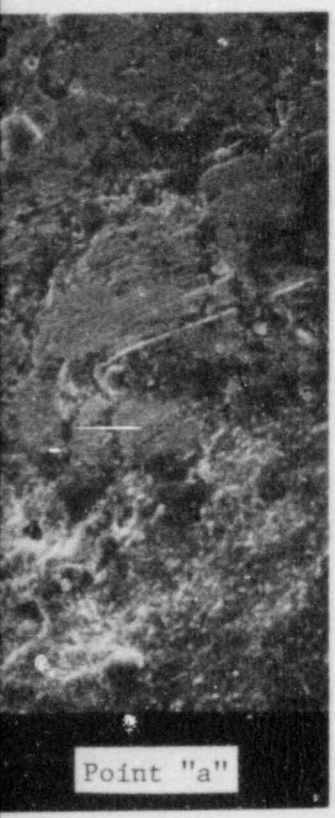

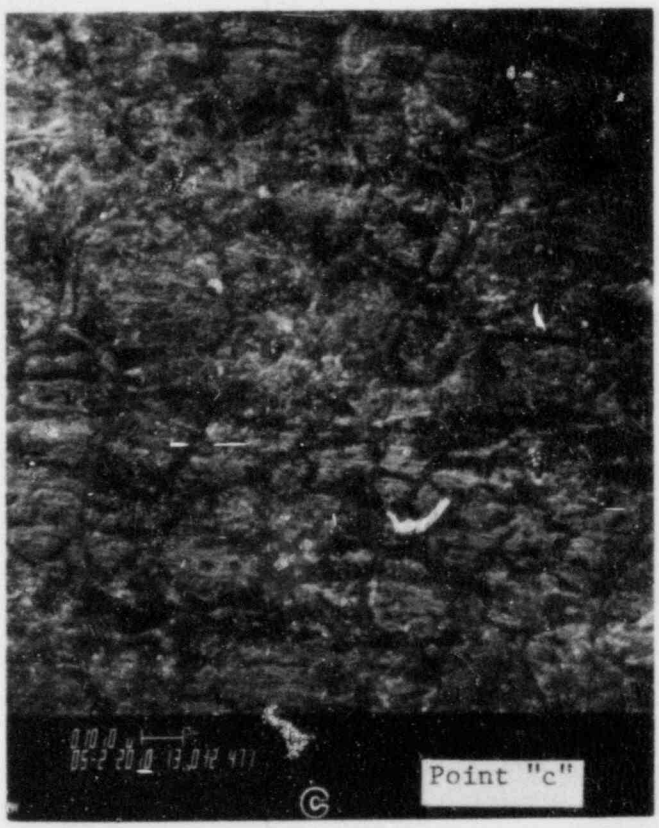

Tube

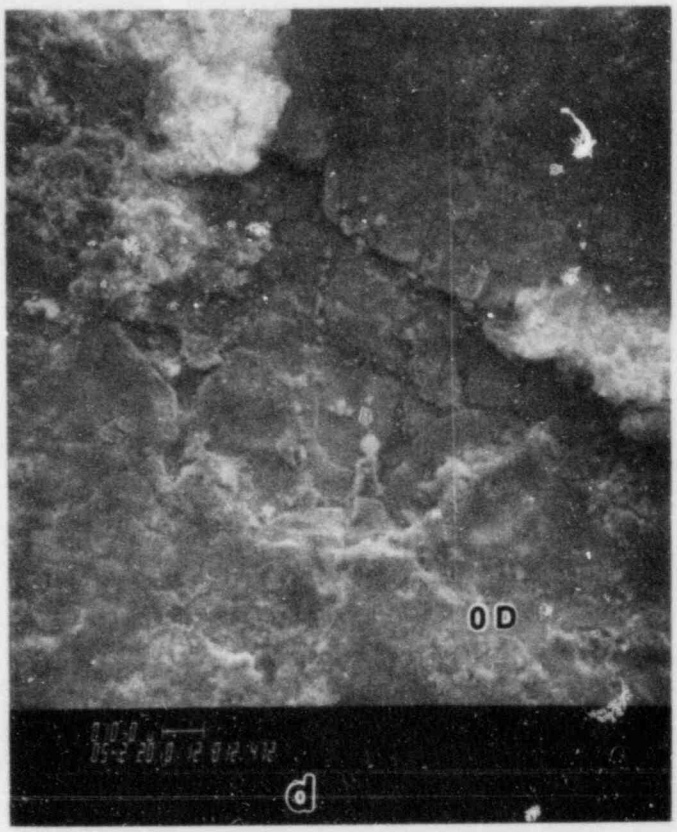

OD Surface Depo

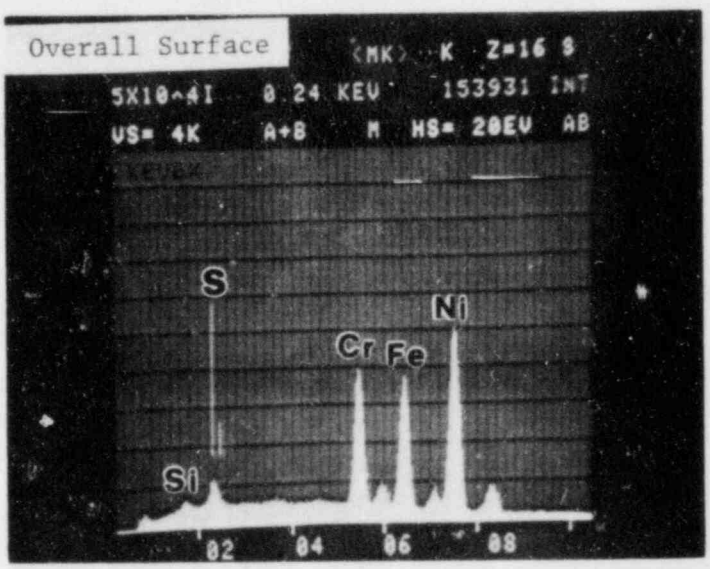

Figure 2-19. SEM Micrographs of Tube B73-8 Area 3

Axis

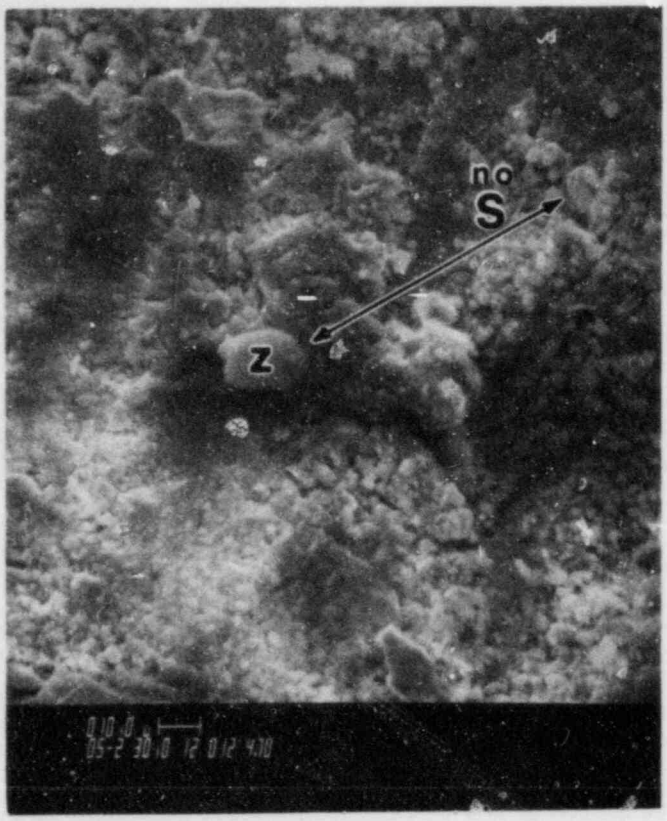

sits

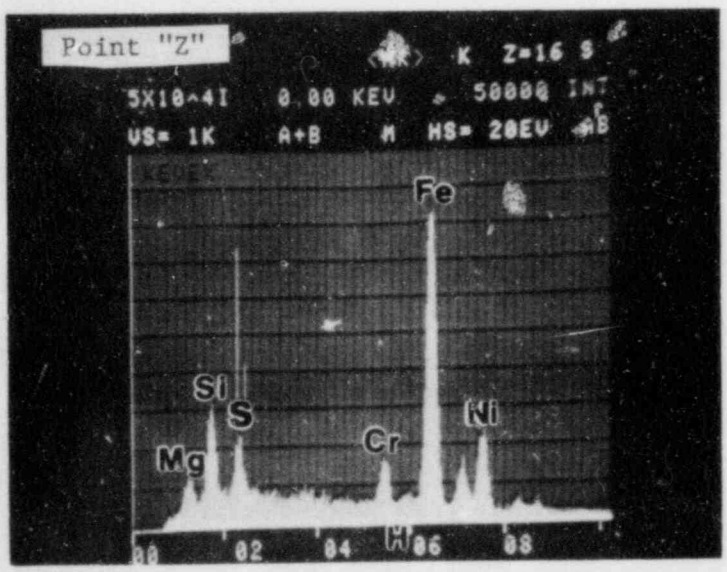

Tube Axis

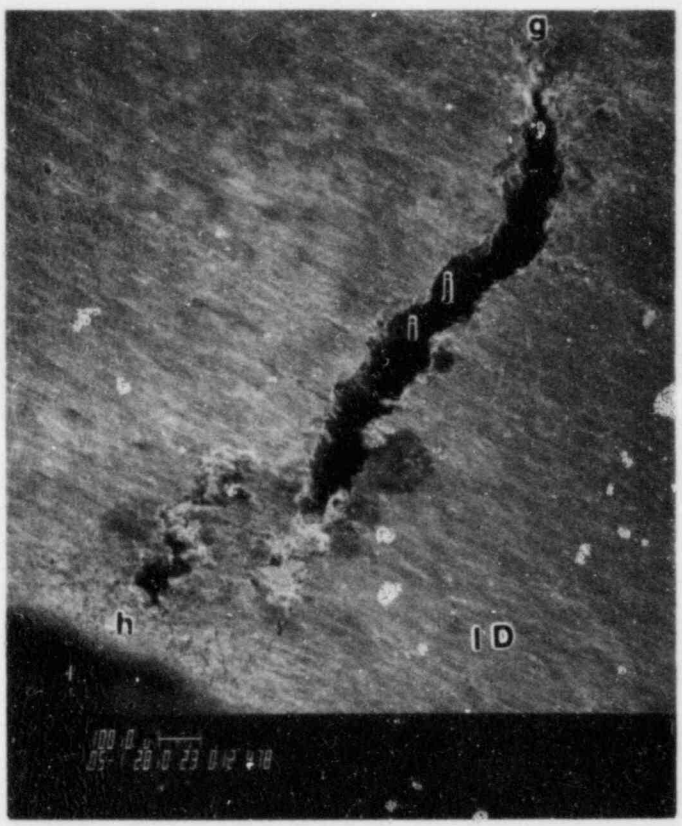

ID Intergranular Circumferential Crack

Figure 2-20. SEM Micrographs of Tube B73-8 Area 2

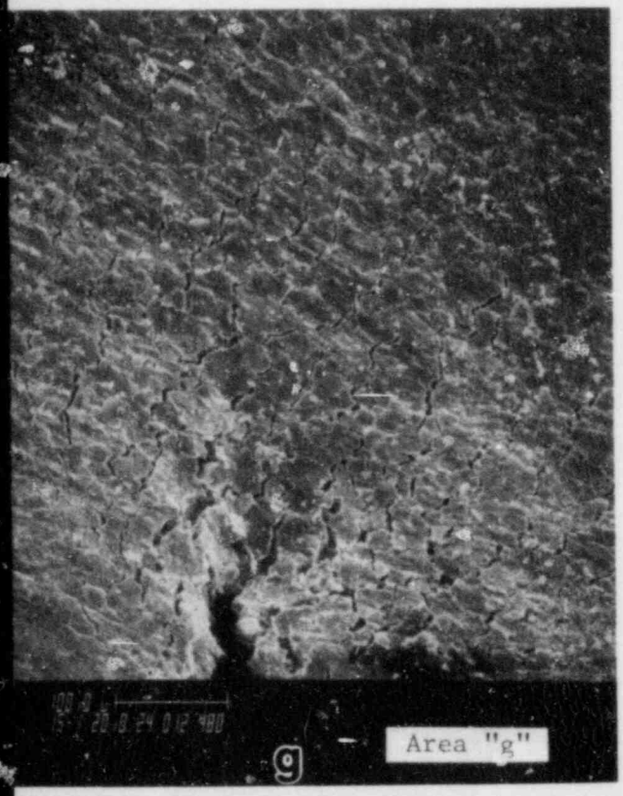

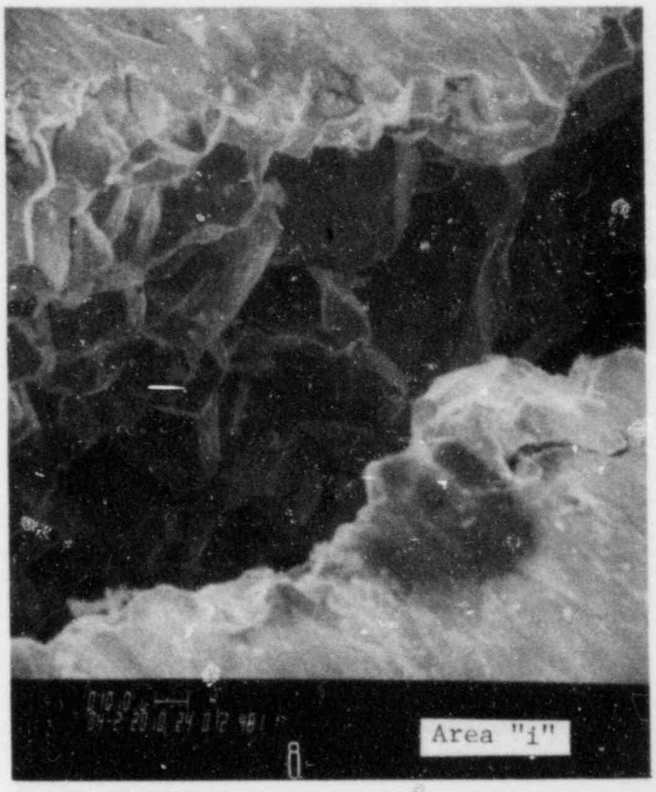

Intergranular Crack Surface

Tube Axis

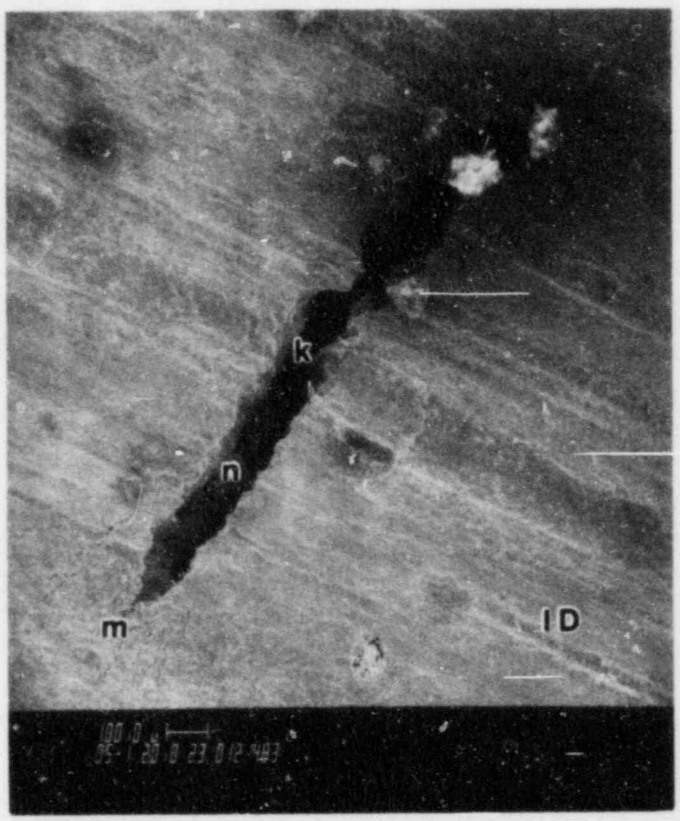

ID Intergranular Circumferential Crack

Figure 2-21. SEM Micrographs of Tube B73-8 Area 3

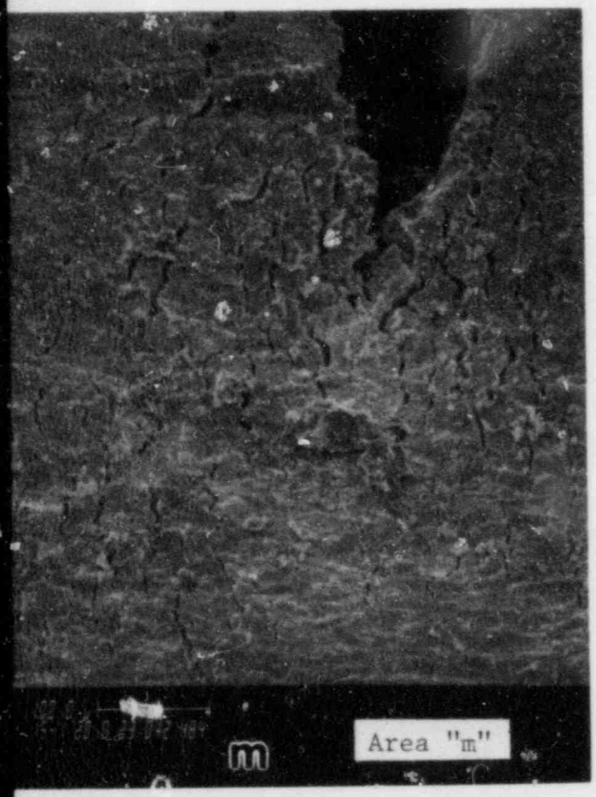

Crack Surface Deposits

Also Available On Aperture Card

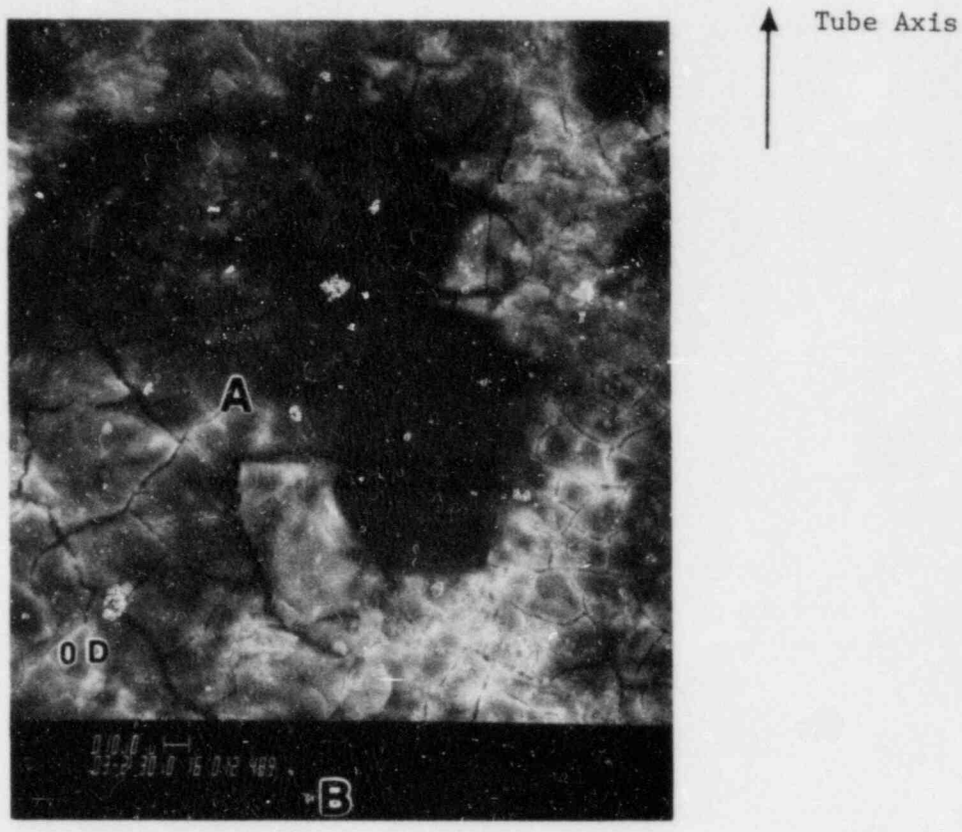

OD Surface Deposits

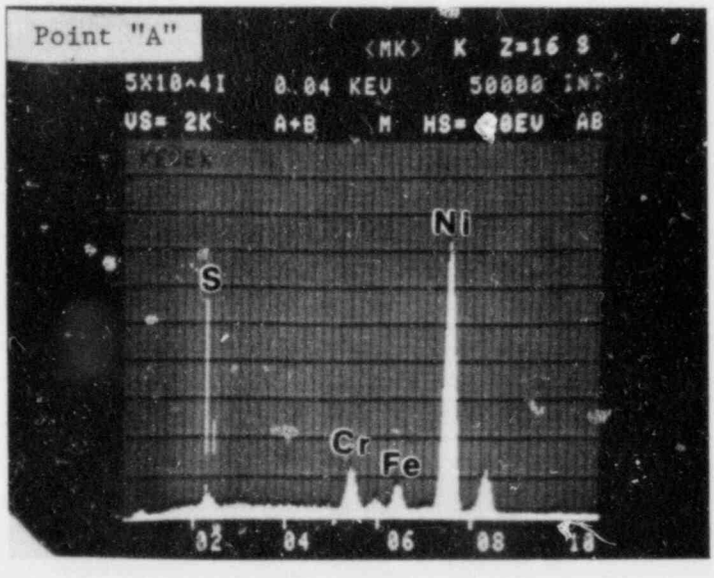

Figure 2-22. SEM Micrographs of Tube B73-8 Area 4

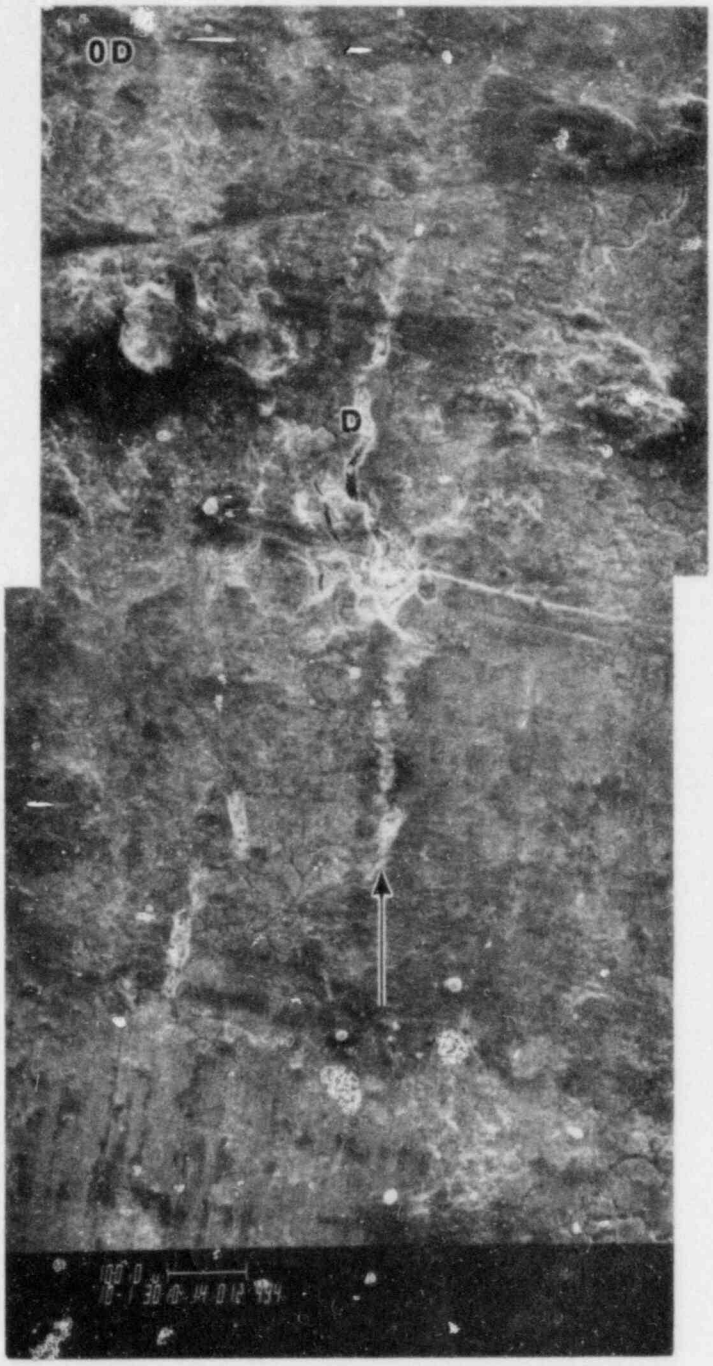

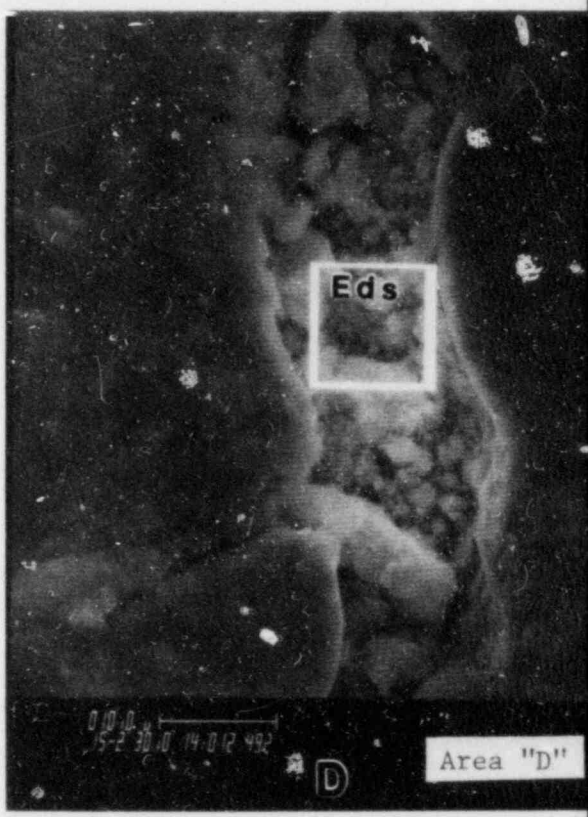

Tube Axis

Crack-like Feature on OD Surface

Also Available On
Aperture Card

Figure 2-23. SEM Micrographs of Tube B73-8 Area 5

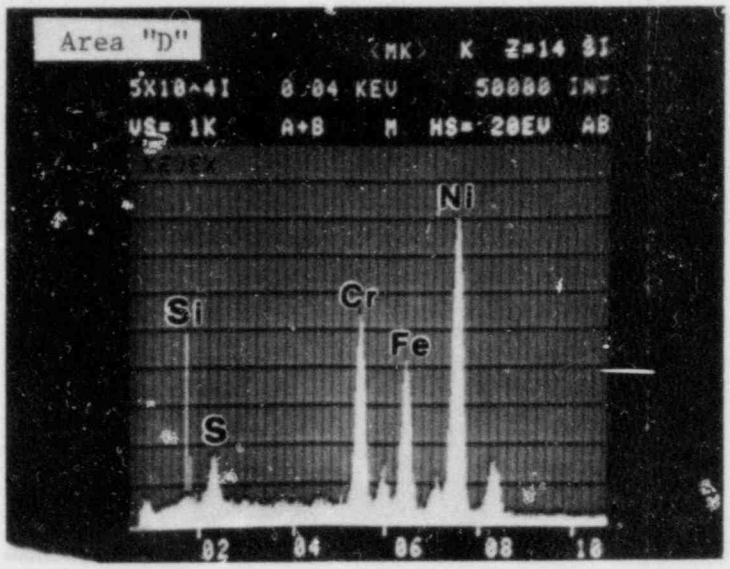

Tube Axis

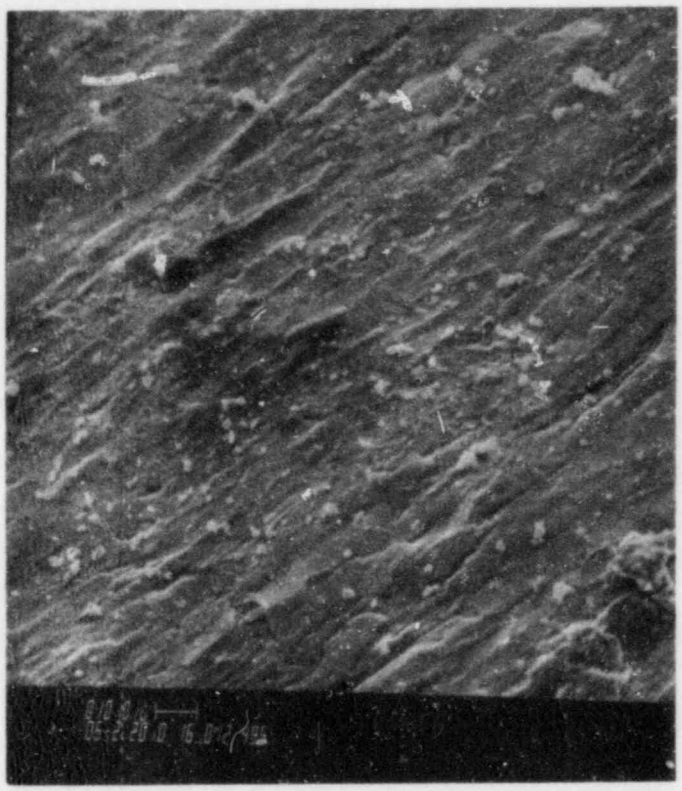

Typical ID Surface

Tube Axis

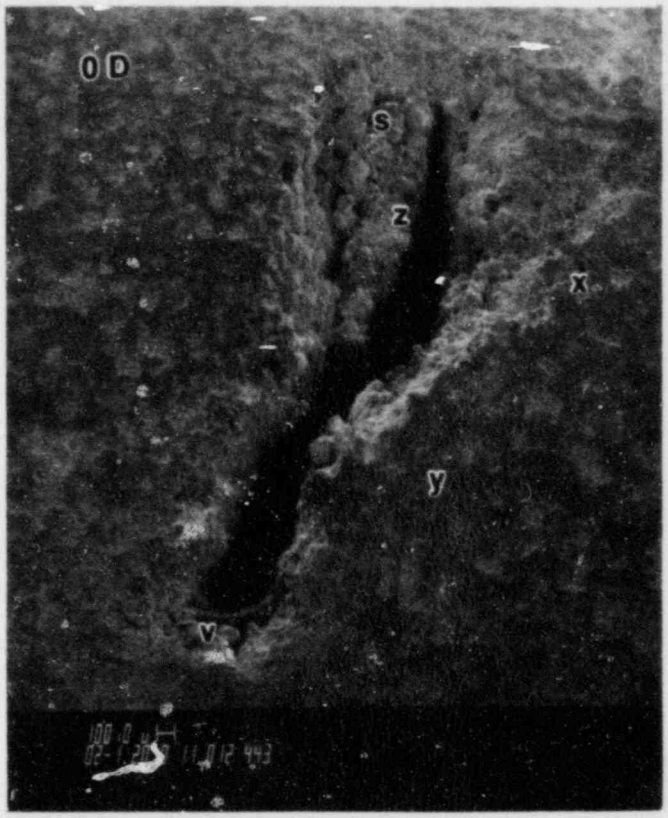

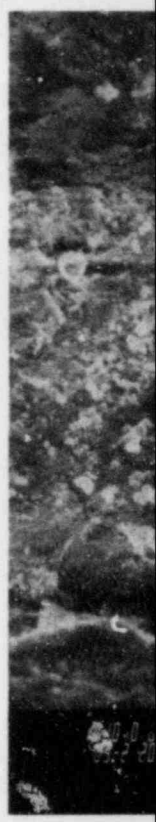

100% Through-Wall Circumferential Intergranular Hole

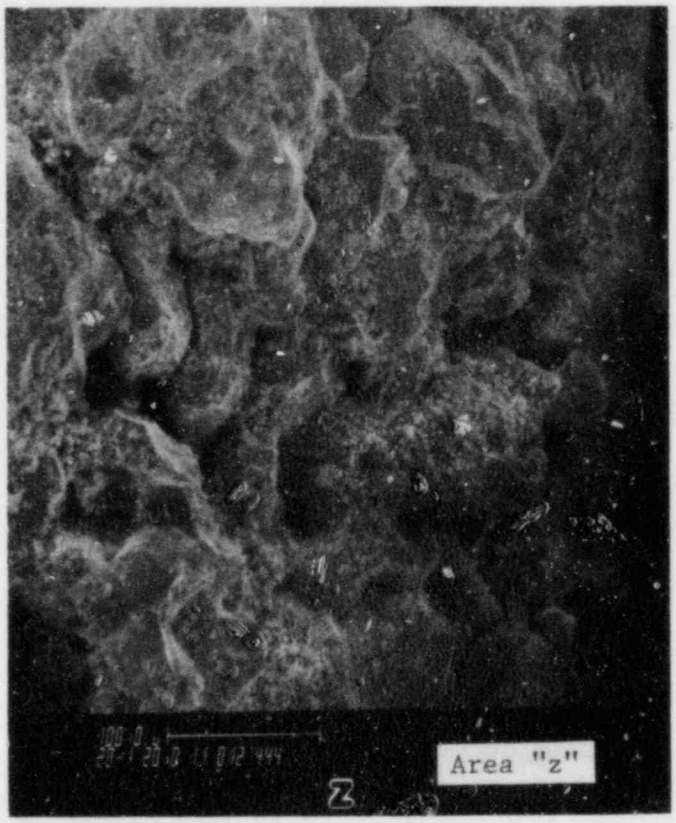

Crack Surface Deposits

Figure 2-24. SEM Micrographs of Tube B73-8 Area 6

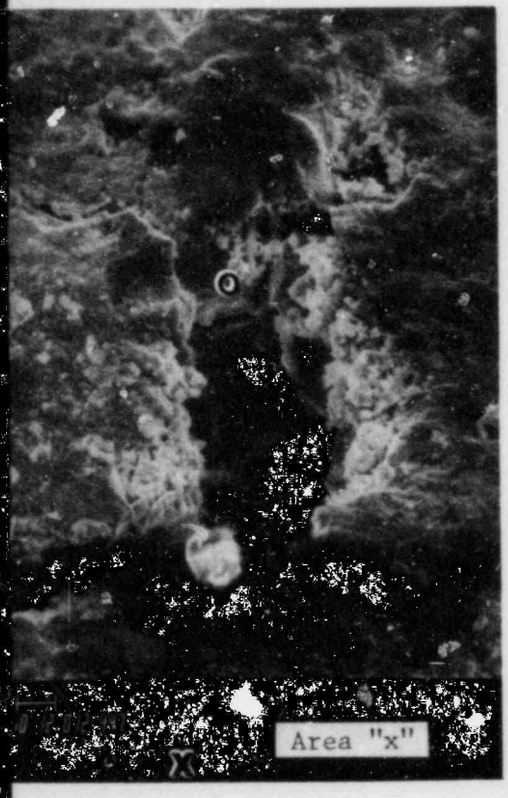

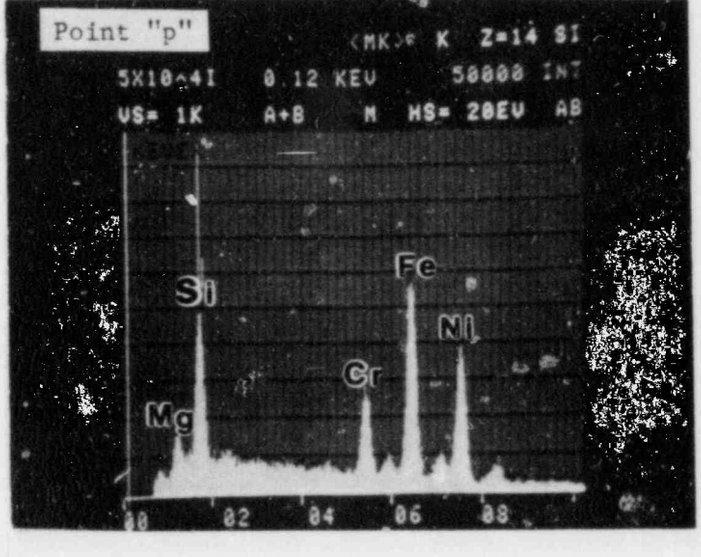

Also Available On Aperture Card

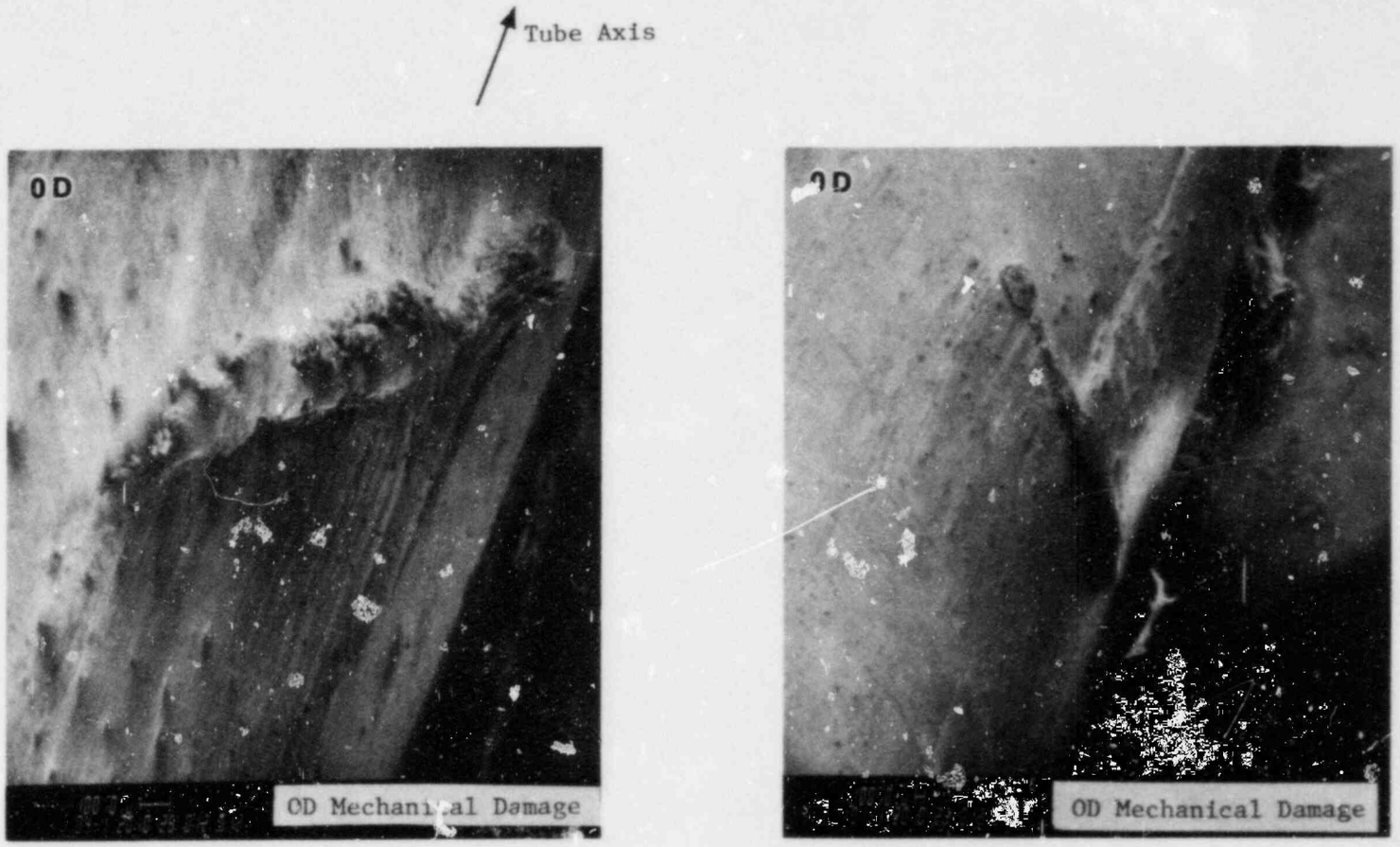

Figure 2-25. SEM Micrographs of Tube B112-19 Area 1

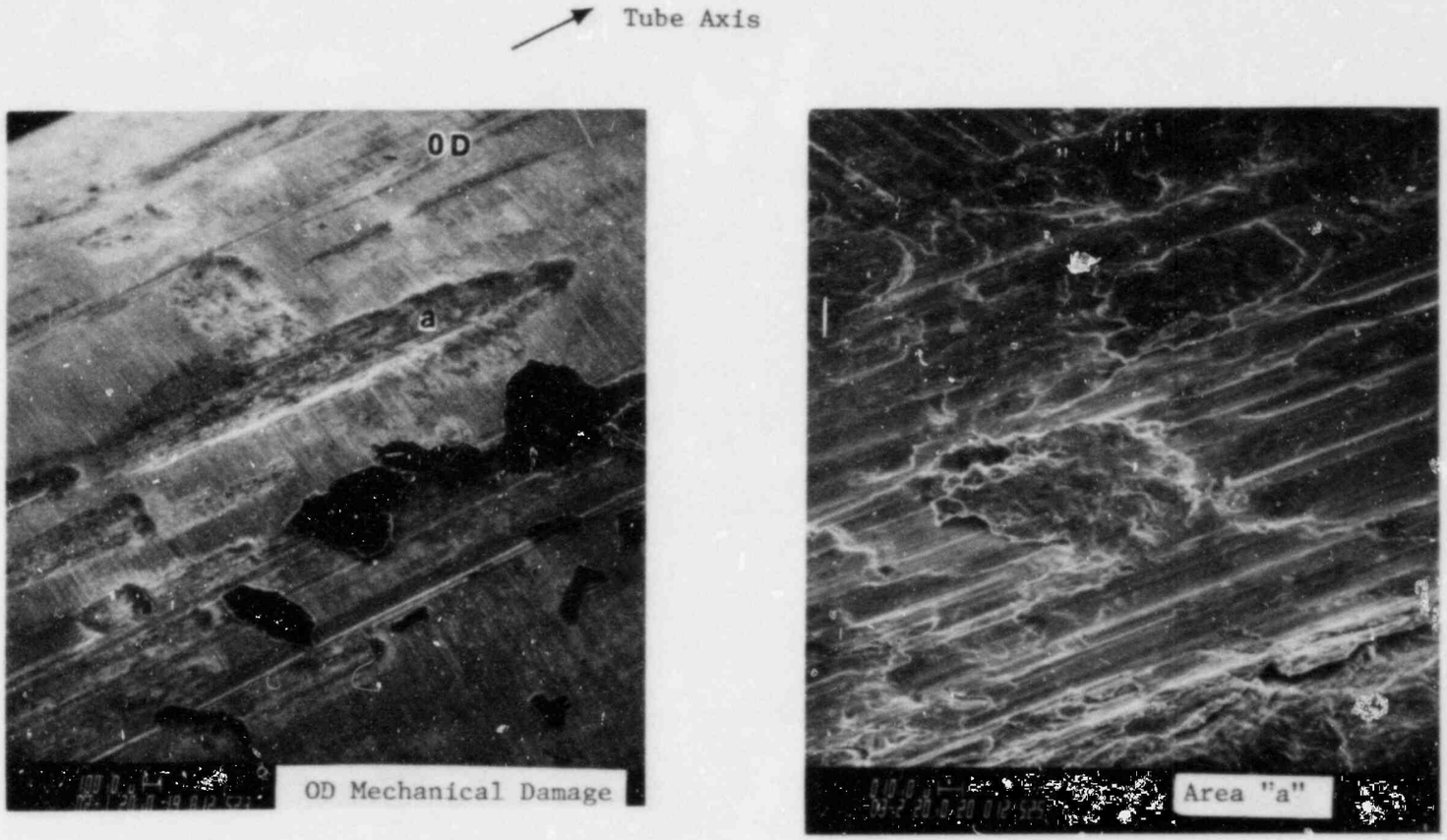

Figure 2-26. SEM Micrographs of Tube B112-19 Area 1 (After Cleaning)

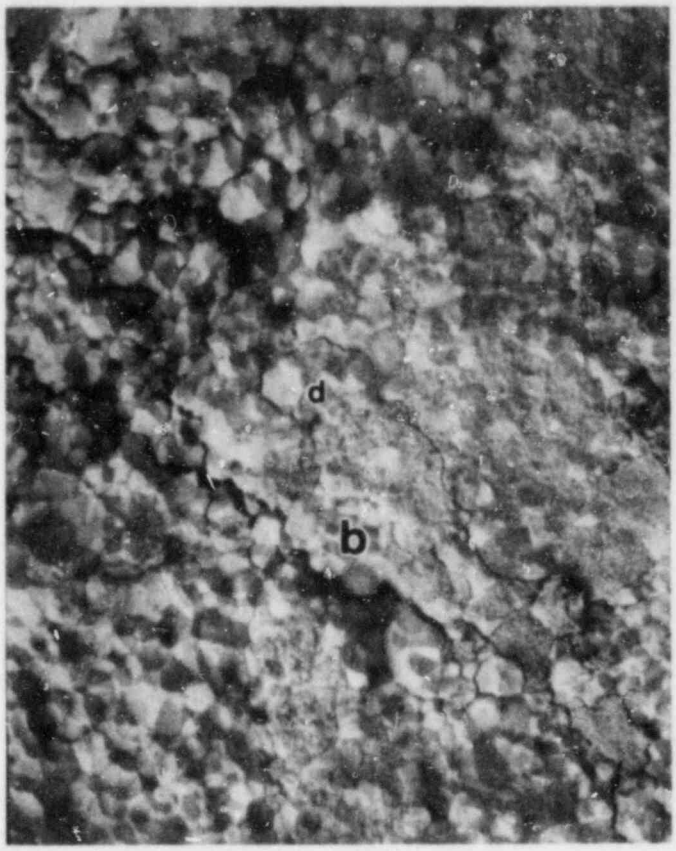

Area "b" (100X)

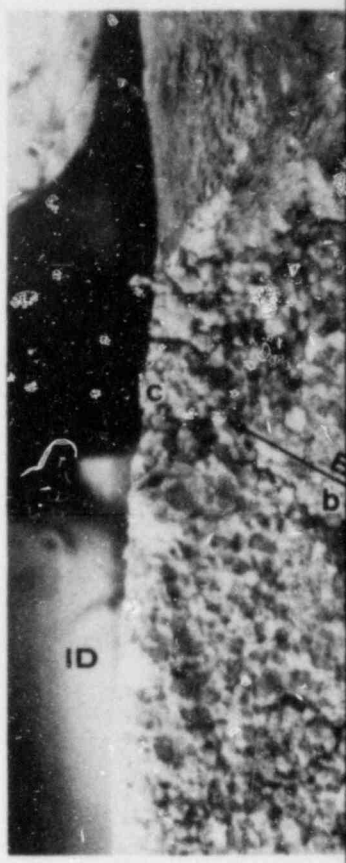

Locato
EMP

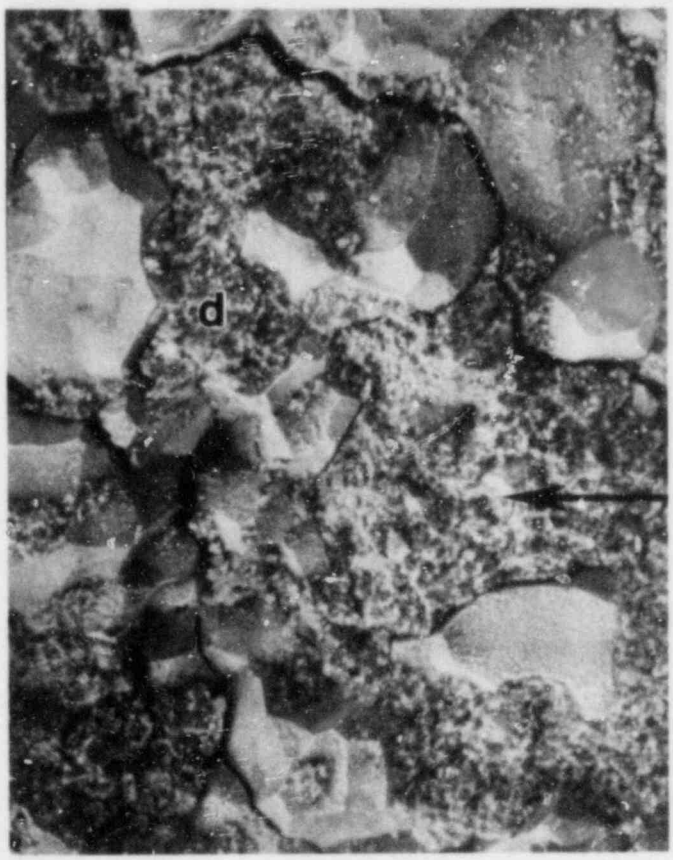

Crack Surface Deposits

Area "d" (500X)

Figure 2-27. SEM Mic
B73-8 A

Also Available On Aperture Card

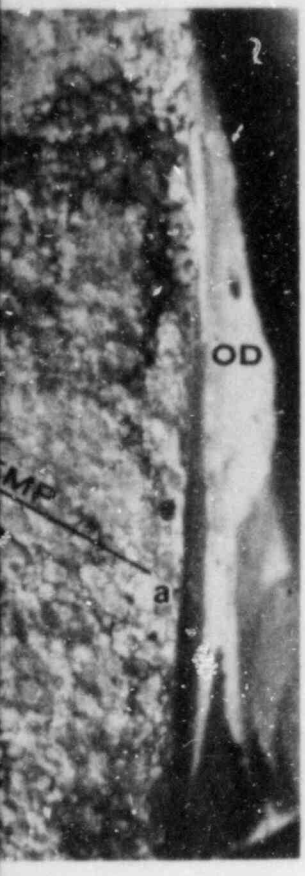

(50X)
ath

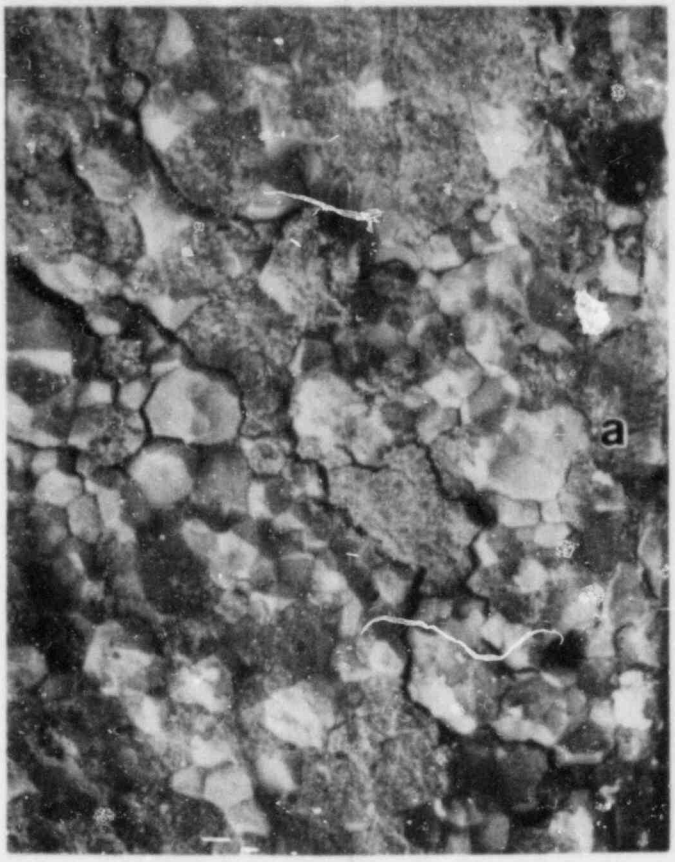

Area "a" (200X)

Clean Crack Surface

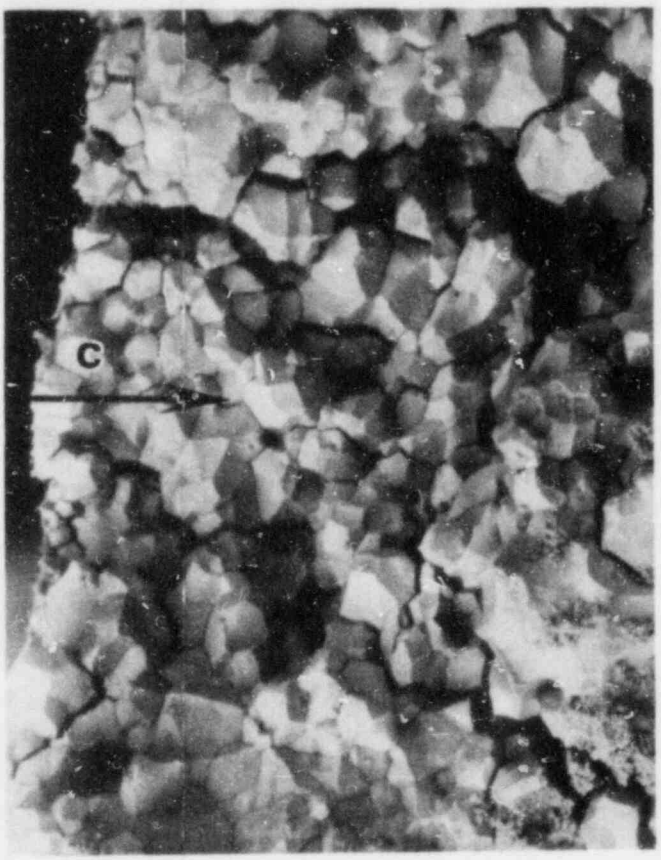

ographs of Tube
ea 1 Crack Surface

Area "c" (200X)

Tube Ax

Intergranular Circumferential Crack
with Extensive Branching

is

Figure 2-28. SEM Micrographs of Tube B73-8 Area 3 (After Bending)

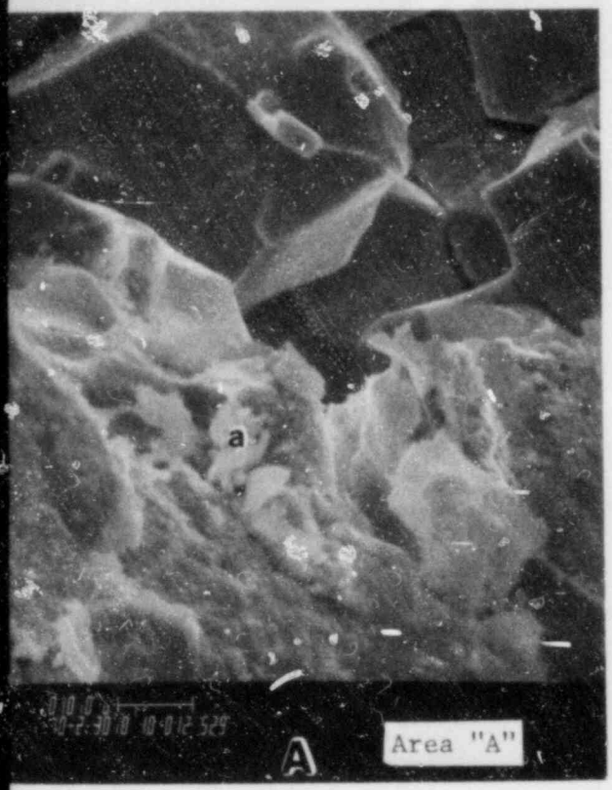

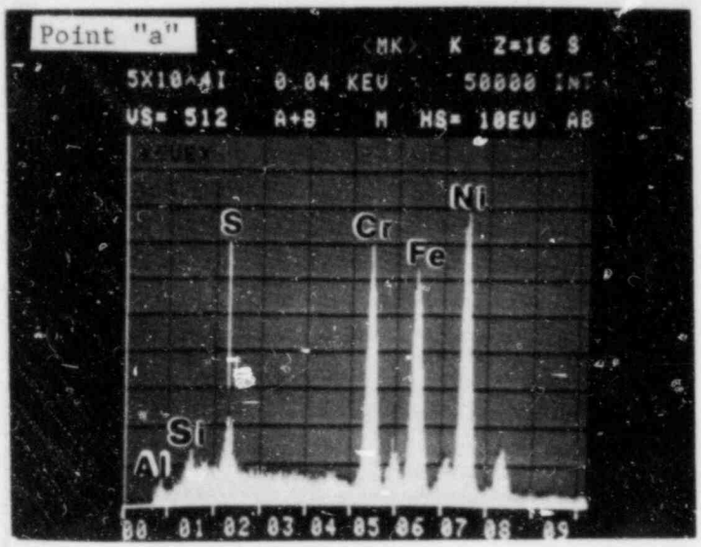

EDX Spectrum Showing Presence of Sulfur in Deposit

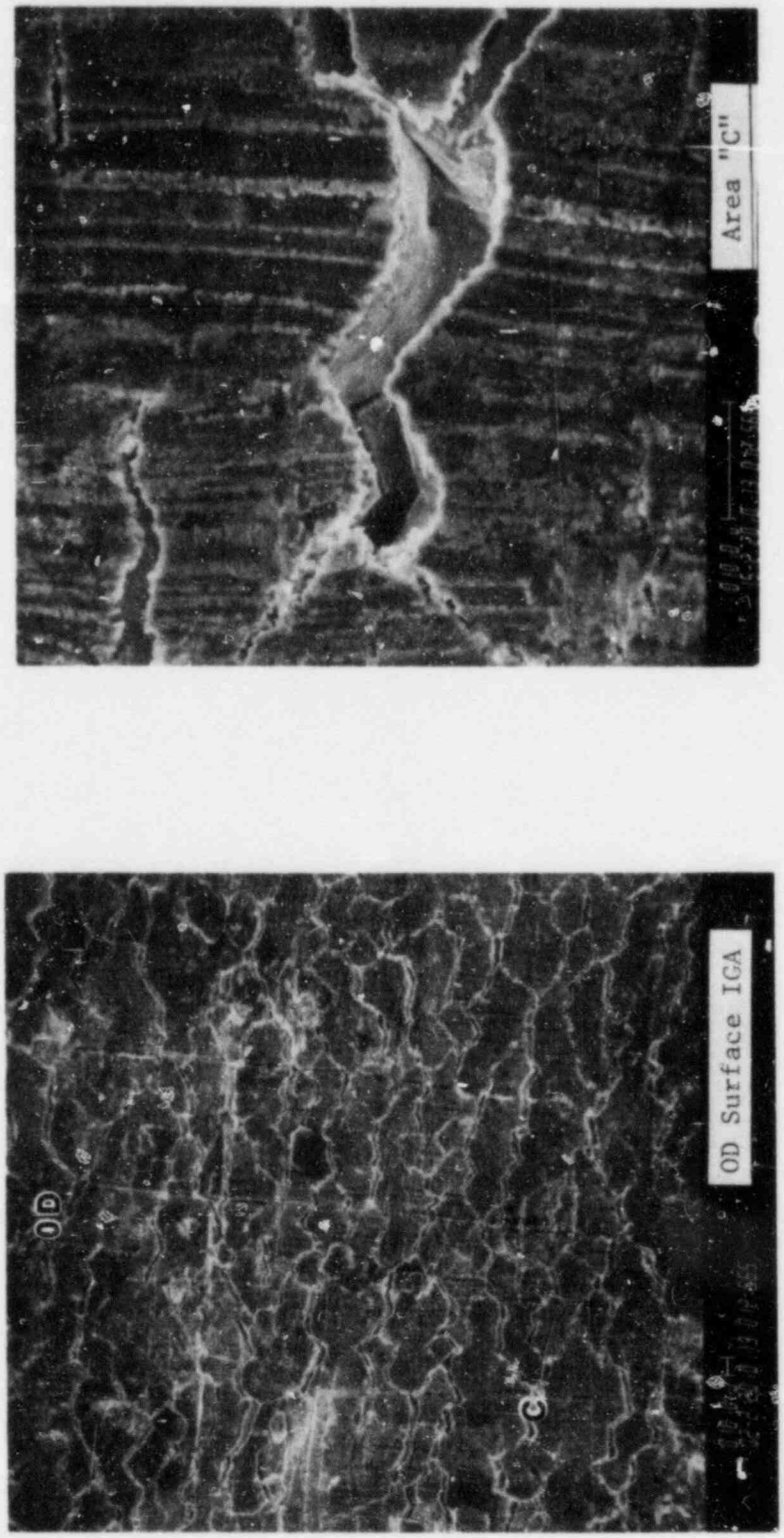

Figure 2-29. SEM Micrographs of Tube B73-8 Area 8 (After Bending)

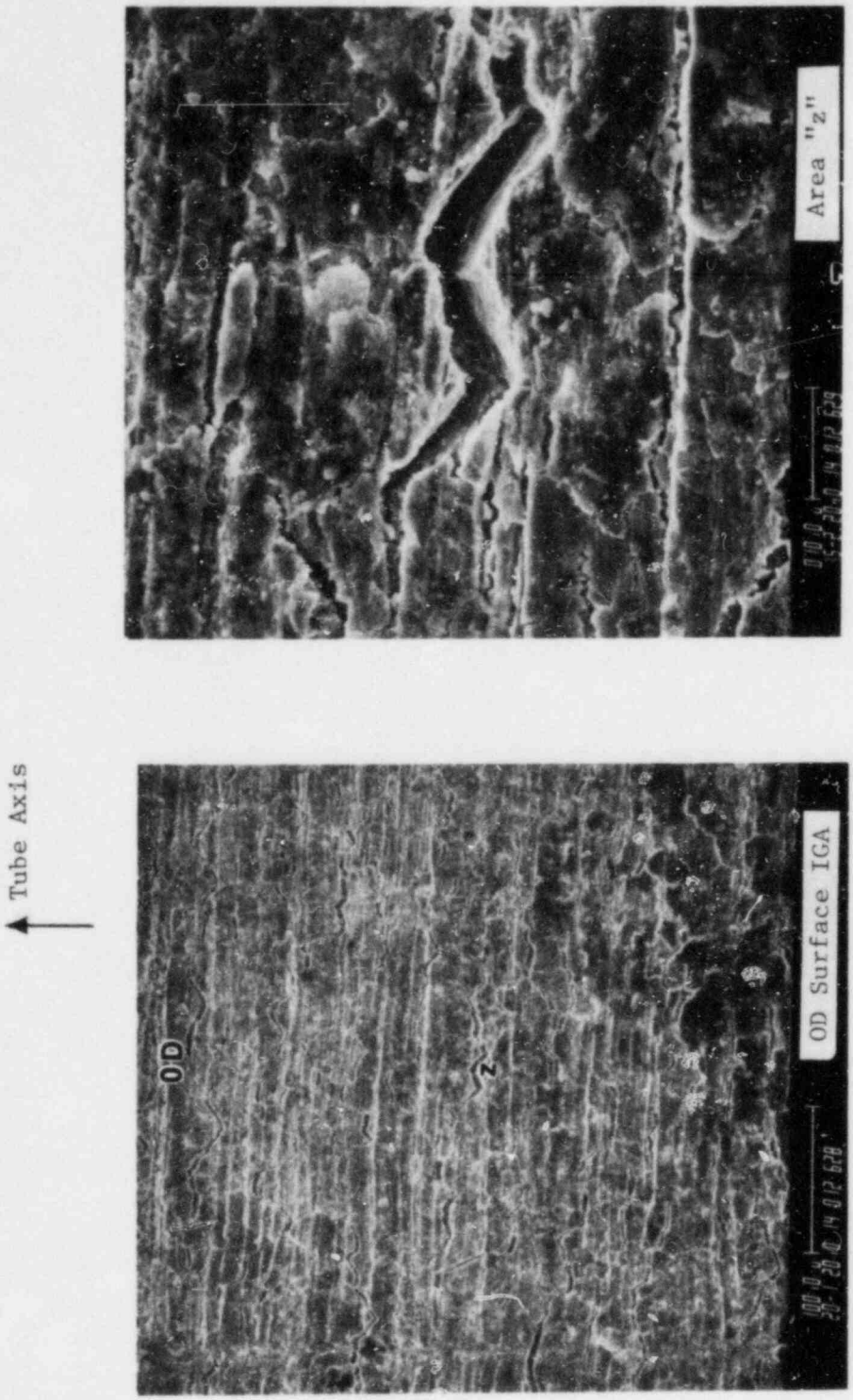

Figure 2-30. SEM Micrographs of Tube B73-8 Area 9 (After Bending)

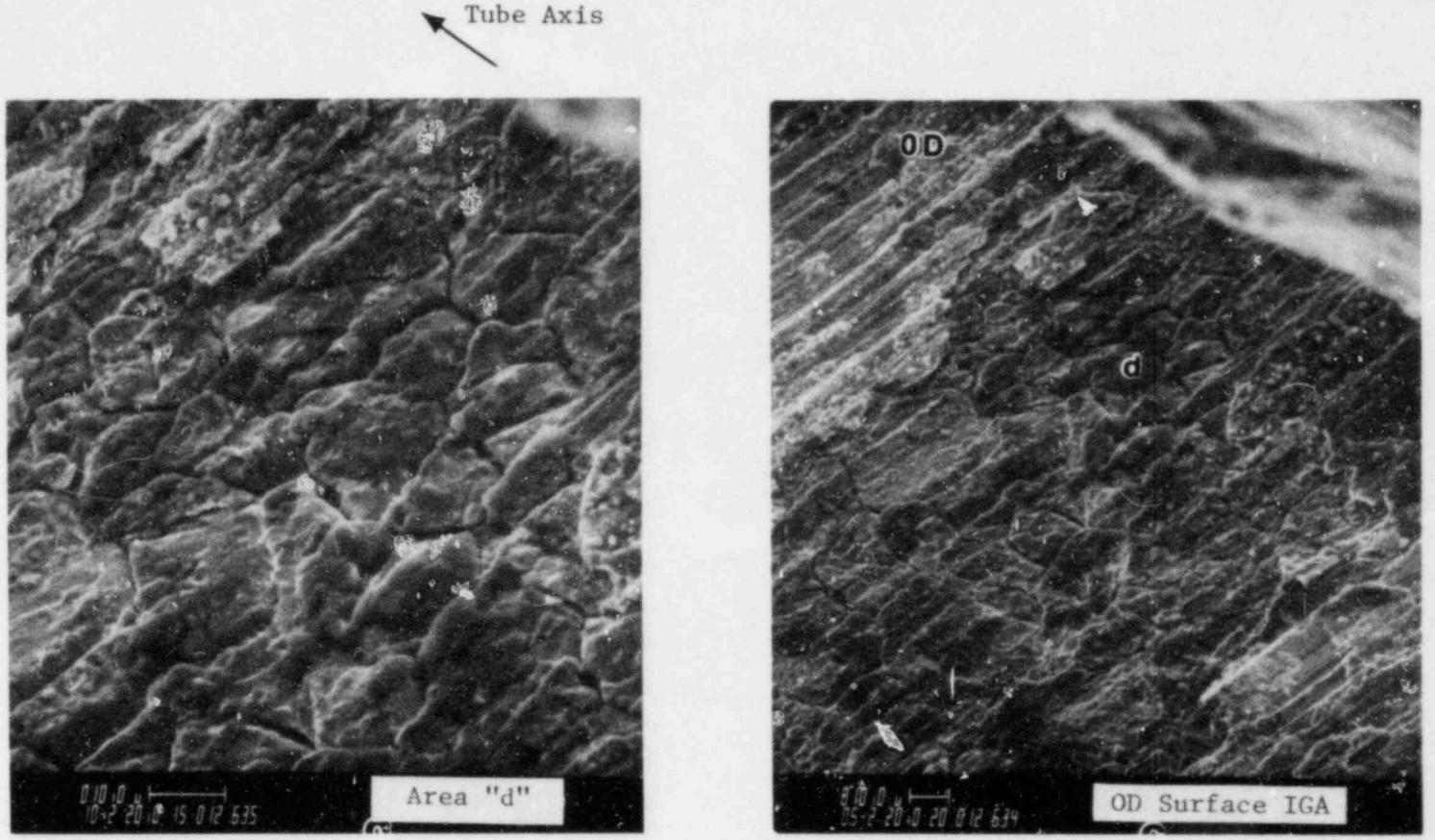

Figure 2-31. SEM Micrographs of Tube B73-8 Area 9 (After Cleaning)

Tube Axis

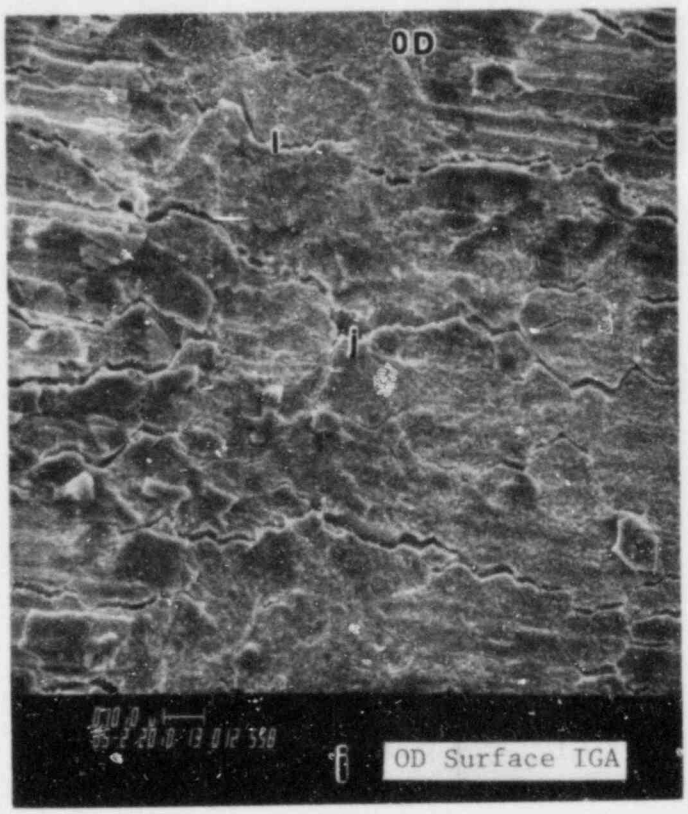

OD Surface IGA

Figure 2-32. SEM Micrographs of Tube B112-19 Area 1 (After Bending)

Also Available On
Aperture Card

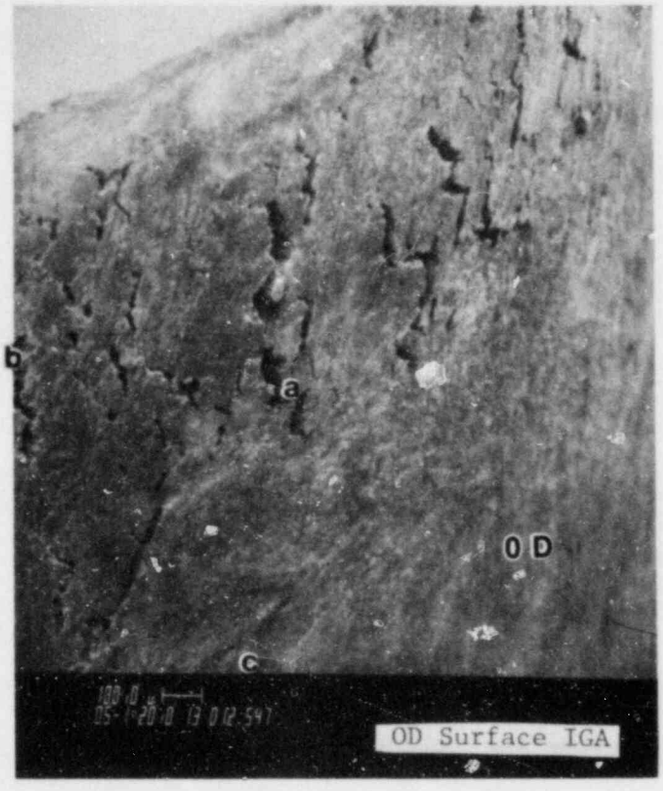

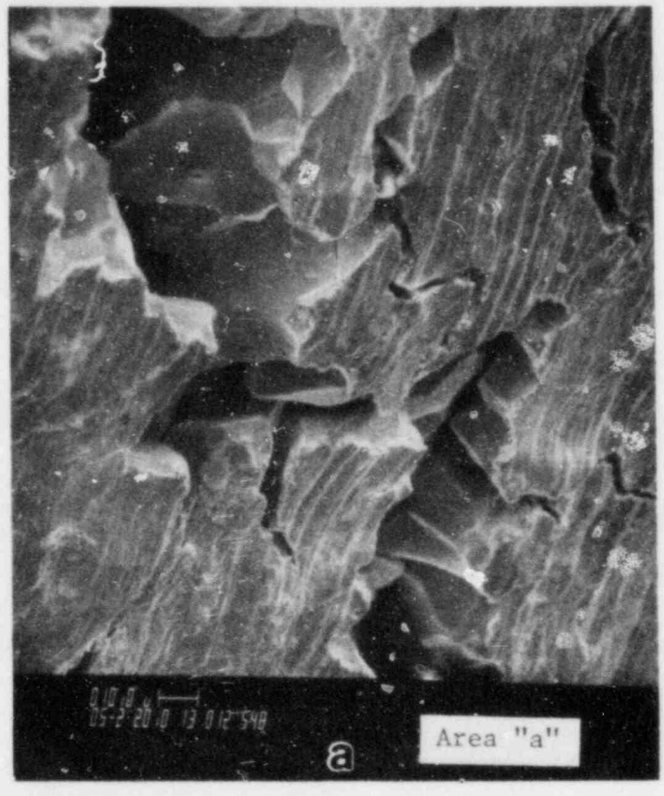

Figure 2-29. SEM Micrographs of Tube B112-19 Area 1 (After Bending)

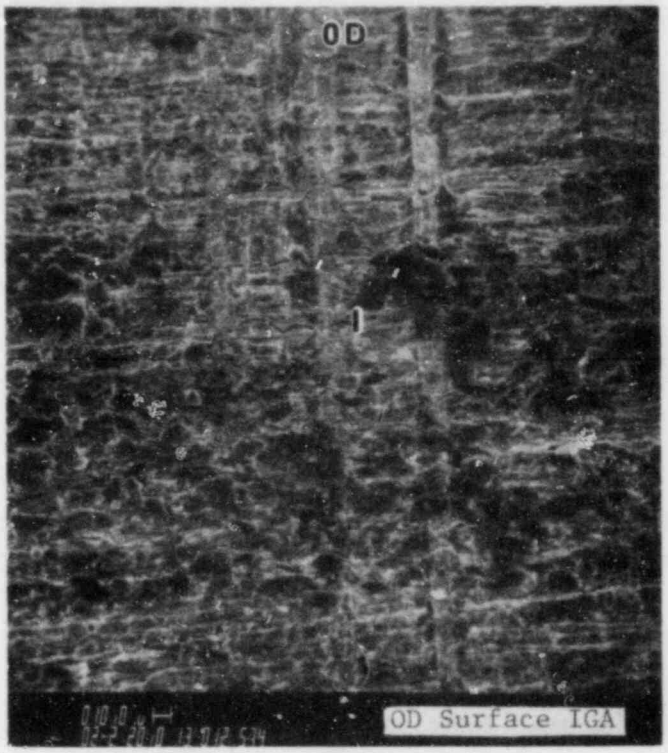

Tube Axis

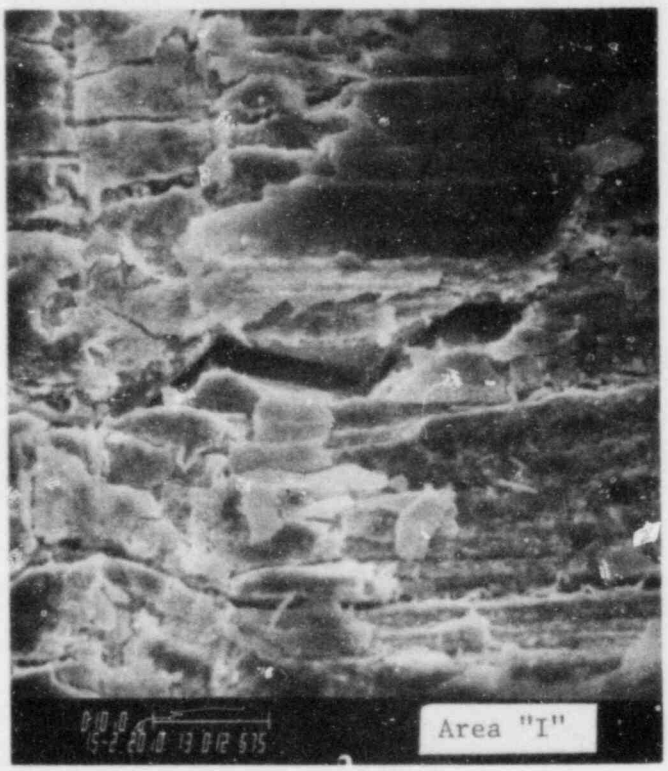

Figure 2-34. SEM Micrographs of Tube B112-19 Area 2 (After Bending)

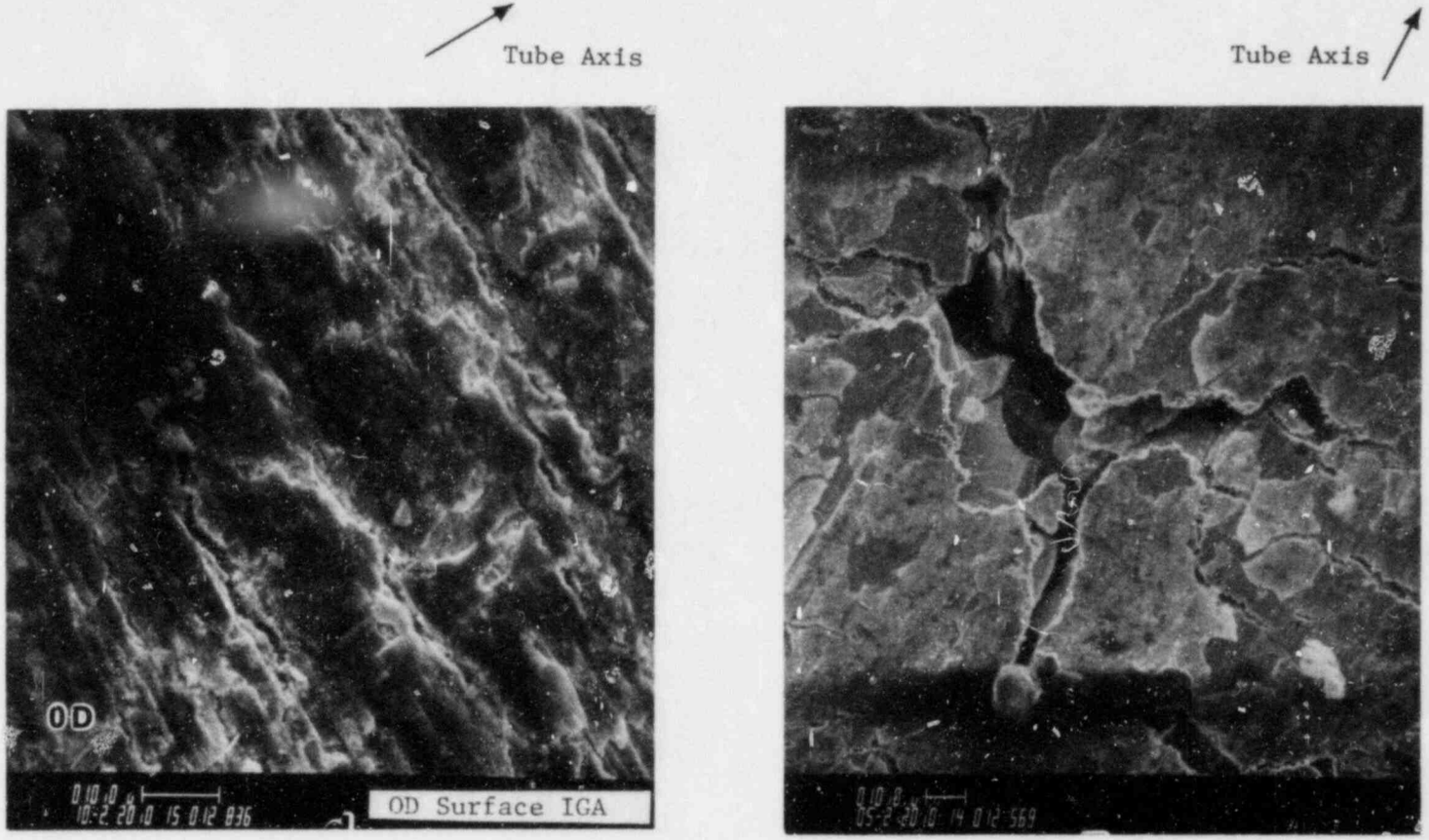

Figure 2-35. SEM Micrographs of Tube B112-19 Area 3 (After Bending)

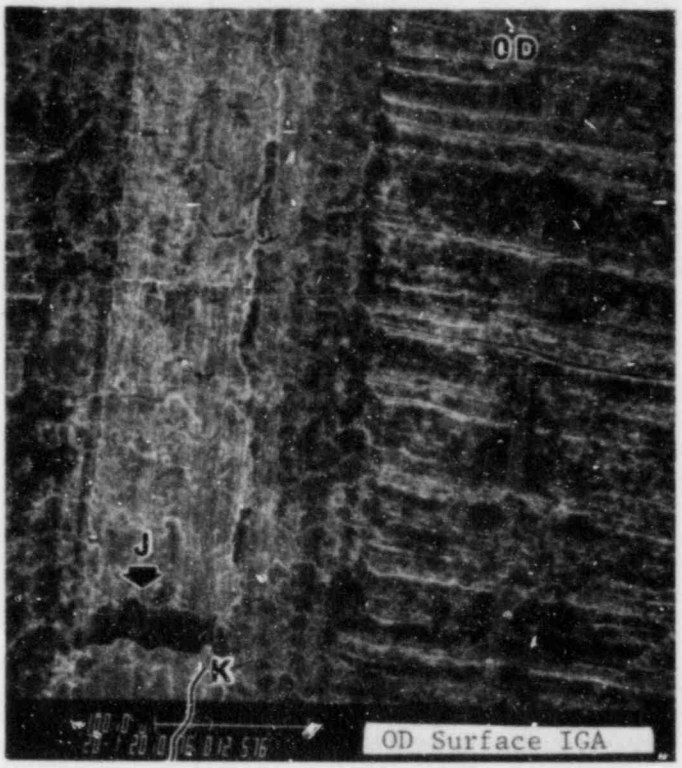

Tube Axis

Tube Axis

Figure 2-36. SEM Micrographs of Tube B112-19 Area 4 (After Bending)

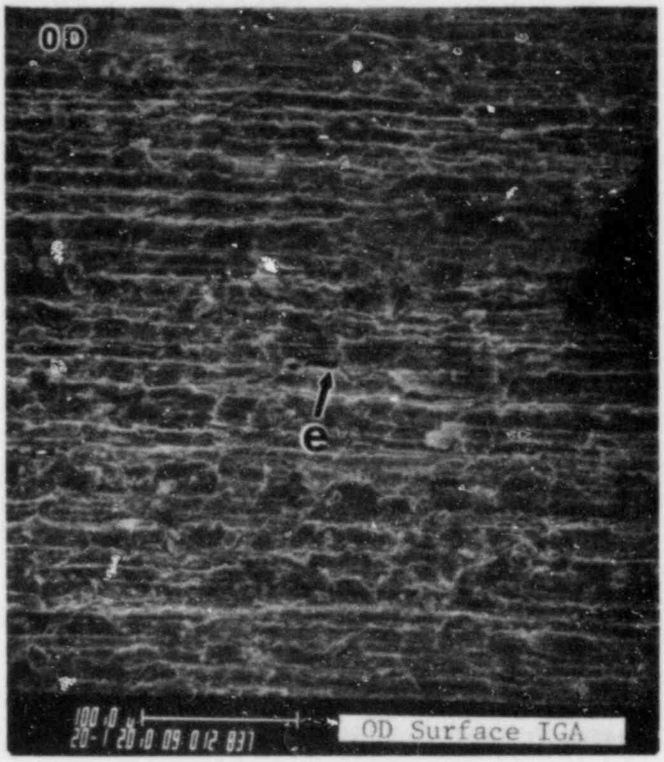

Tube Axis

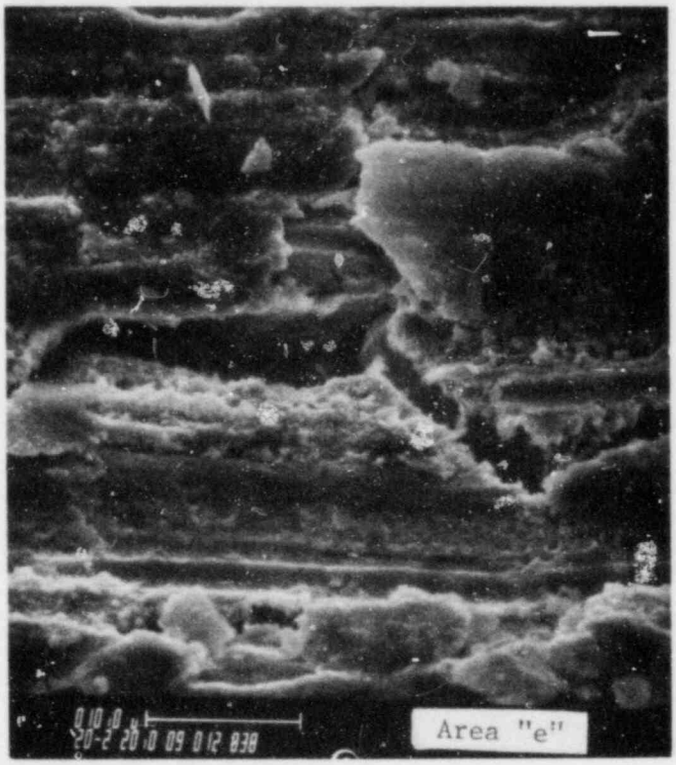

Figure 2-37. SEM Micrographs of Tube B112-19 Area 5 (After Bending)

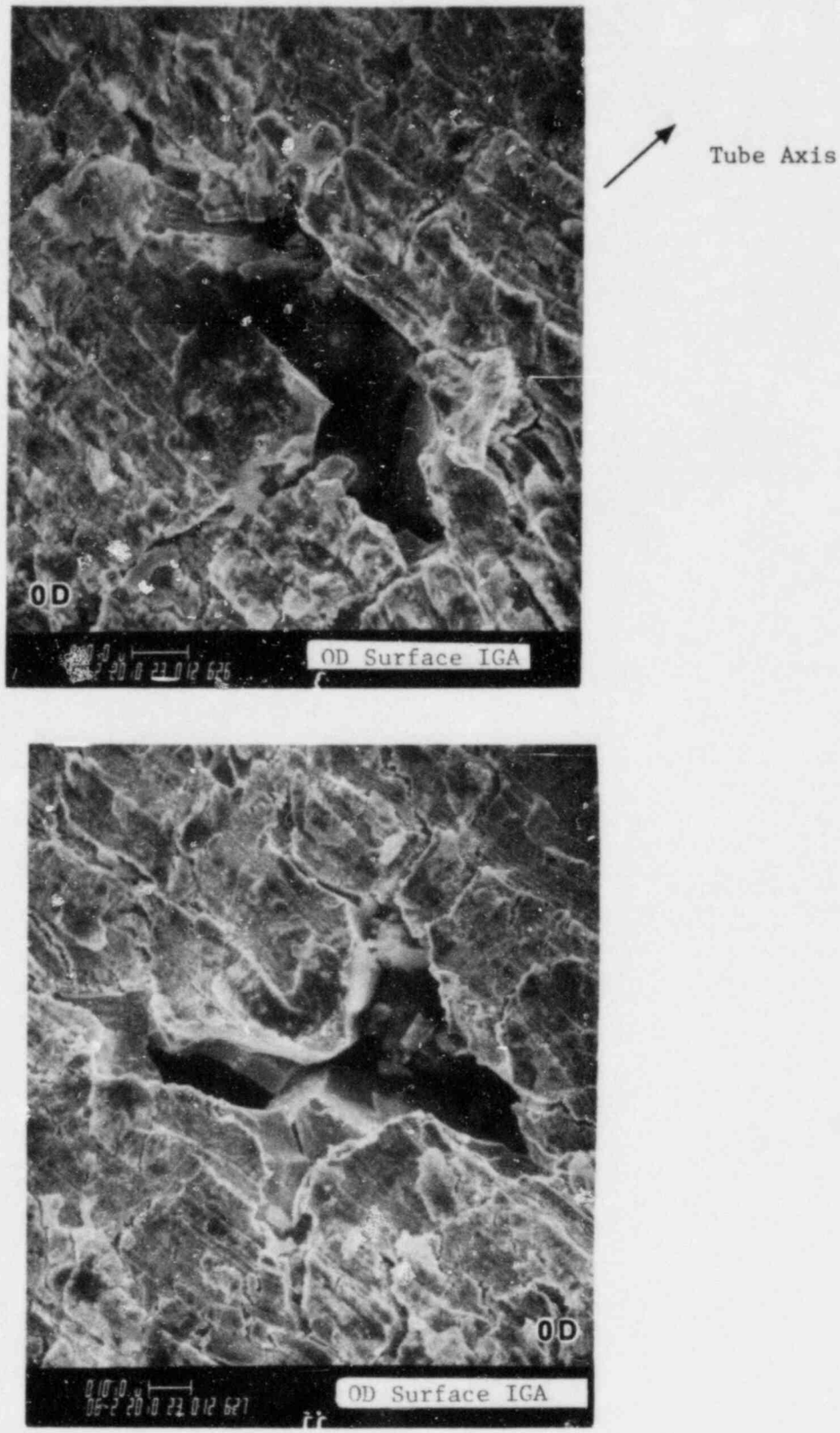

Figure 2-38. SEM Micrographs of Tube B112-19 Area 6 (After Bending)

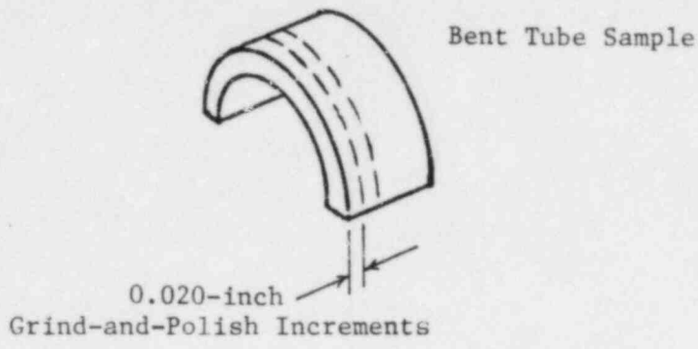

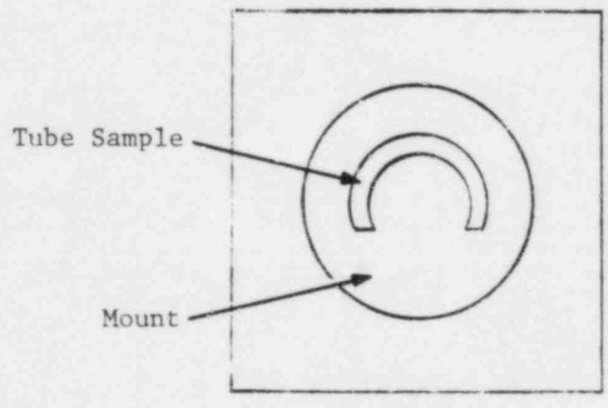

Mounted Metallographic Specimen

Figure 2-39. Longitudinal Metallographic Examination Technique

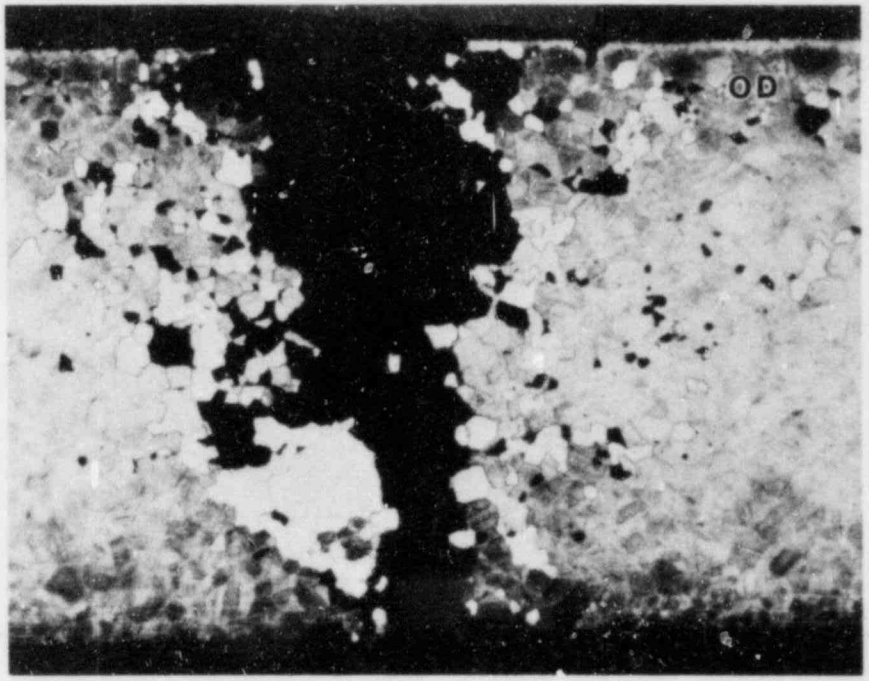

(75X)

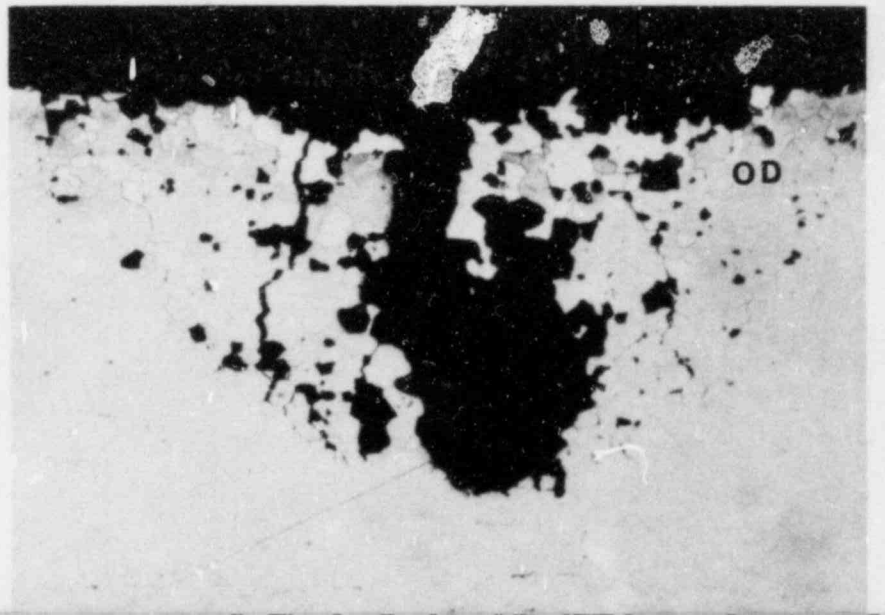

Figure 2-40. Micrographs of Tube B73-8 Area 2

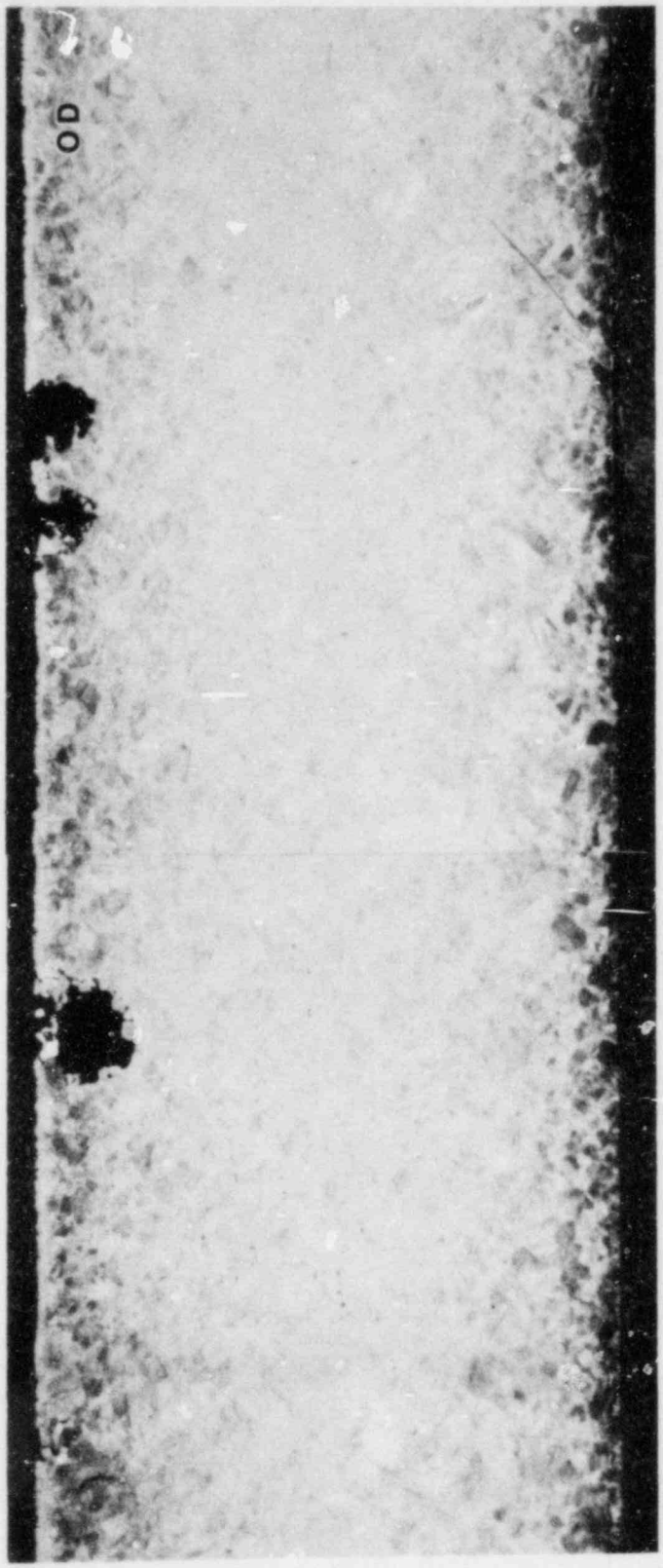

(75X)

(75X)

Successive Longitudinal Grinding Steps Through 100% Throughwall Circumferential Crack

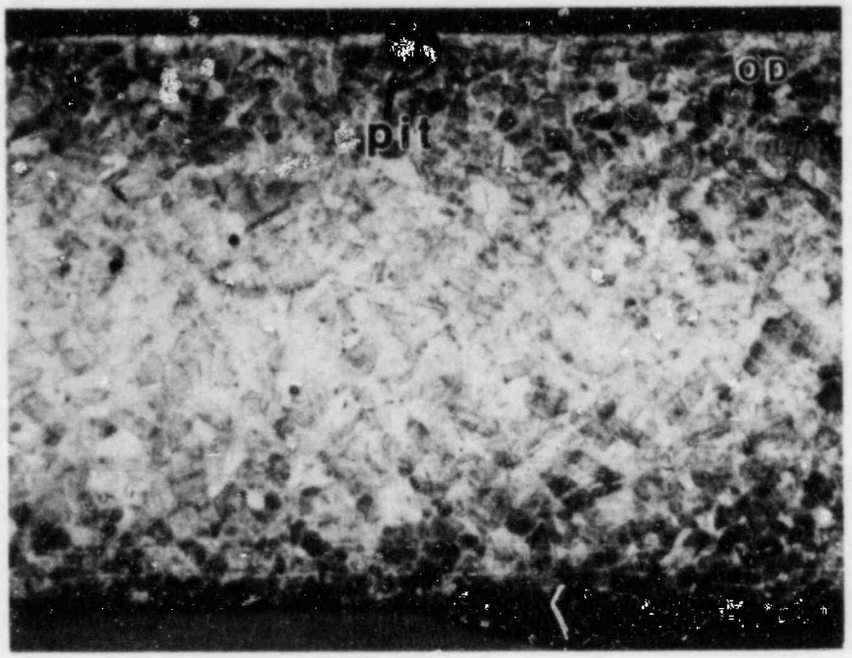

(75X)

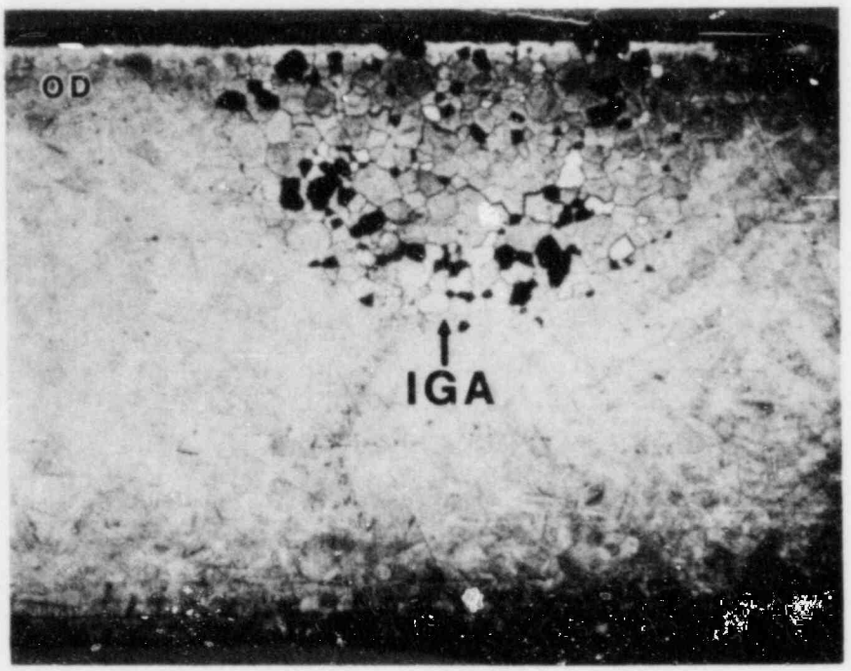

Figure 2-41. Micrographs of Tube B73-8 Area 2

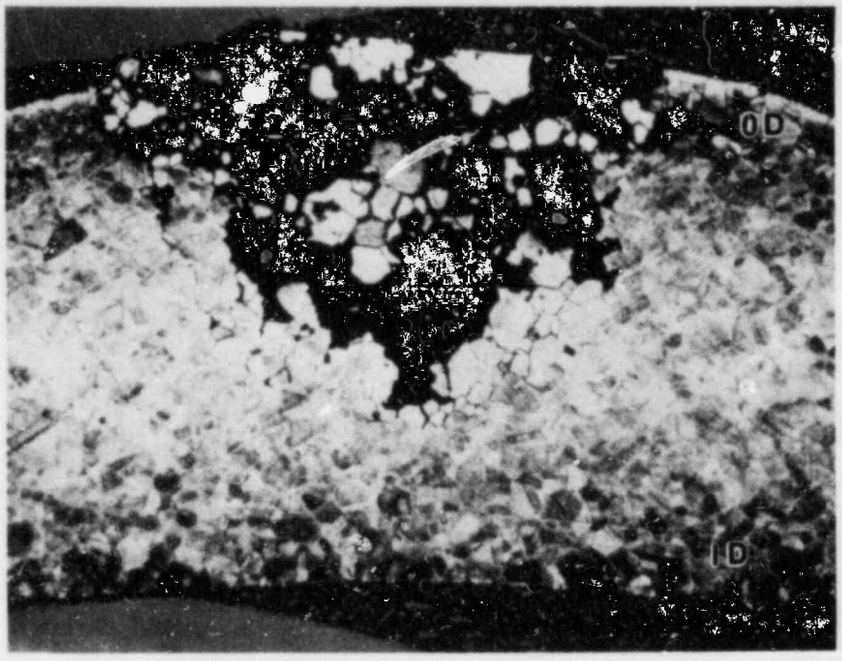

70% Throughwall Intergranular
Circumferential Crack

(66.5X)

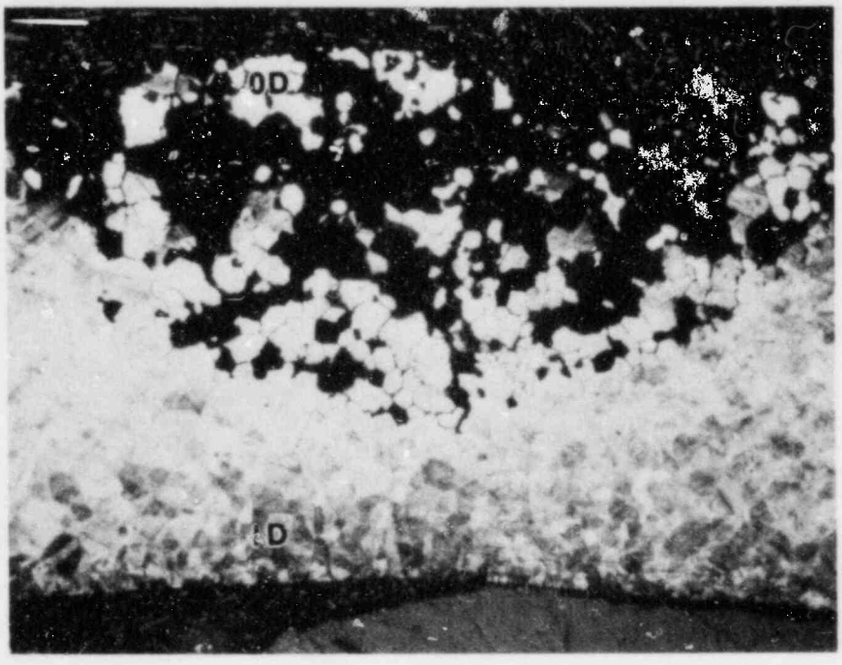

Figure 2-42. Micrographs of Tube B73-8 Area 4

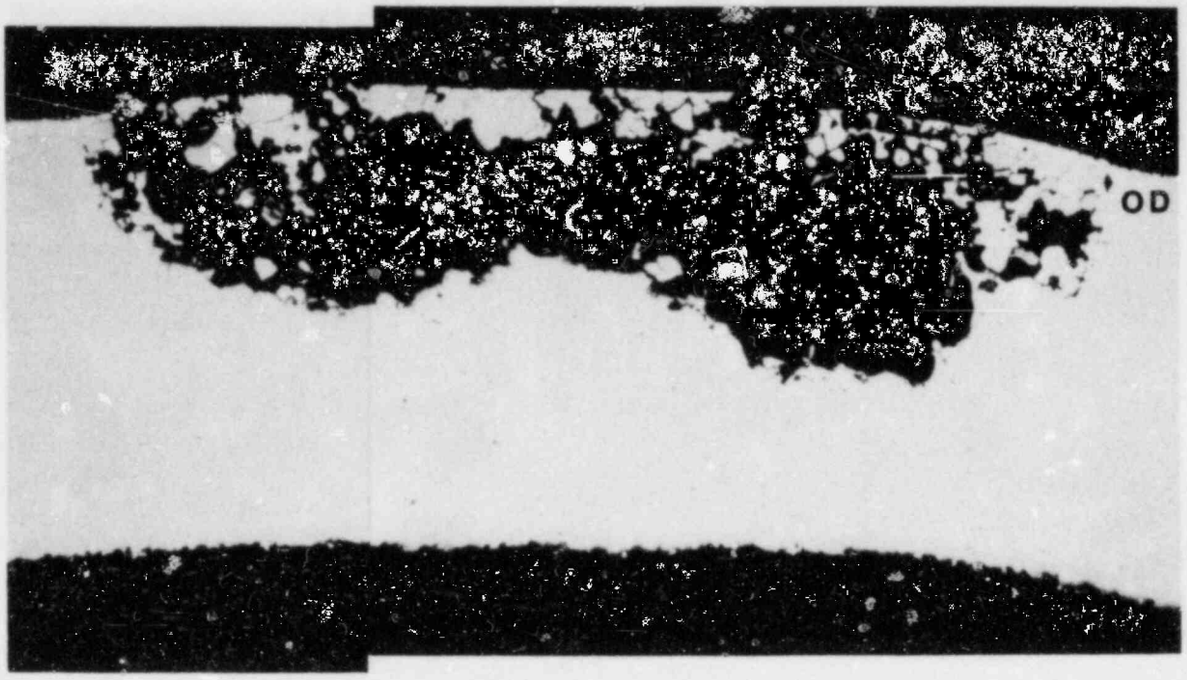

(50X)

60% Throughwall Intergranular
Circumferential Crack

Figure 2-43. Micrographs of Tube B73-8 Area 5

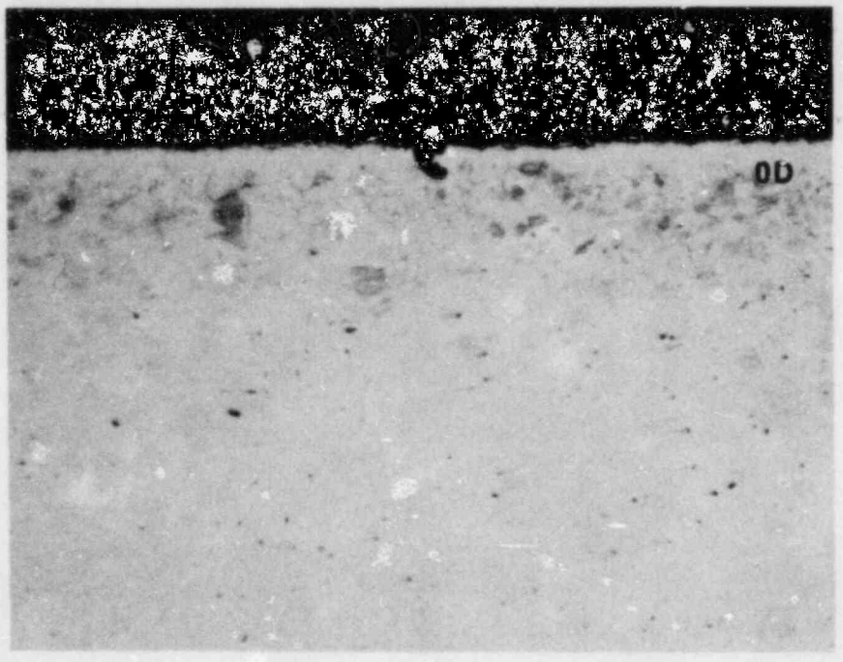

OD Pitting
(50X)

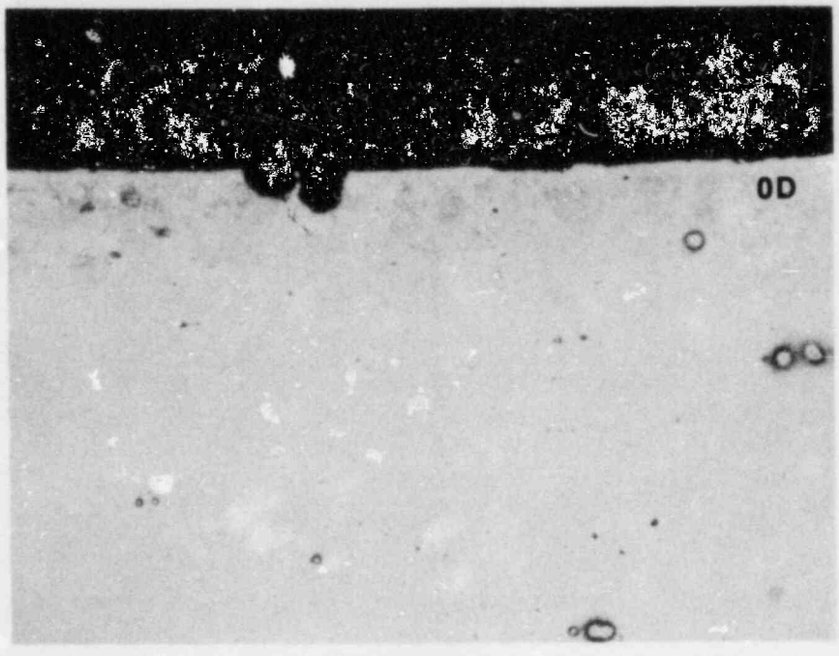

Figure 2-44. Micrographs of Tube B73-8 Area 7

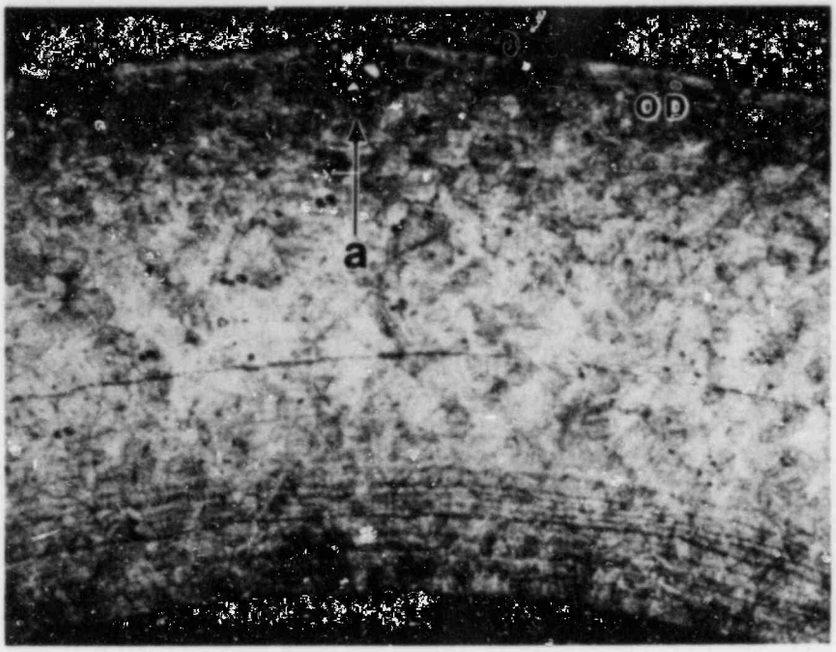

(75X)
OD Surface IGA

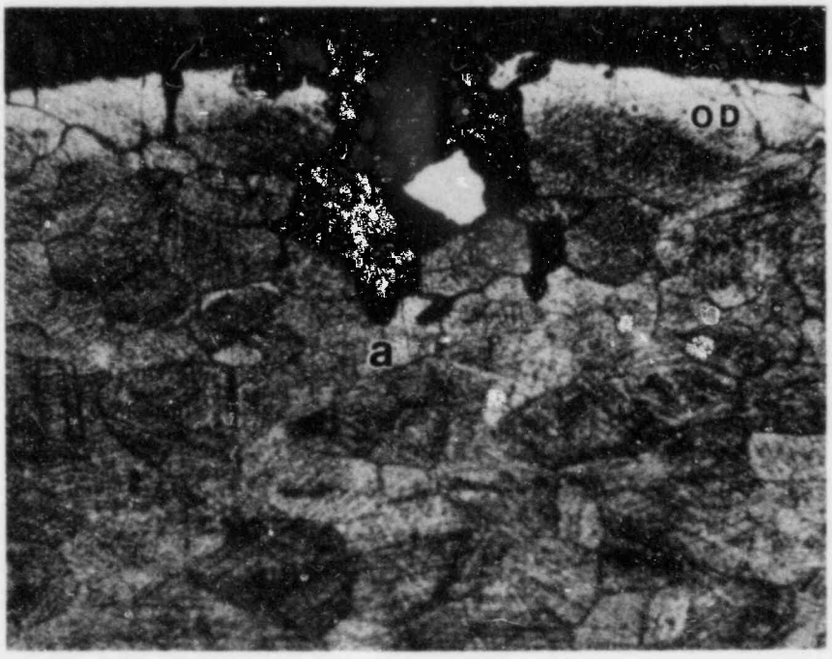

(532X)

Figure 2-45. Micrographs of Tube B73-8 Area 8

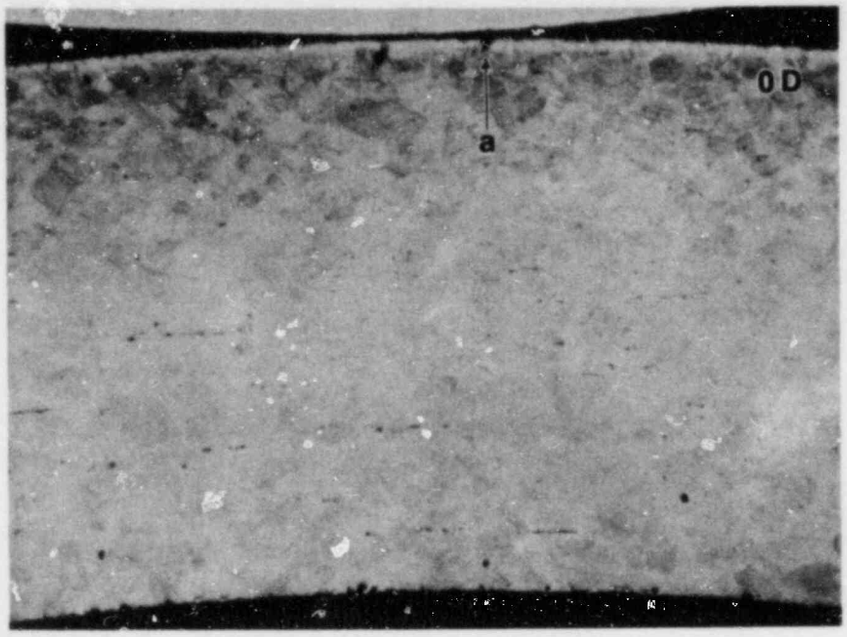

(66.5X)

OD Surface IGA

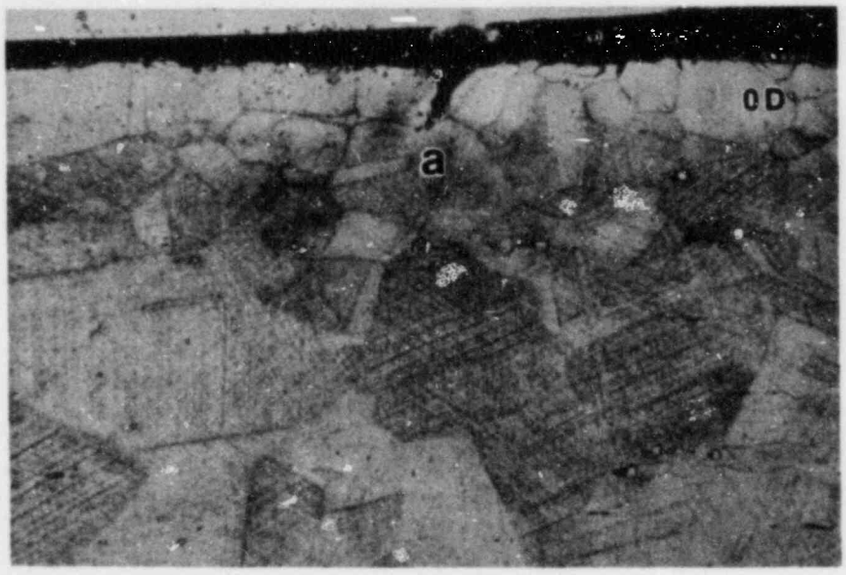

(400X)

Figure 2-46. Micrographs of Tube B73-8 Area 9

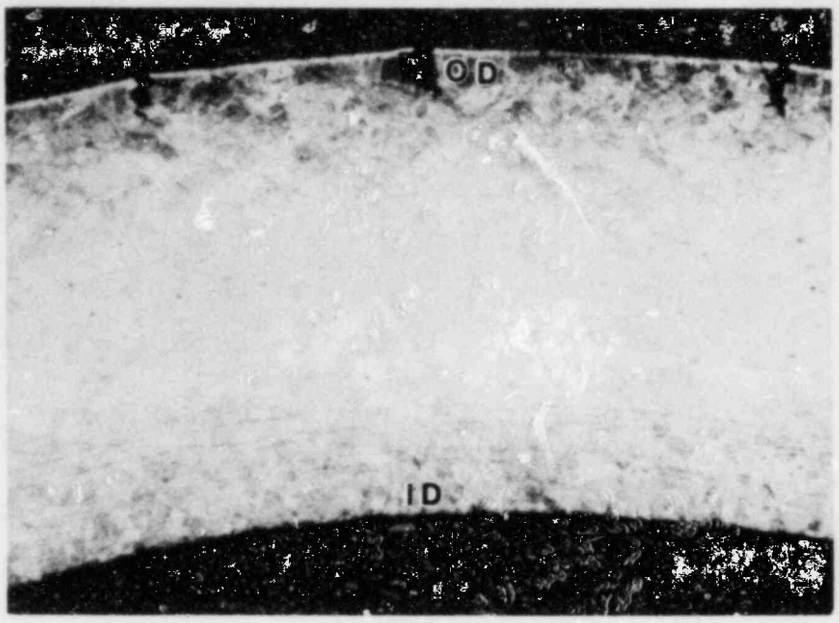

Successive Longitudinal Grind-and-Polish
Steps of General OD Surface IGA
(50X)

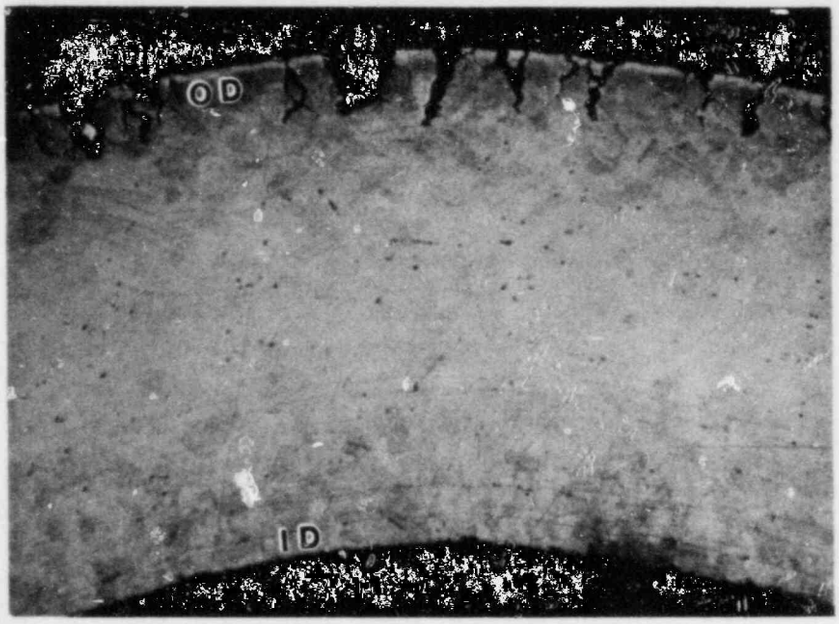

Figure 2-47. Micrographs of Tube B112-19 Area 1

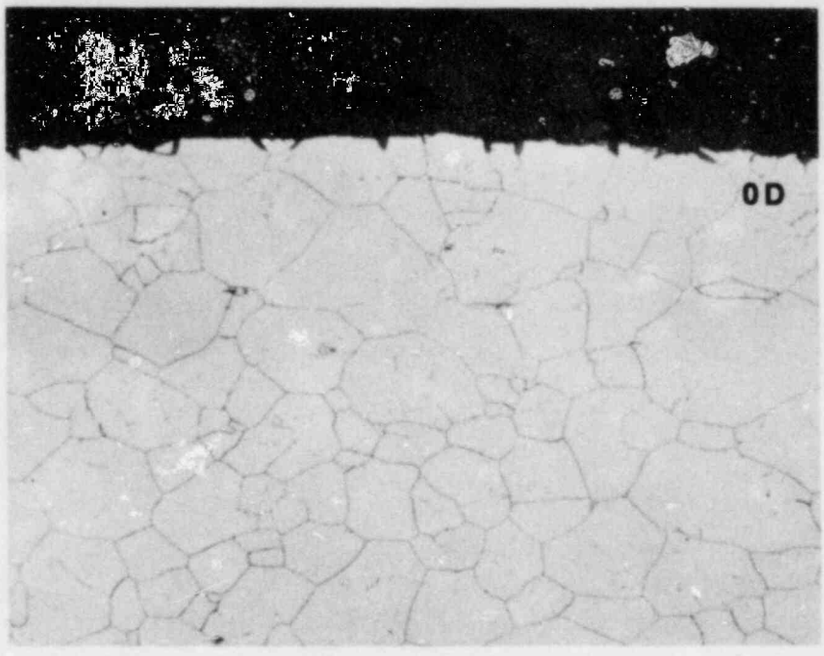

Area 3 (300X)
OD Surface IGA

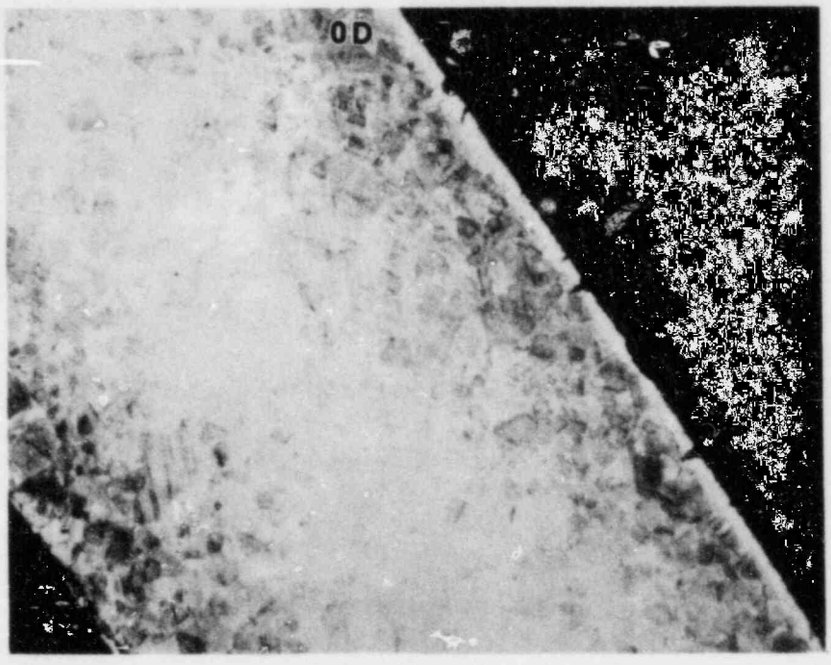

Area 2 (75X)

Figure 2-48. Micrographs of Tube B112-19 Areas 2 and 3

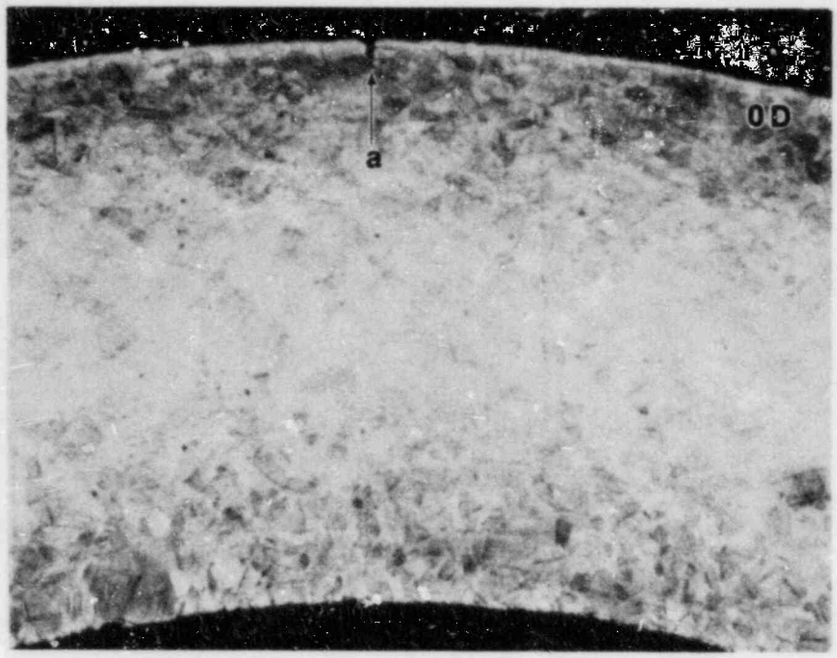

(66.5X)

OD Surface IGA

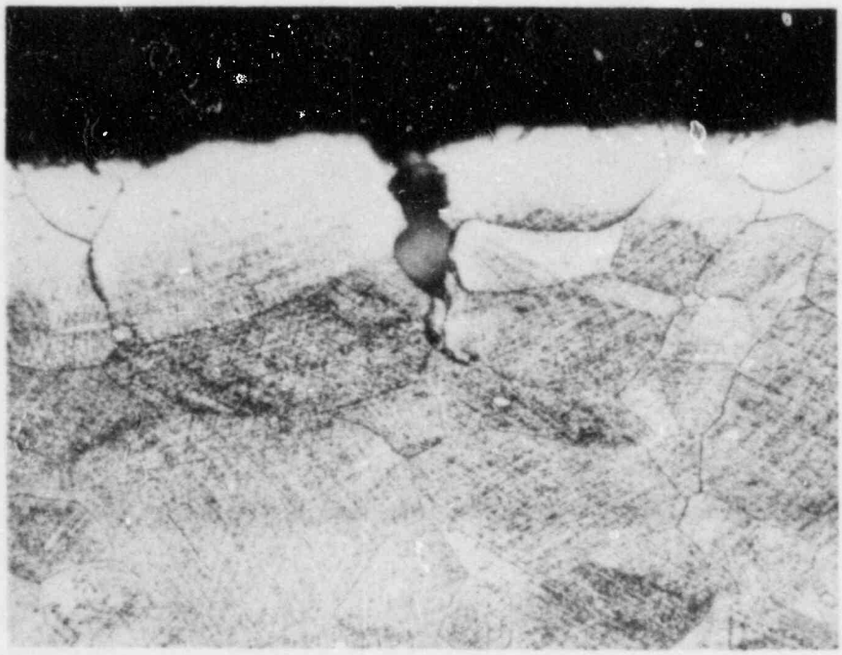

(532X)

Area "a"

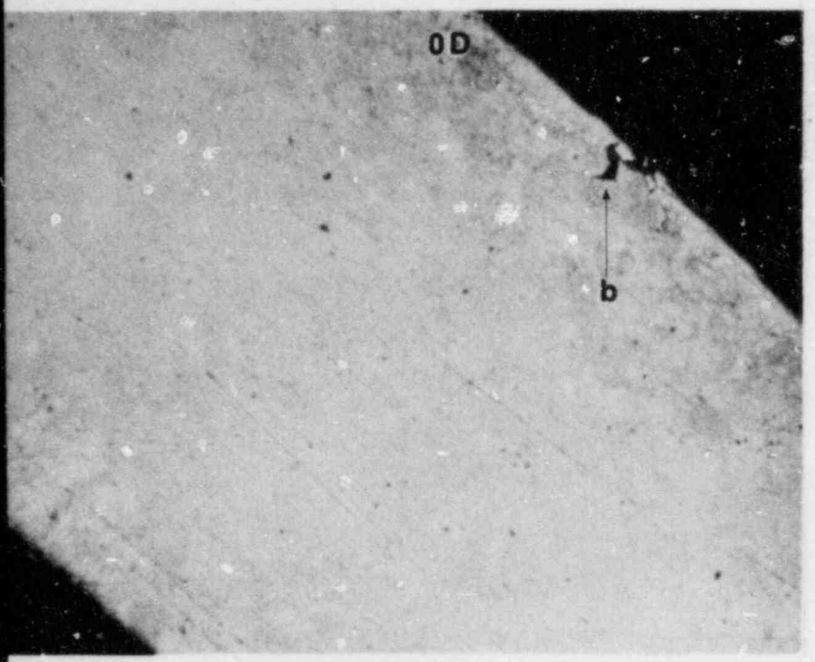

(100X)

Figure 2-49. Micrographs of Tube B112-19 Area 4

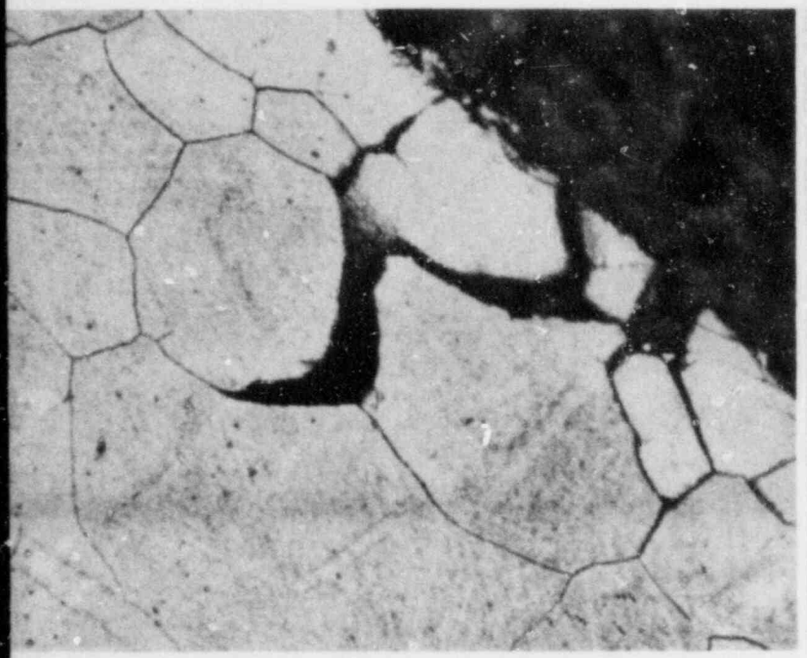

(750X)
Area "b"

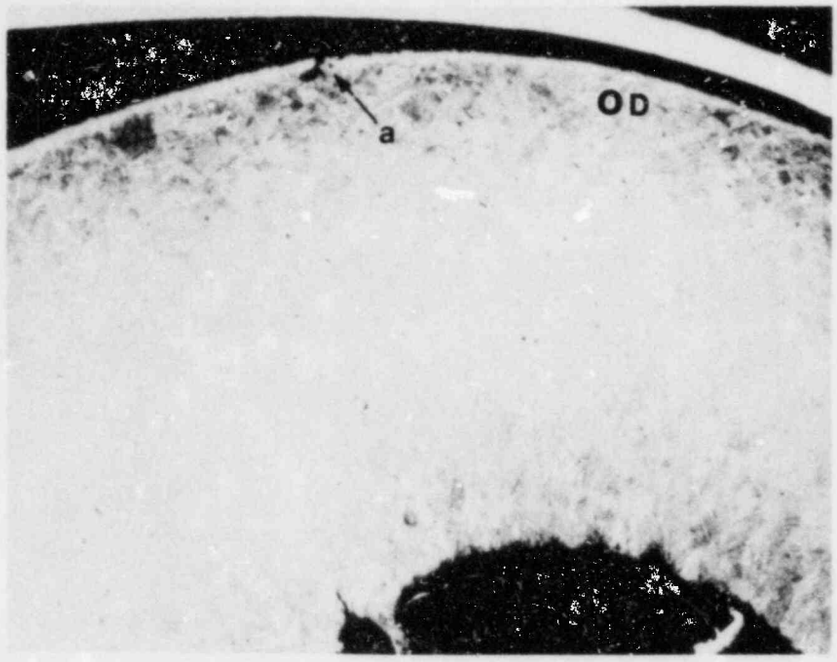

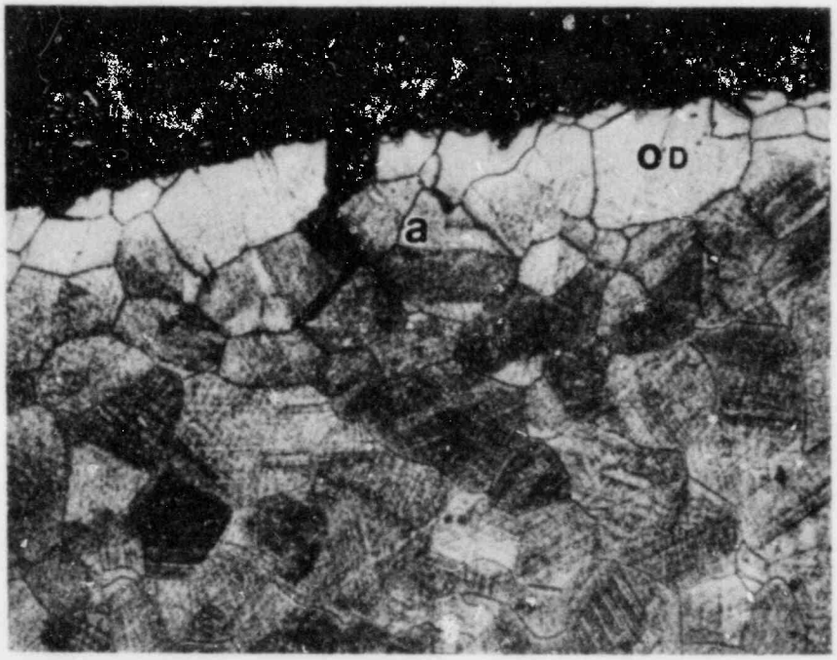

Figure 2-50. Micrographs of Tube B112-19 Area 6

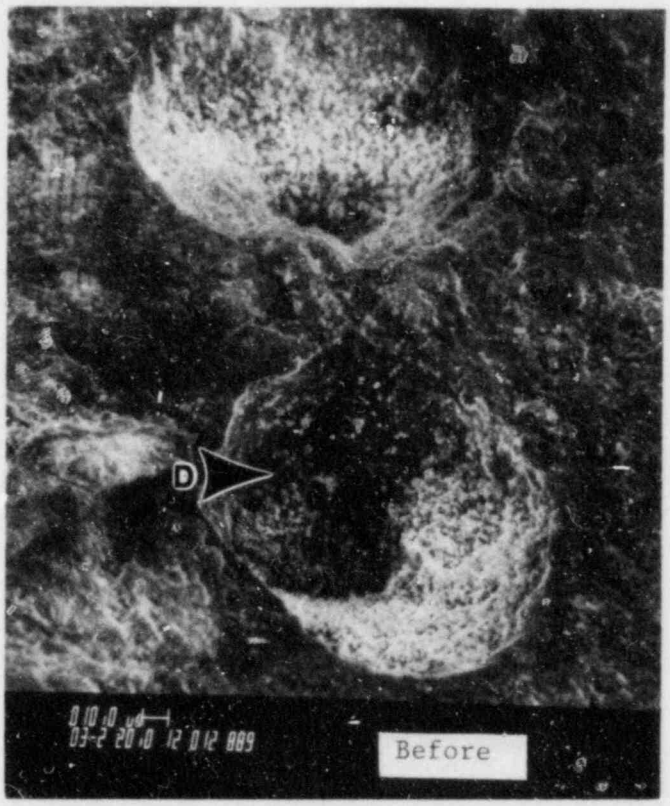

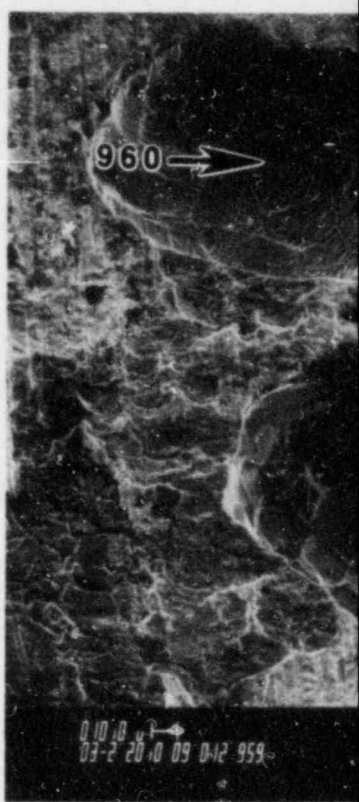

Pitting with Light Granular Deposits

Figure 2-51. SEM Micrographs of Tube B73-8 Near Area 6 (Before and After Cleaning)

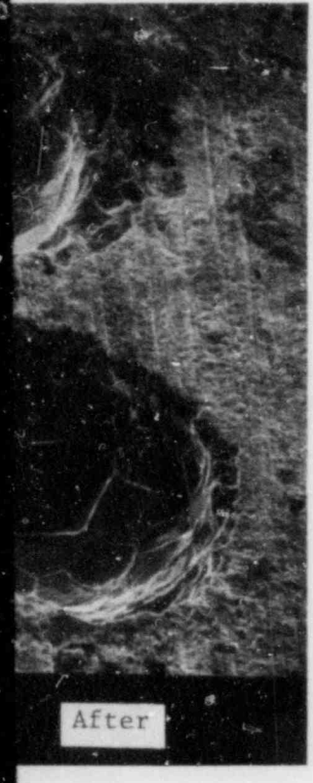

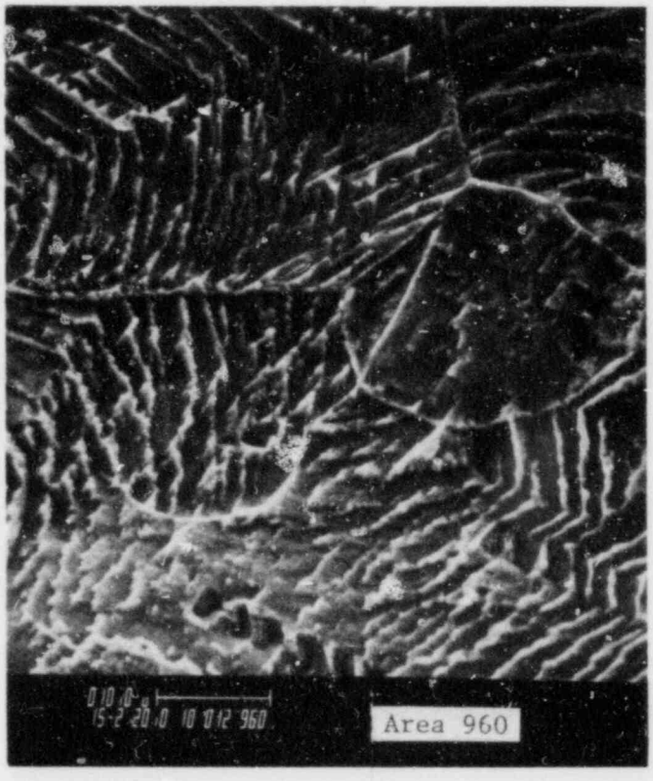

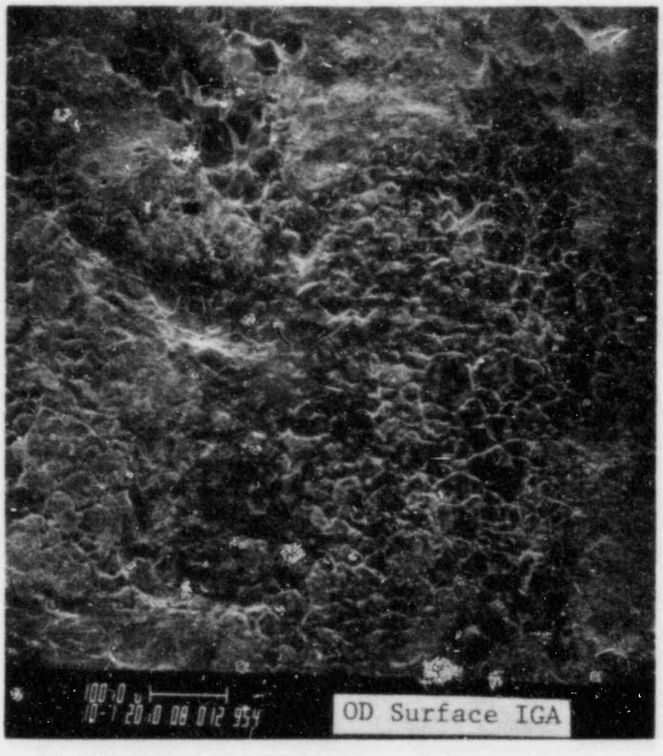

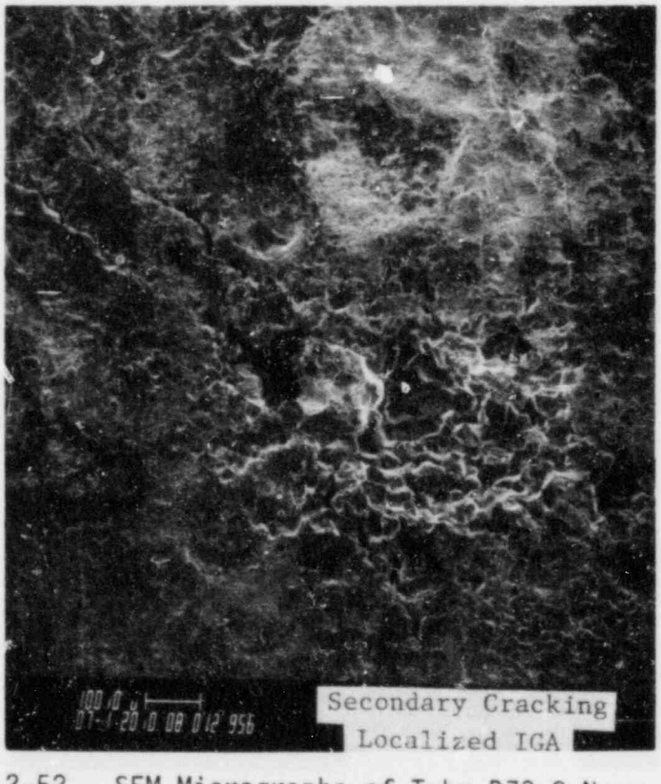

Figure 2-52. SEM Micrographs of Tube B73-8 Near Area 6 (After Cleaning)

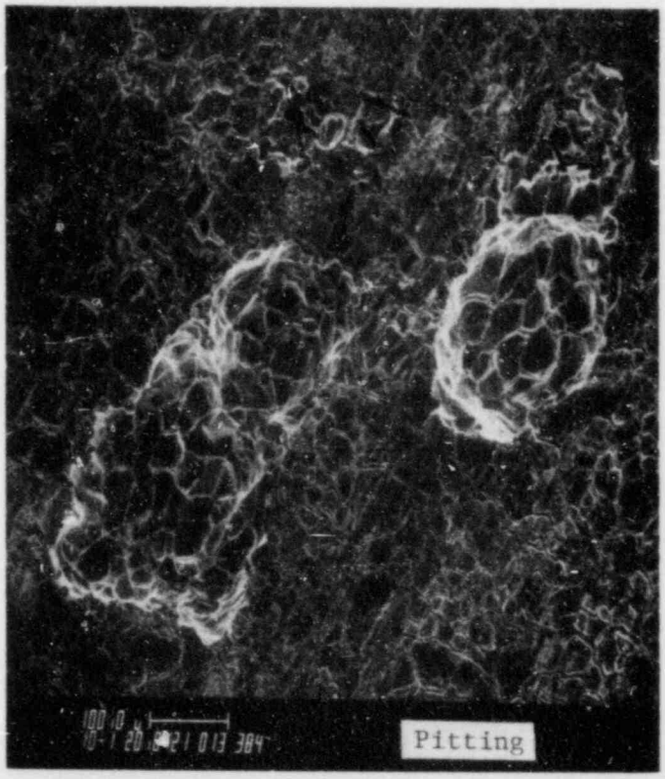

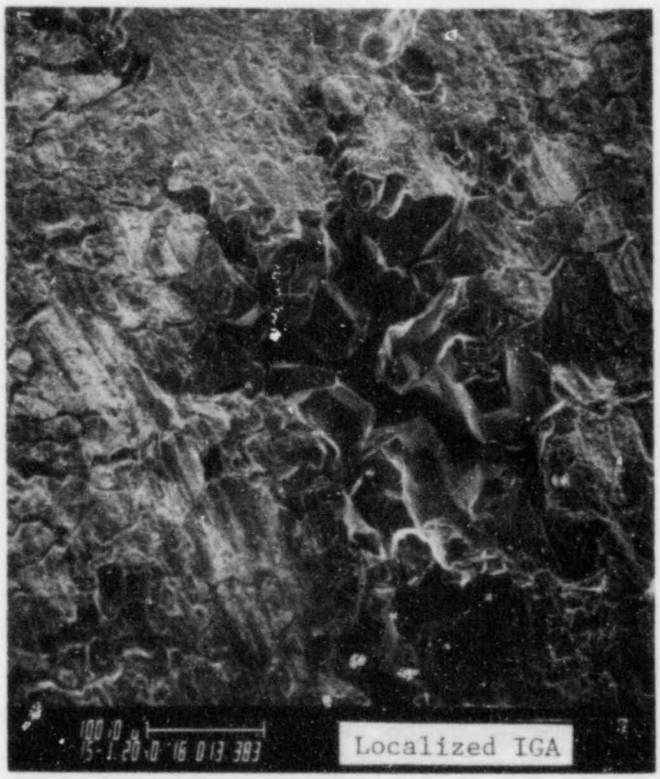

Figure 2-53. SEM Micrographs of Tube B73-8 Area 7
(After Cleaning)

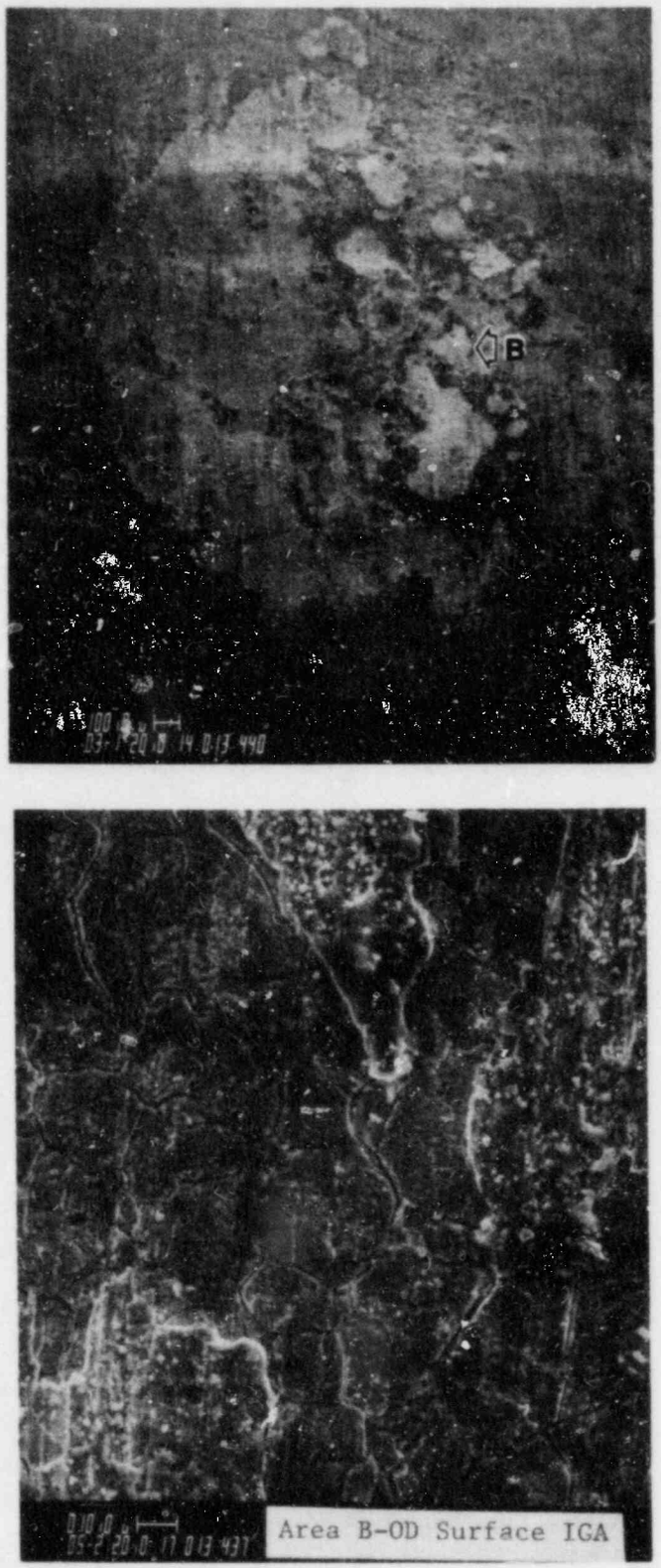

Figure 2-54. SEM Micrographs of Tube B73-8 Area 10

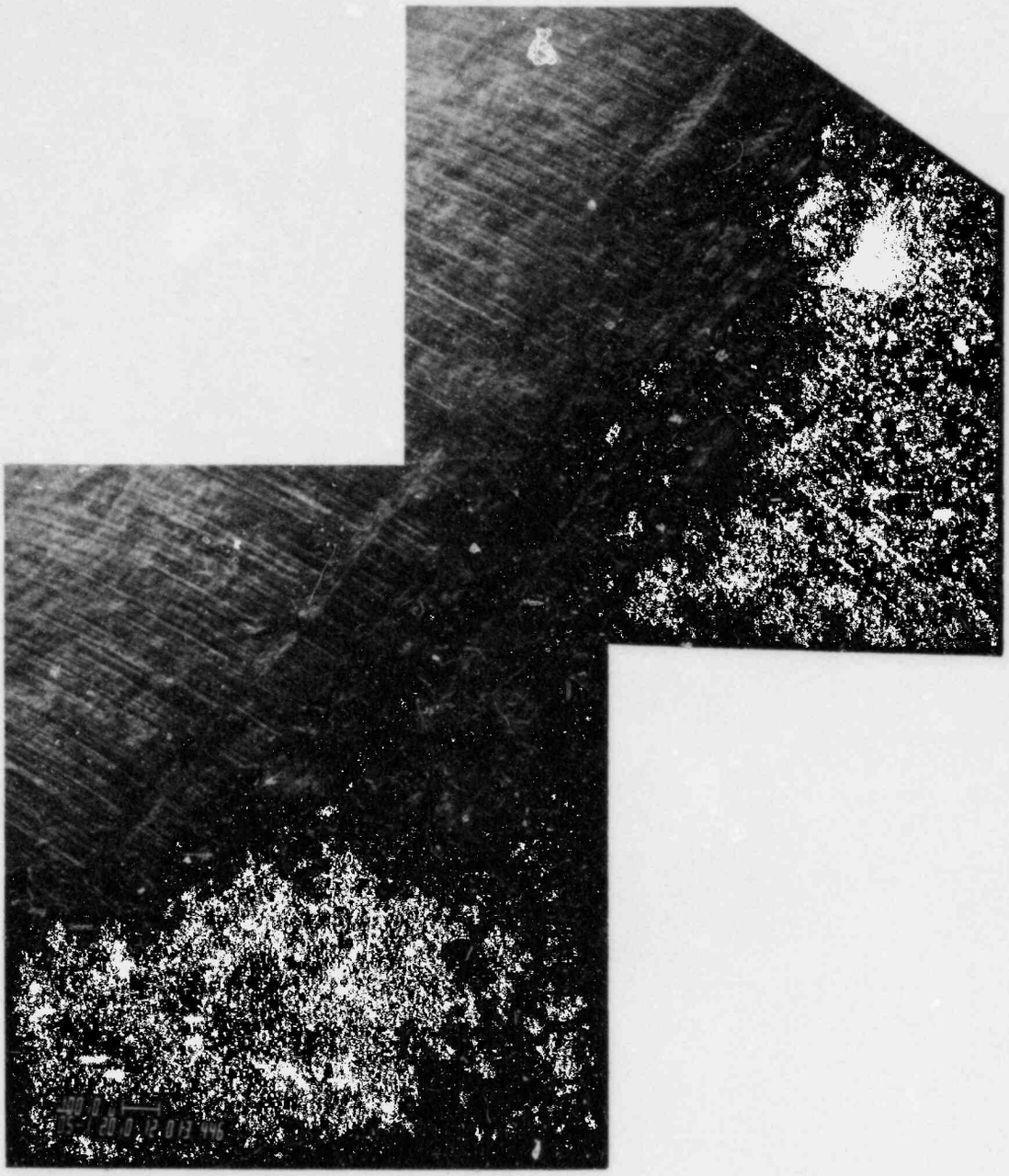

Figure 2-55. SEM Micrographs of Tube B73-8 Area 10 (After Cleaning)

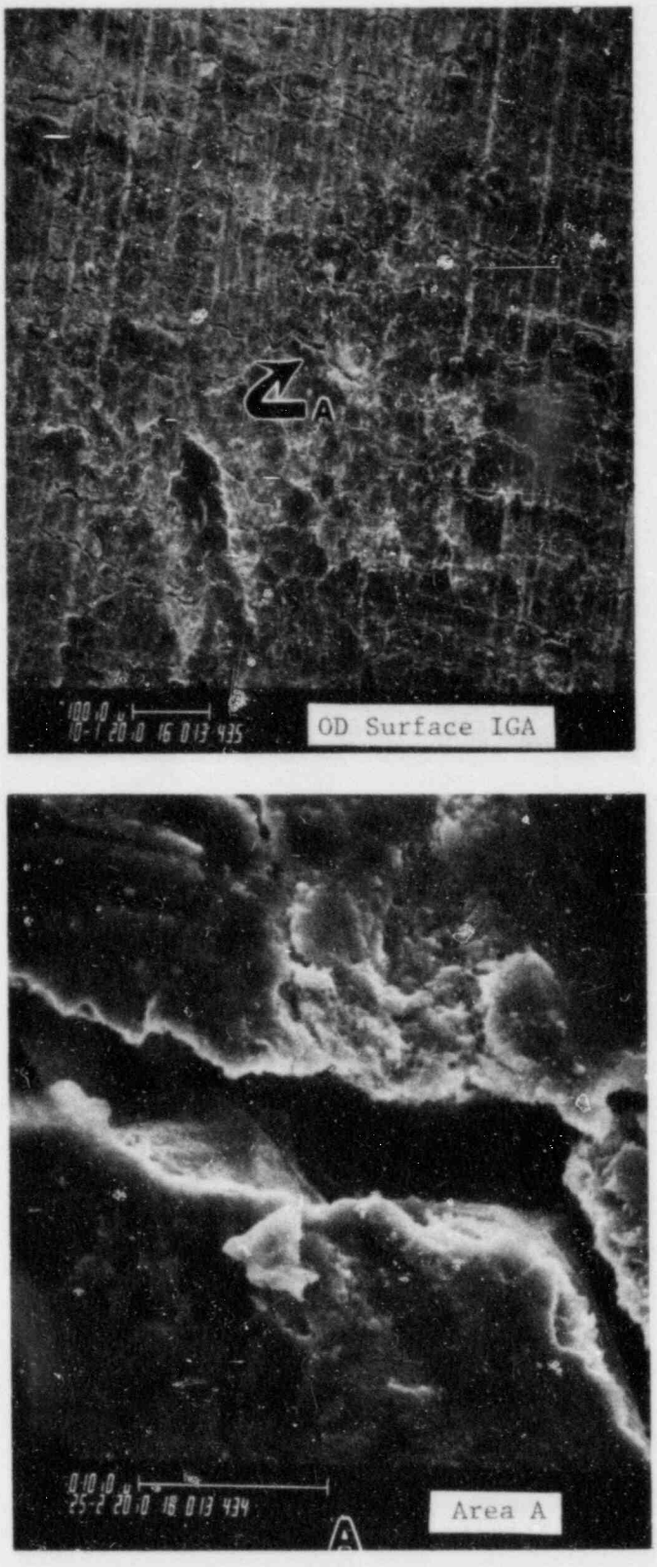

Figure 2-56. SEM Micrographs of Tube B73-3 Area 11

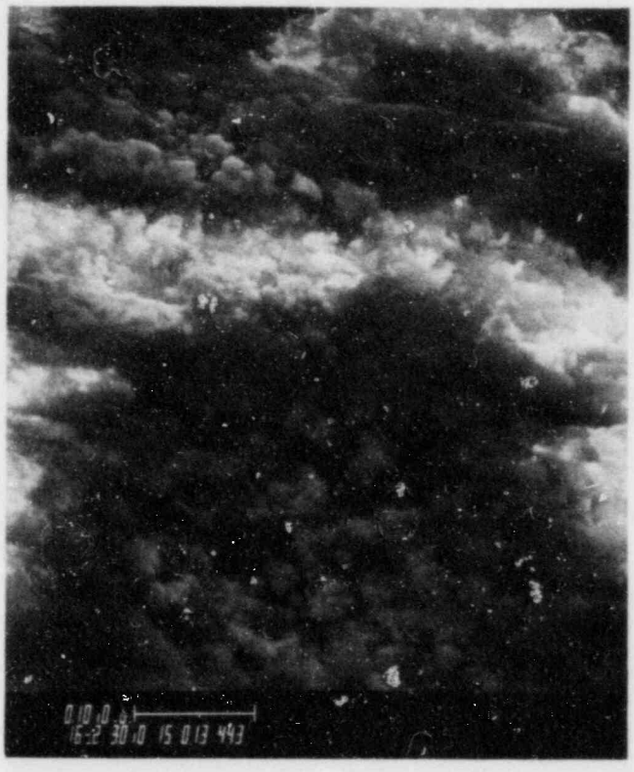

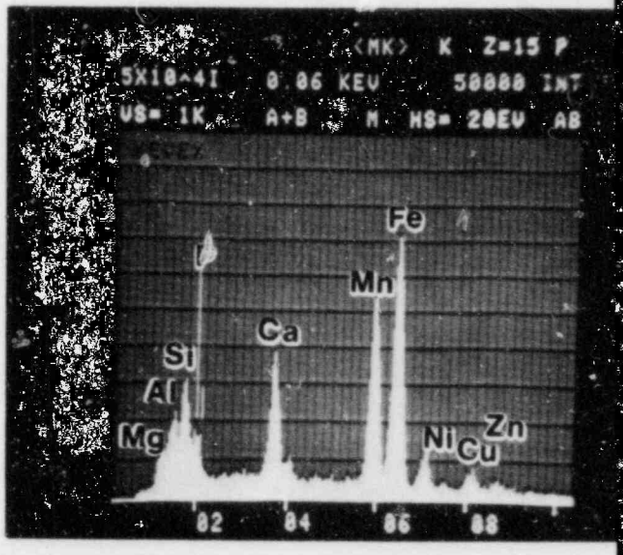

← Surface Deposit Before Cleaning

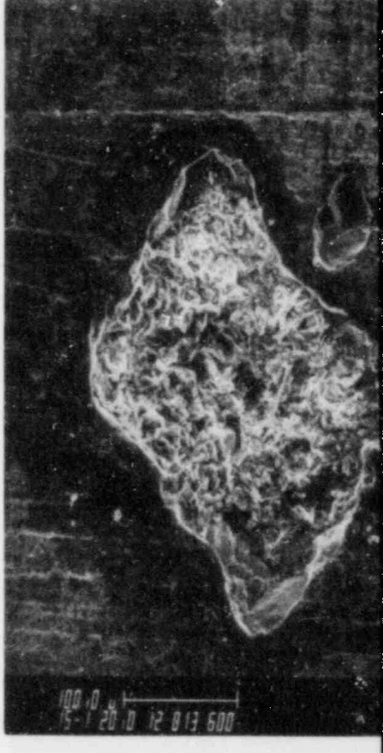

Pitting

Figure 2-57. SEM Micrographs of Tube B73-8 Area 12 (Before and After Cleaning)

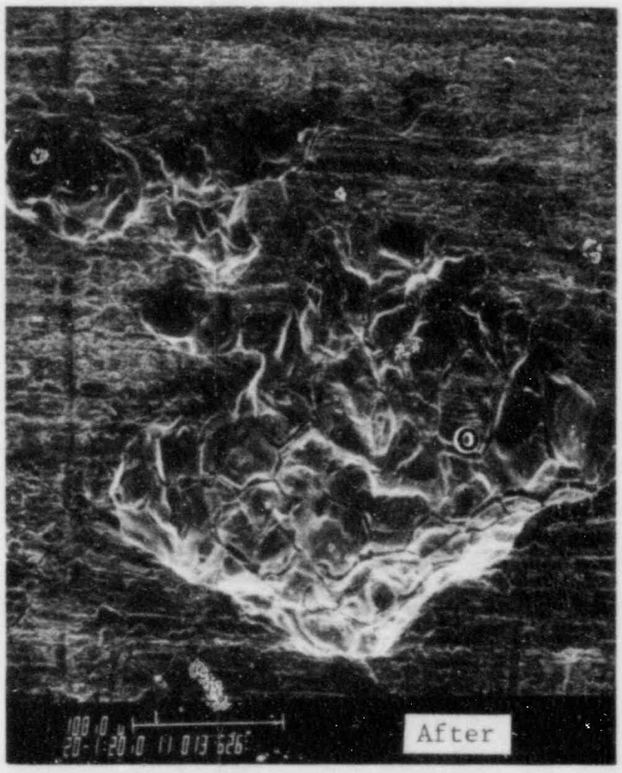

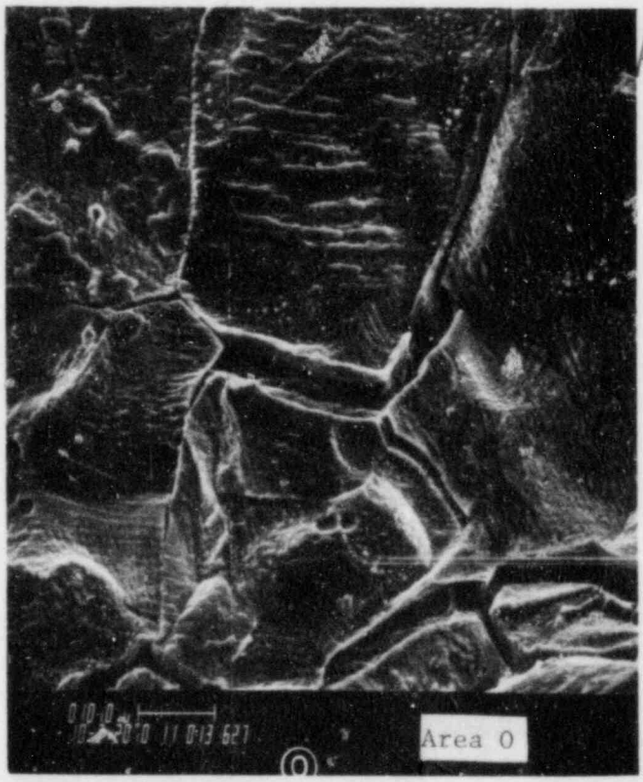

OD Surface
Deposits

Figure 2-58. SEM Micrographs of Tube B112-19 Area 7
(After Cleaning)

3. DISCUSSION

The precise conditions and environment within the ANO-1 OTSGs is not known. Based on the data obtained during this examination and facts known of Inconel 600 corrosion, the most probable attack mechanism involves a reduced sulfur species in an acid environment. Conditions necessary for this type of attack are: 1) presence of sulfur, 2) aqueous acidic environment, 3) low temperatures (<212°F), and 4) oxidizing conditions. The SIGA detected in this examination is preferential attack of the Cr depleted grain boundaries (stress-relieved state of OTSG Inconel 600), a microstructure susceptible to sulfur attack. Tube examination chemistry data confirms that sulfur was present. Chemistry data also showed a chlorine species to be present, which may have helped create a locally acidic environment. An aqueous environment and oxidizing conditions may occur during low temperature reactor shutdown conditions. Since circumferential cracks were detected within the UTS crevice of only a lane region tube (B73-8) and mainly along one axis, axial stress may have played some role in their formation. A concentrated impurity environment within the crevices of lane region tubes could have been provided by the heavy OD surface deposits at the UTS secondary face. Within the UTS crevices, the SIGA may have eventually formed into through-wall cracks either during reactor shutdown or operation.(3) Possible sources of reduced sulfur species include 1) accidental injection into the secondary system of lubricating oils or chemicals such as sodium thiosulfate, 2) decomposition of condensate polisher resins, and 3) the reduction of sulfates (e.g., by hydrazine).

4. CONCLUSIONS

- General intergranular attack exists essentially uniform on the OD surfaces from the top of both tubes to the 15th TSP of B73-8 and the 14th TSP of B112-19.

- Through-wall cracking exists within the UTS crevice of the lane region tube (B73-8).

- The entire OD tube surfaces were covered with deposit layers which were high in iron. The heaviest deposits were located near the UTS secondary face.

- Laboratory and site eddy current inspection techniques were effective in detecting UTS crevice cracking ($\geq$60% through-wall), but were not effective in detecting the surface intergranular attack.

- Significant concentrations of sulfur (about 2.5 wt. %) and chlorine (about 1.2 wt. %) were detected on a crack surface within the UTS crevice.

- The most probable corrosive mechanism supported by the tube examination data is intergranular attack of the chromium depleted Inconel 600 grain boundaries by an acidic sulfur species in an aqueous environment.

5. REFERENCES

(1) Memorandum from W. M. Latham to S. C. Inman, dated February 18, 1983, "Eddy Current Exam of Pulled ANO Steam Generator Tubes," (in Appendix B).

(2) S. C. Inman, "Examination of OTSG Tubes from TMI-1 Third Pulling Sequence - Final Report," Babcock & Wilcox RDD:83:5068-03:03, December 1982.

(3) M. A. Rigdon, R. E. Ricker, and L. W. Sarver, "Final Report on Tube 77-17 From Arkansas Nuclear One," Babcock & Wilcox LR:78:6206-01:4, July 24, 1978.

(4) M. A. Rigdon and E. B. S. Pardue, "Evaluation of Tube Samples From TMI-1," B&W Document No. 77-1135317.

APPENDIX A

X-Ray Radiographs

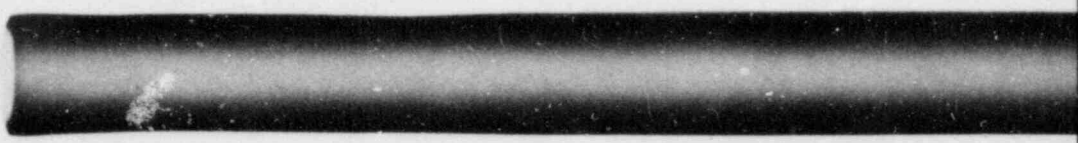

0°

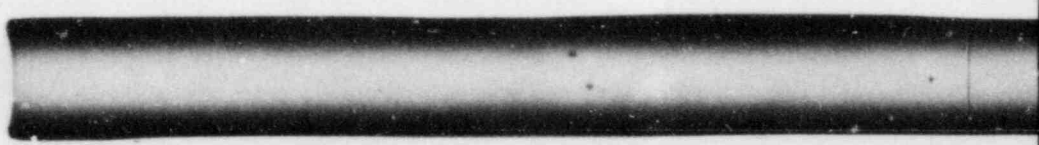

90°

Tube B73-8 P

Also Available On
Aperture Card

iece 1

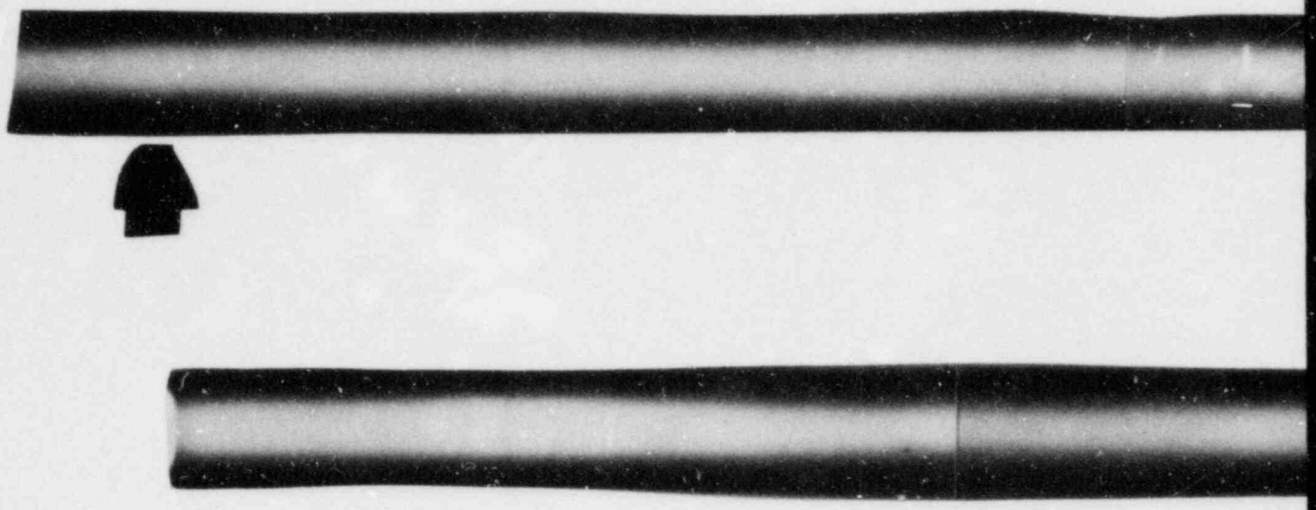

0°

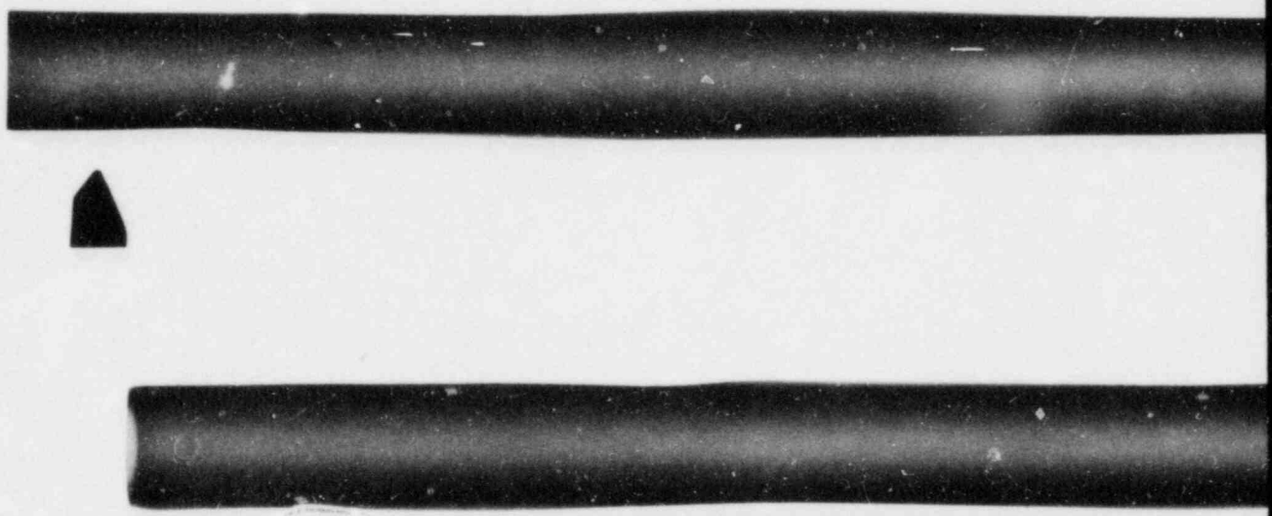

90

Tube B7

8-8 Piece 2

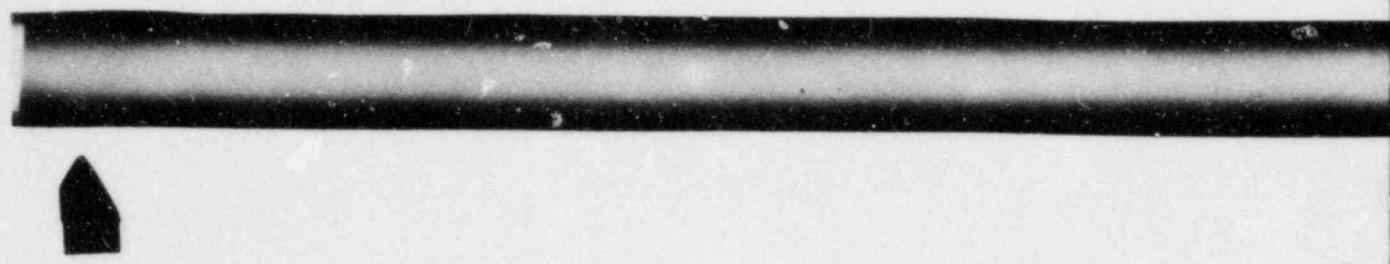

0°

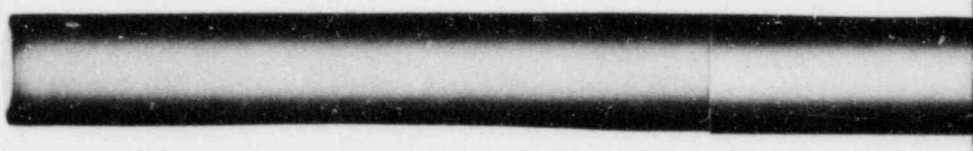

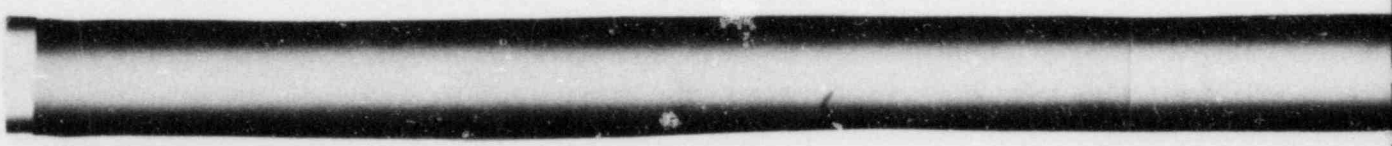

90°

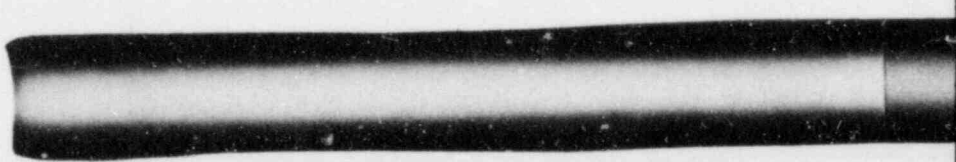

Tube B73-8

Also Available On
Aperture Card

Piece 3

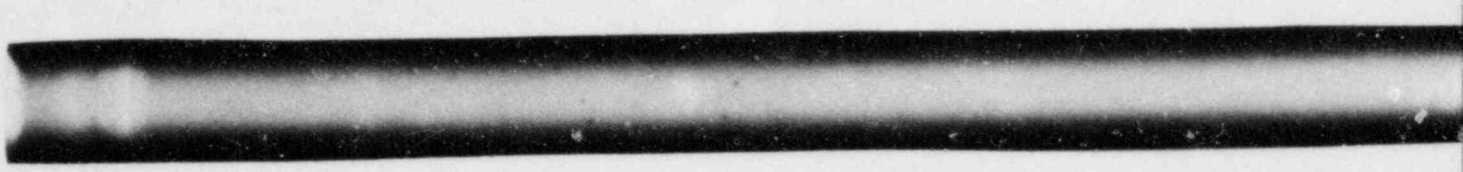

0°

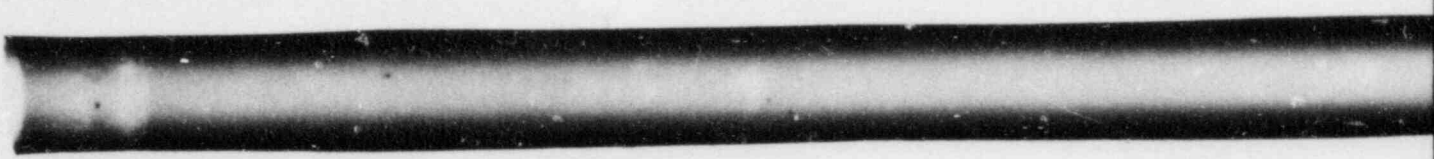

90°

Tube B73-8

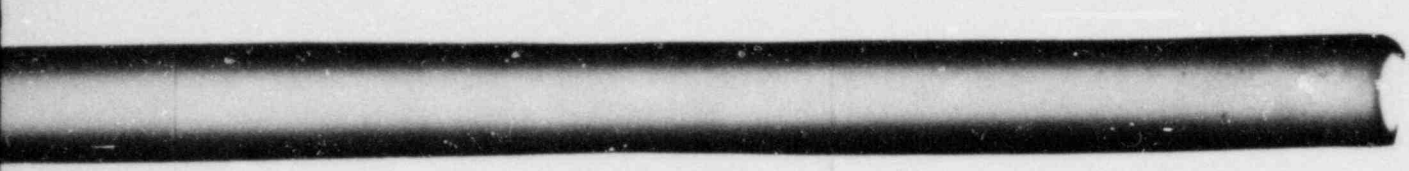

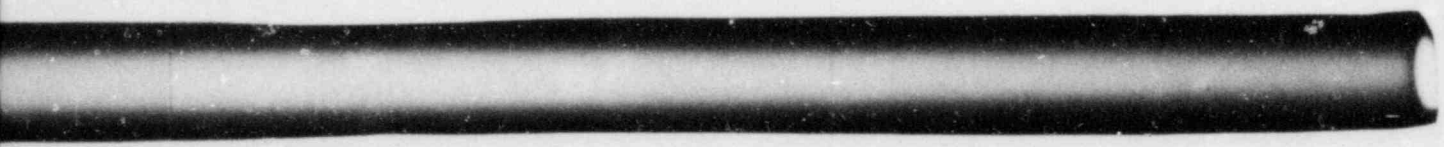

Also Available On
Aperture Card

Piece 4

[redacted]

[redacted]

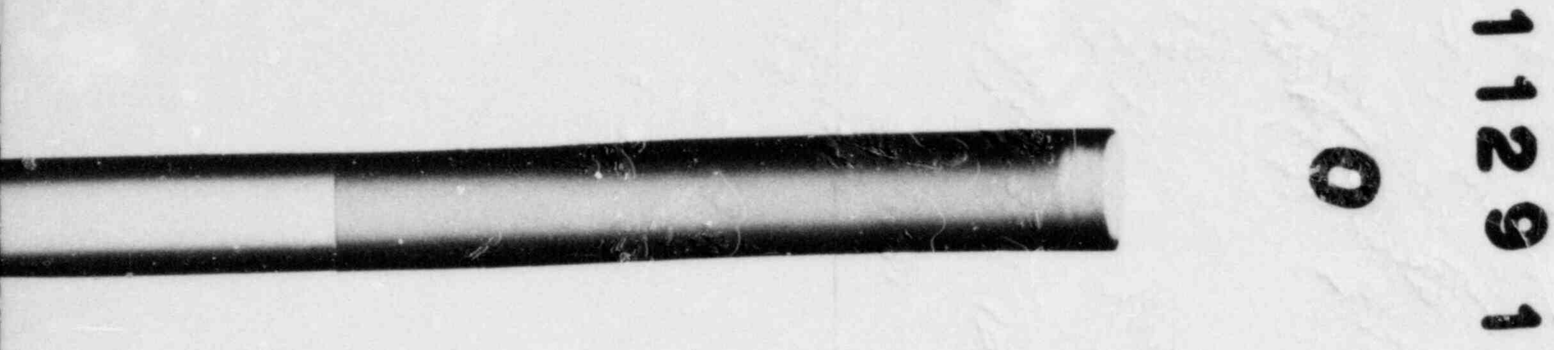

0°

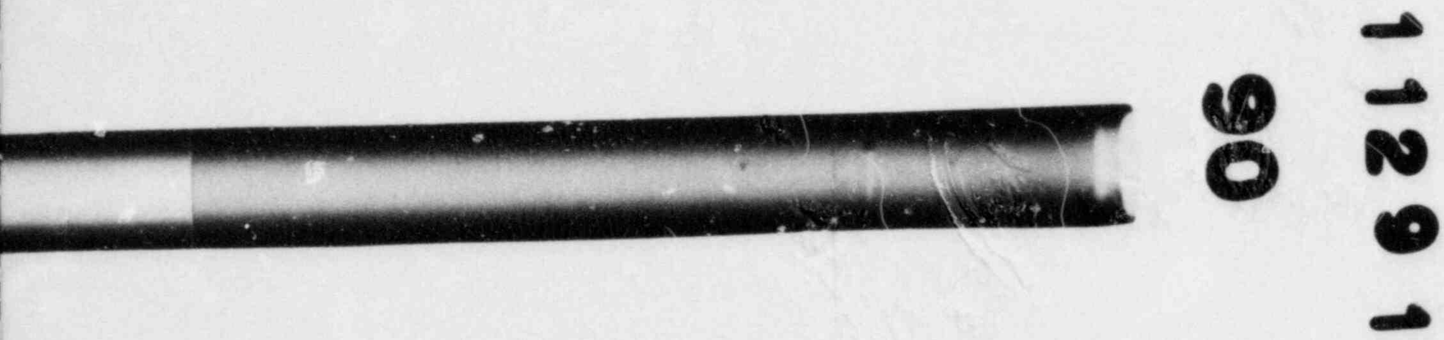

90°

Tube B112-19 Piece 1

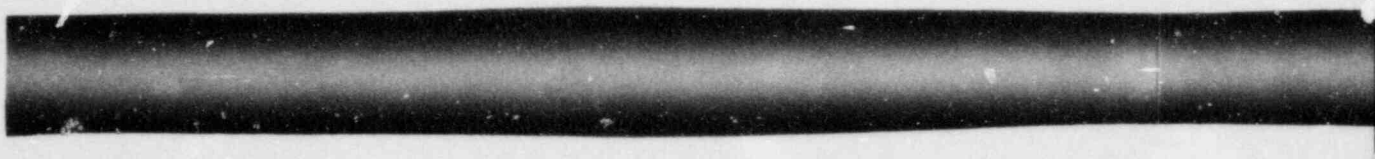

0°

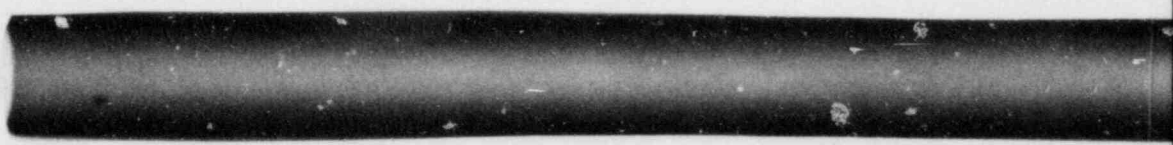

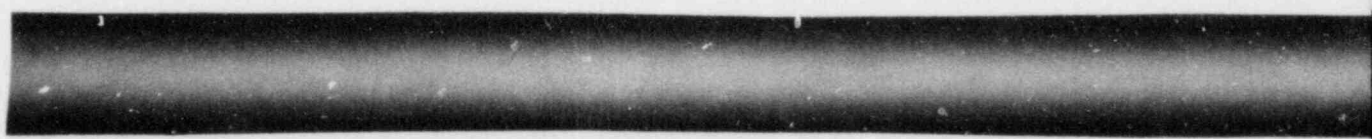

90°

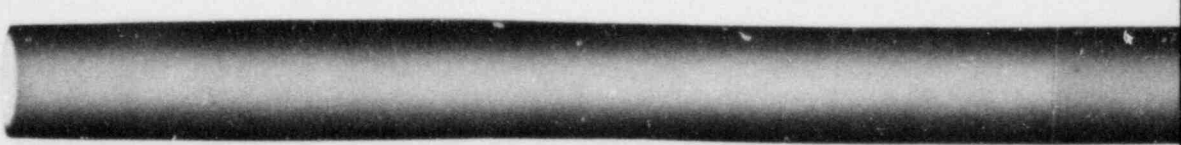

Tube B112-

11802

11803

9 Piece 2

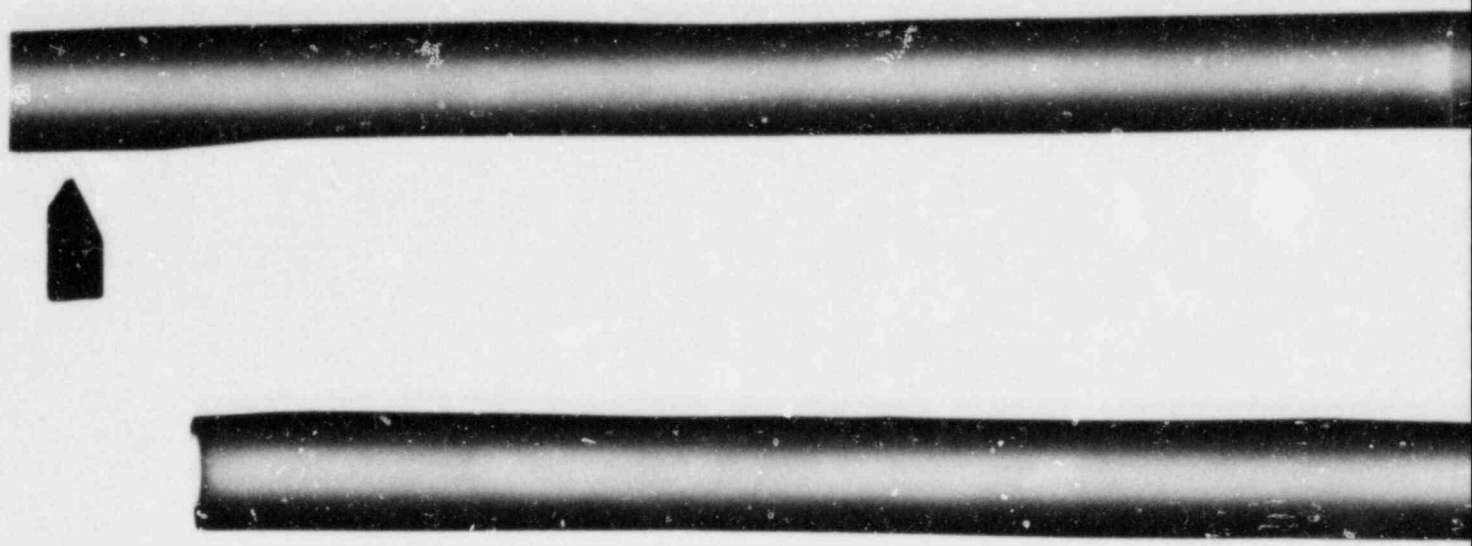

0°

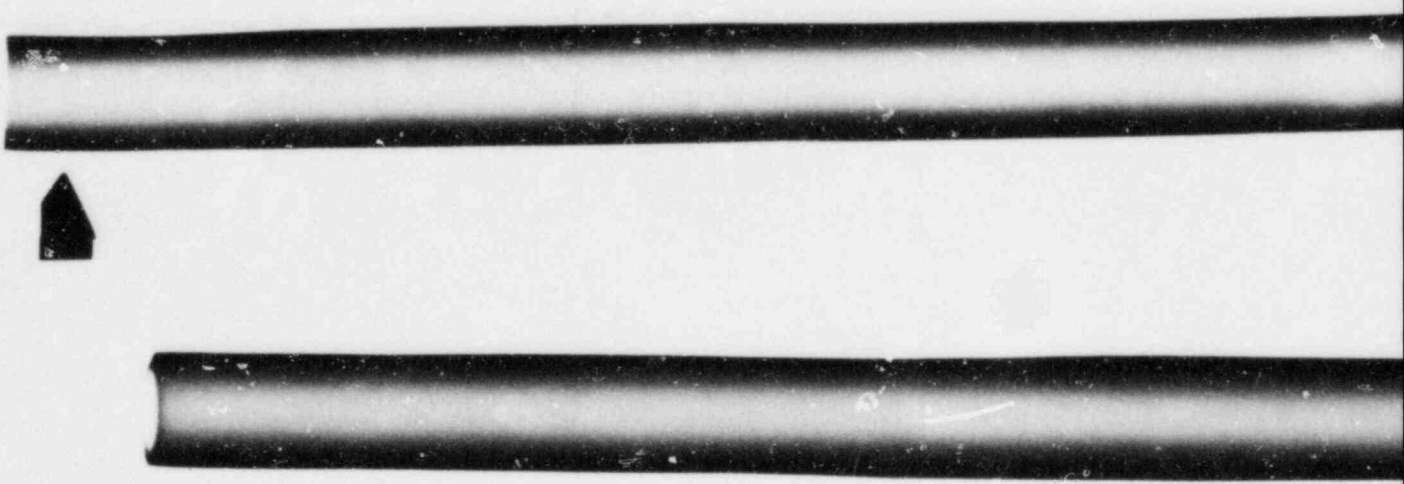

90°

Tube B112-1

Also Available On
Aperture Card

Piece 3

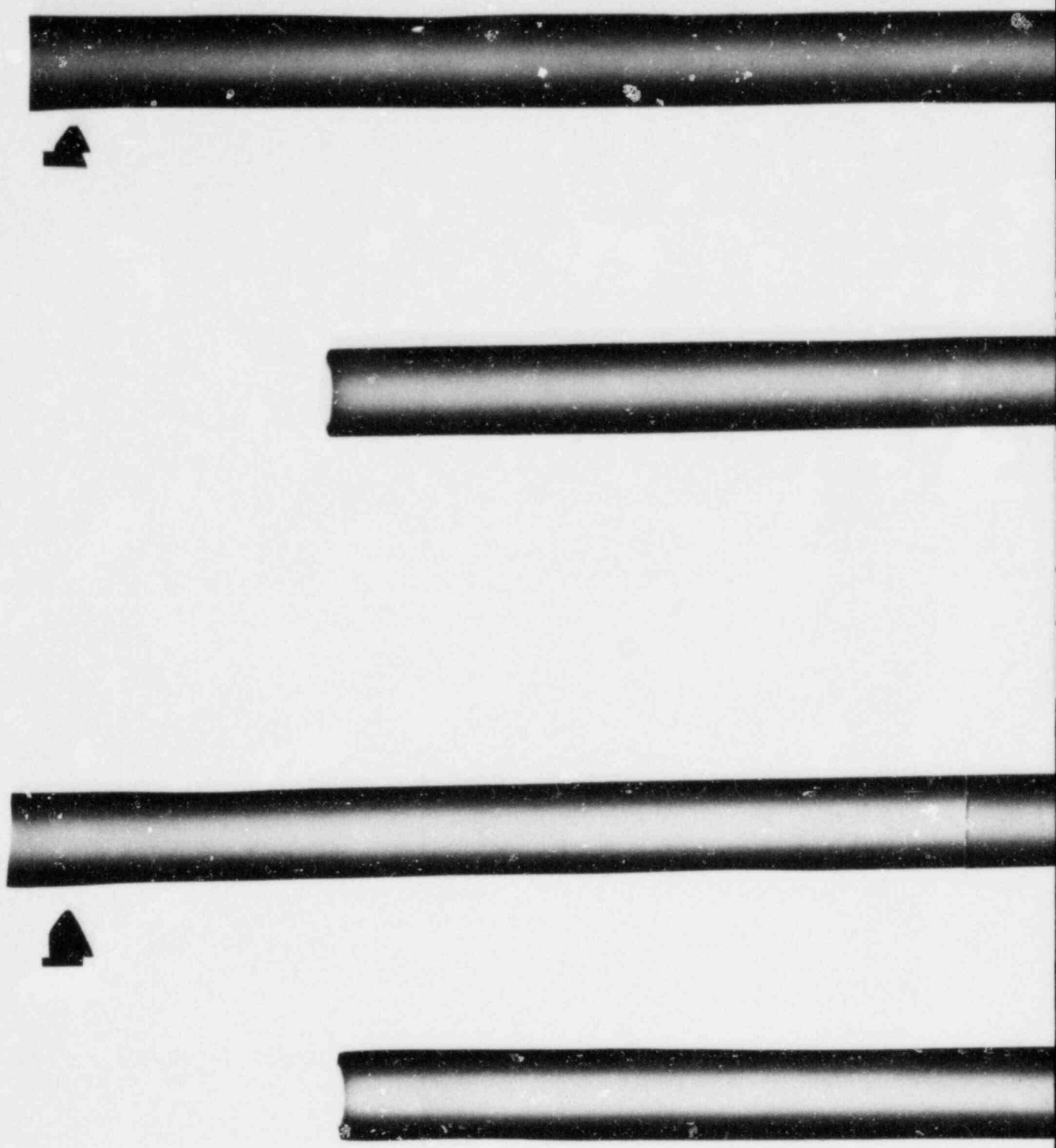

Tube B

112-19 Piece 4

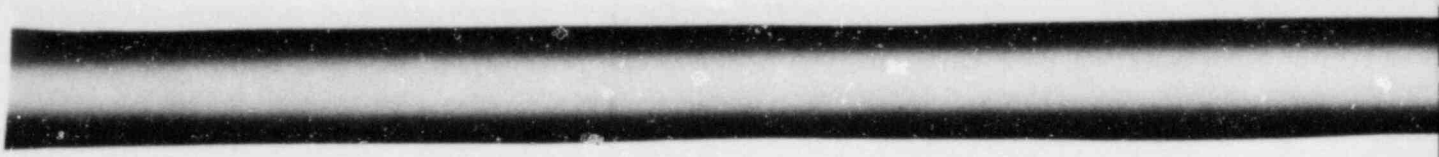

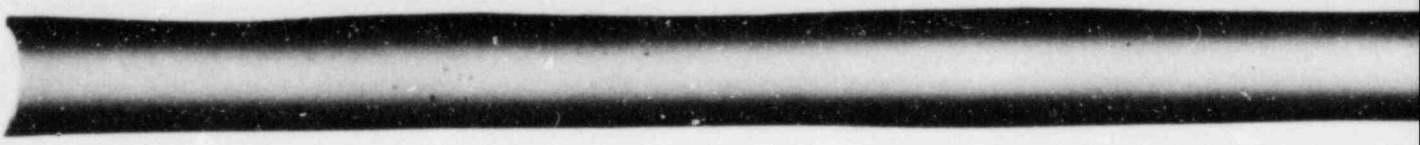

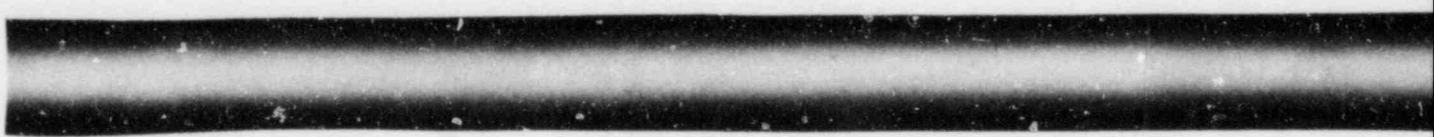

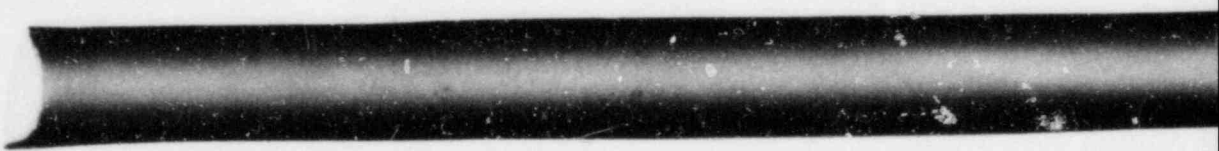

Tube Bl

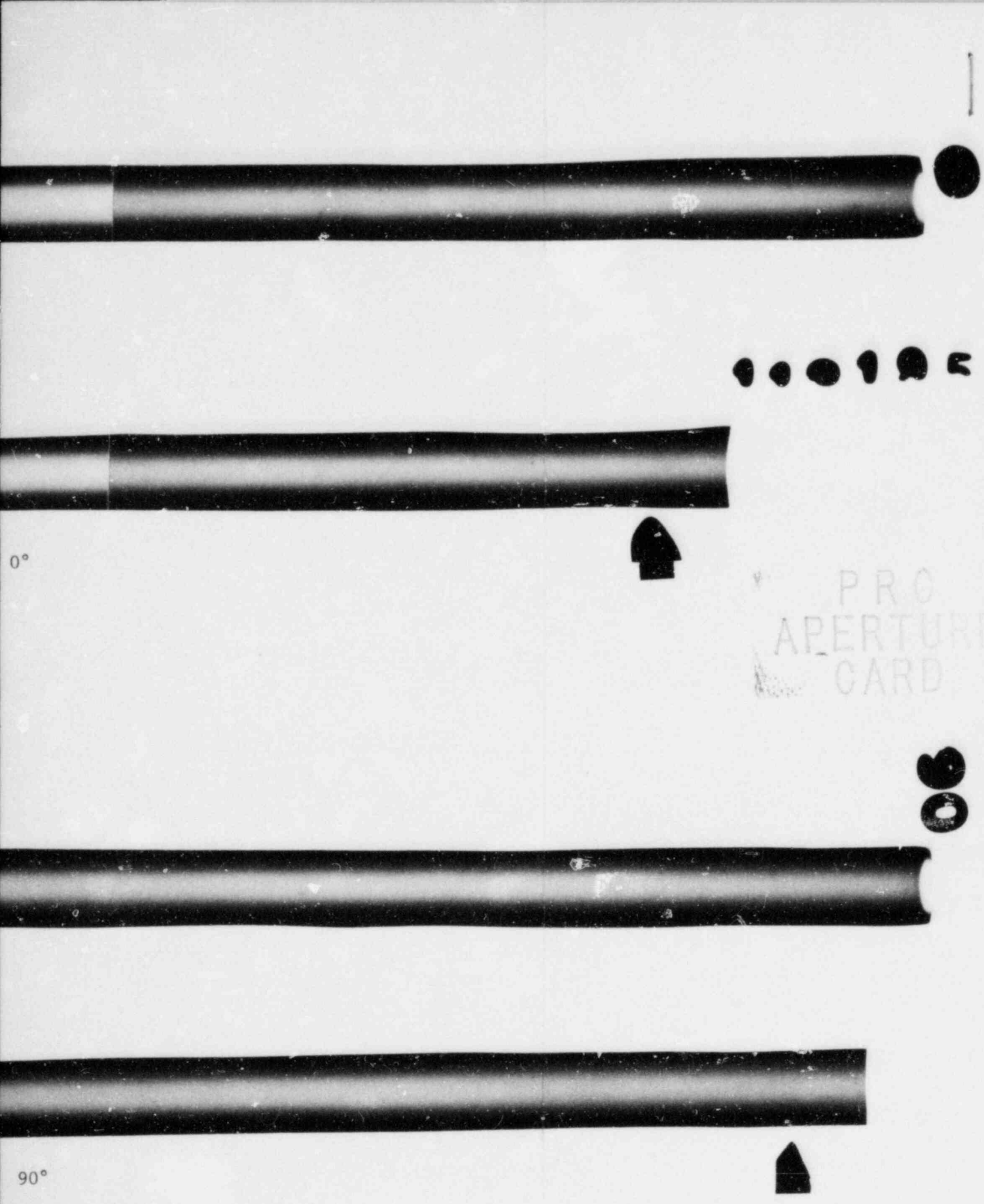

12-19 Piece 5

Also Available On
Aperture Card

APPENDIX B

Eddy Current Inspection Details

Babcock & Wilcox
a McDermott company

Research and Development Division
Lynchburg Research Center
Lynchburg, Virginia 24505

cc: G. M. Bain
A. E. Holt
S. R. Lester
A. E. Wehrmeister
H. L. Whaley

To
S. C. INMAN, NUCLEAR MATERIALS, LRC

From
W. M. LATHAM - NDM&D, LRC

Cust.
AP&L

File No. or Ref.
5303

Subj.
EDDY CURRENT EXAM OF PULLED ANO STEAM GENERATOR TUBES

Date
FEBRUARY 18, 1983

On February 15 and 16, 1983, sections of two tubes removed from an ANO steam generator were examined at the LRC Hot Cell using several different eddy current techniques. All tube sections were examined initially using a 0.500" diameter annular differential probe, a mix of 400 kHz and 200 kHz for support plate response suppression, and 600 kHz, in order to simulate the site eddy current inspection. Although several sections were damaged by the tube removal process, only one section, tube B73-8 piece 2, was conclusively found to contain defect indications. After documenting the axial location of defect indications, a carbon steel upper tubesheet (UTS) simulation was placed over the tube section. The mockup was located at the suspected in situ UTS interface and scans were made while recording the data on magnetic tape. Several scans were performed after moving the simulation slightly above and below the interface for possible comparison with site results at a later date. In addition to the 0.500" diameter differential probe, tube B73-8, piece 2 was examined with a 0.125" diameter radial absolute coil (O.D. surface scanning probe) to determine the circumferential location and extent of the defects. A through-wall hole was found 11 1/2 inches from the top and was located at approximately 80° clockwise from the x-axis as viewed from the top end. Numerous circumferential cracks were found to be centered at approximately 180° from the x-axis with approximately 45° circumferential extent. The inspection results for all tubes are summarized in more detail in the attached table.

Tube B112-19, piece 4 reportedly contained a 63% of wall O.D. defect below the 15th TSP region. This section was examined with three additional eddy current techniques, but no conclusive defect indications were found. It should be noted, however, that the 15th TSP region was damaged during tube removal (denting and smeared metal), possibly obscuring defect information. The piece was inspected with a 0.540" diameter annular differential probe which would not pass the region of interest because of tube denting. Examination with the 0.125" diameter radial absolute coil showed no conclusive defect indication. Finally, piece 4 was inspected with a 0.500" diameter annular differential probe using a 400 kHz/900 kHz mix to suppress the response to denting. Again, no defect indications were seen.

W. M. Latham

WML/ntq
Attachment

SUMMARY OF RESULTS

Tube Number	Scan Direction	Defect Location	Depth Estimate (% of Wall)	Additional Comments
B73-8 piece 1	Bottom to top	No loss-of-metal type defect indications		Minor denting 6 1/2" from top
B73-8 piece 2	Bottom to top	11 1/2" from top	100% Through-wall	
"		8 9/16" - 8 1/2" from top	Difficult to determine because of distorted signal patterns.	Multiple-defects at least 2, probably 3 occuring over a very short distance axially.
"		7 3/8" from top	83%	Appear to be OD initiated circumferential cracks
"		6 15/16" from top	88%	Located with radial absolute "pencil" probe
"		6 7/16" from top	92%	Located ≈180° from tube X-axis. Circumferential extent 45°
B73-8 piece 3	Bottom to top	No Loss-of-metal type defect indications		Slightly damaged during tube removal process
B73-8 piece 4	Bottom to top			Heavily damaged during tube removal process
B112-19 piece 1	Top to bottom	No loss-of-metal type defect indications		Slight diameter increase 8 1/2" from top
B112-19 piece 2	Bottom to top			Small dent - 13 7/16" from top

SUMMARY OF RESULTS (Cont'd.)

Tube Number	Scan Direction	Defect Location	Depth Estimate (% of Wall)	Additional Comments
B112-19 piece 3	Bottom to top			Damaged from tube removal process - section contains large diameter increase.
B112-19 piece 4	Top to bottom	No loss-of-metal type defect indications		Extensive denting near 15th TSP region metal smeared from tube removal process 15th TSP region examined using three different techniques: (1) 0.540" annular differential probe (2) 0.500" annular differential probe with dent mix (3) 0.125" radial absolute O.D. surface scanning probe
B112-19 piece 5	Top-bottom			

APPENDIX C

Tube Diameter Data

B73-8 - Piece 1

	Avg. ID, Inches	Avg. OD, Inches	Tubewall, Inches
1	.552	.6296	.0388
2	.5525	.6294	.0385
3	.5525	.6293	.0384
4	.553	.6292	.038[illegible]
5	.5525	.6295	.0385
6	.5525	.6293	.0384
7	.552	.6292	.0386
9	.552	.6292	.0386
10	.552	.6293	.0387
11	.5525	.6287	.0381
12	.552	.6282	.0381
13	.5525	.6294	.0385
14	.5515	.6292	.0389
15	.5515	.6295	.0390
16	.552	.6294	.0387
17	.552	.6292	.0386
18	.552	.6293	.0387
19	.552	.6291	.0386

B73-8 - Piece 2

	Avg. ID, Inches	Avg. OD, Inches	Tubewall, Inches
1	.5505	.6273	.0384
2	.5525	.6277	.0376
3	.552	.6275	.0378
4	.553	.6281	.0376
5	.5535	.6275	.0370
6	.552	.6277	.0379
7	.5515	.6279	.0382
8	.5495	.6275	.0390
9	.550	.6282	.0391
10	.551	.6277	.0384
11	.5495	.6277	.0391
12	.550	.6265	.0383
13	.549	.6262	.0386
14	.5495	.6268	.0387
15	.550	.6277	.0389
16	.550	.6271	.0386
17	.5505	.6278	.0387
18	.550	.6274	.0387
19	.5505	.6286	.0391
20	.551	.6276	.0383
21	.550	.6273	.0387
22	.551	.6271	.0381
23	.5485	.6272	.0394
24	.551	.6282	.0386
25	.552	.6348	.0414
26	.5515	.6358	.0422
27	.553	.6373	.0422
28	.552	.6352	.0416

B73-8 - Piece 2 (Cont'd)

	Avg. ID, Inches	Avg. OD, Inches	Tubewall, Inches
29	.552	.6227	.0354
30	.552	.6310	.0395
31	.552	.6328	.0404
32	.552	.6316	.0398
33	.552	.6298	.0389
34	.5515	.6294	.0390
35	.552	.6294	.0387
36	.5525	.6293	.0384
37	.5525	.6295	.0385
38	.5525	.6295	.0385
39	.553	.6296	.0383

B73-8 - Piece 3

	Avg. ID, Inches	Avg. OD, Inches	Tubewall, Inches
1	.5485	.6281	.0398
2	.5475	.6121	.0323
3	.535	.6127	.0389
4	.533	.6097	.0384
5	.531	.6078	.0384
6	.5265	.6126	.0431
7	.537	.6149	.0390
8	.539	.6152	.0381
9	.540	.6147	.0374
10	.5395	.6149	.0377
11	.5405	.6149	.0372
12	.540	.6148	.0374
13	.540	.6150	.0375
14	.540	.6149	.0375
15	.540	.6152	.0376
16	.5405	.6153	.0374
17	.5405	.6157	.0376
18	.5405	.6162	.0379
19	.5415	.6169	.0377
20	.5415	.6175	.0380
21	.5415	.6163	.0374
22	.540	.6152	.0376
23	.5395	.6147	.0376
24	.5395	.6145	.0375
25	.539	.6140	.0375
26	.538	.6125	.0373
27	.539	.6154	.0382
28	.541	.6159	.0375
29	.541	.6160	.0375

B73-8 - Piece 3 (Cont'd)

	Avg. ID, Inches	Avg. OD, Inches	Tubewall, Inches
30	.541	.6157	.0374
31	.5405	.6158	.0377
32	.5405	.6160	.0378
33	.541	.6157	.0374
34	.5405	.6161	.0378
35	.541	.6167	.0379
36	.541	.6163	.0377
37	.541	.6157	.0374
38	.5405	.6159	.0377
39	.5405	.6163	.0379
40	.5405	.6164	.0380
41	.541	.6162	.0376

B73-8 - Piece 4

	Avg. ID, Inches	Avg. OD, Inches	Tubewall, Inches
1	.540	.6158	379
2	.541	.6165	378
3	.541	.6162	376
4	.5405	.6157	376
5	.5395	.6159	382
6	.540	.6156	378
7	.5405	.6157	376
8	.5405	.6157	383
9	.5405	.6158	377
10	.5405	.6158	377
11	.5405	.6156	376
12	.5405	.6159	377
13	.541	.6157	374
14	.541	.6165	378
15	.5415	.6170	378
16	.541	.6167	379
17	.5405	.6169	382
18	.541	.6167	379
19	.5405	.6176	386
20	.5415	.6165	375
21	.5455	.6221	383
22	.544	.6189	375
23	.5485	.6174	345
24	.541	.6247	419
25	.5545	.6259	357
26	.540	.6165	383
27	.5495	.6156	331

B112-19 - Piece 1

	Avg. ID, Inches	Avg. OD, Inches	Tubewall, Inches
1	.5502	.6293	.0637
2	.5500	.6291	.0396
3	.5500	.6291	.0396
4	.5499	.6291	.0396
5	.5497	.6290	.0397
6	.5494	.6291	.0399
7	.5497	.6290	.0397
8	.5499	.6291	.0396
9	.5499	.6290	.0396
10	.5500	.6292	.0396
11	.5499	.6291	.0396
12	.5499	.6290	.0396
13	.5499	.6288	.0395
14	.5499	.6288	.0395
15	.5499	.6290	.0396
16	.5499	.6290	.0396
17	.5499	.6292	.0397
18	.5504	.6291	.0394
19	.5504	.6291	.0394

B112-19 - Piece 2

	Avg. ID, Inches	Avg. OD, Inches	Tubewall, Inches
1	.5505	.6290	.0620
2	.5295	.6290	.0498
3	.5505	.6290	.0393
4	.550	.6291	.0646
5	.550	.6291	.0396
6	.5505	.6288	.0392
7	.550	.6291	.0396
8	.550	.6291	.0396
9	.5495	.6291	.0398
10	.550	.6291	.0396
11	.5505	.6291	.0393
12	.5505	.6291	.0393
13	.550	.6290	.0395
14	.5505	.6290	.0393
15	.5505	.6290	.0393
16	.5505	.6289	.0392
17	.5505	.6291	.0393
18	.551	.6290	.0390
19	.5505	.6290	.0393
20	.5515	.6291	.0388
21	.5515	.6291	.0388
22	.551	.6292	.0391
23	.551	.6291	.0391
24	.551	.6292	.0391
25	.5515	.6291	.0388
26	.551	.6278	.0384
27	.5515	.6290	.0390
28	.5505	.6281	.0388
29	.550	.6291	.0396

B112-19 - Piece 2 (Cont'd)

	Avg. ID, Inches	Avg. OD, Inches	Tubewall, Inches
30	.550	.6291	.0396
31	.550	.6291	.0396
32	.550	.6290	.0395
33	.5505	.6291	.0393
34	.5505	.6295	.0395
35	.5505	.6291	.0393
36	.551	.6291	.0391
37	.551	.6292	.0391
38	.5505	.6295	.0395
39	.5505	.6290	.0393
40	.5505	.6290	.0393
41	.551	.6290	.0390
42	.550	.6290	.0395

B112-19 - Piece 3

	Avg. ID, Inches	Avg. OD, Inches	Tubewall, Inches
1	.5505	.6291	.0393
2	.551	.6290	.0390
3	.551	.6291	.0391
4	.551	.6291	.0391
5	.552	.6291	.0386
6	.553	.6292	.0381
7	.552	.6293	.0387
8	.551	.6291	.0391
9	.551	.6292	.0391
10	.551	.6291	.0391
11	.551	.6290	.0390
12	.5535	.6296	.0381
13	.551	.6289	.0390
14	.5505	.6291	.0393
15	.5505	.6289	.0392
16	.5505	.6291	.0393
17	.5505	.6291	.0393
18	.551	.6292	.0391
19	.551	.6291	.0391
20	.551	.62905	.0390
21	.551	.6290	.0390
22	.551	.6290	.0390
23	.551	.6290	.0390
24	.551	.6290	.0390
25	.551	.62905	.0390
26	.551	.6290	.0391
27	.551	.6291	.0391
28	.551	.6289	.0390
29	.551	.6290	.0390

B112-9 - Piece 3 (Cont'd)

	Avg. ID, Inches	Avg. OD, Inches	Tubewall, Inches
30	.551	.6289	.0390
31	.551	.6289	.0390
32	.551	.6291	.0391
33	.551	.6290	.0390
34	.5505	.6290	.0393
35	.550	.6290	.0395
36	.549	.6289	.0400
37	.5485	.6289	.0402
38	.549	.6290	.0400
39	.549	.6290	.0400
40	.5495	.6290	.0390
41	.5495	.6292	.0399

B112-19 - Piece 4

	Avg. ID, Inches	Avg. OD, Inches	Tubewall Inches
1	.5505	.6295	.0395
2	.551	.6292	.0391
3	.551	.6292	.0391
4	.551	.6291	.0391
5	.551	.6291	.0391
6	.5515	.6291	.0388
7	.5512	.6292	.0391
8	.5505	.6292	.0394
9	.550	.6291	.0396
10	.550	.6291	.0396
11	.5505	.6291	.0393
12	.551	.6290	.0390
13	.5505	.6289	.0392
14	.5505	.6291	.0393
15	.5505	.6290	.0393
16	.5505	.6290	.0393
17	.5505	.6290	.0393
18	.5505	.6291	.0393
19	.5505	.6291	.0393
20	.551	.6291	.0391
21	.5505	.6291	.0393
22	.551	.6292	.0391
23	.551	.6290	.0390
24	.551	.6291	.0391
25	.551	.6291	.0391
26	.551	.6291	.0391
27	.551	.6293	.0392
28	.551	.6293	.0392
29	.5505	.6295	.0395

B112-19 - Piece 4 (Cont'd)

	Avg. ID, Inches	Avg. OD, Inches	Tubewall, Inches
30	.551	.6293	.0392
31	.551	.6282	.0386
32	.549	.6273	.0392
33	.5453	.6262	.0406
34	.5455	.6251	.0398
35	.548	.6259	.0390
36	.548	.6263	.0392
37	.548	.6264	.0392
38	.548	.6263	.0392
39	.548	.6262	.0391
40	.548	.6262	.0391
41	.548	.6263	.0392

B112-19 - Piece 5

	Avg. ID, Inches	Avg. OD, Inches	Tubewall, Inches
1	.549	.6264	.0375
2	.549	.6267	.0389
3	.548	.6265	.0393
4	.548	.6265	.0393
5	.5475	.6263	.0394
6	.547	.6265	.0398
7	.5475	.6265	.0395
8	.548	.6264	.0392
9	.5485	.6265	.0390
10	.5485	.6263	.0389
11	.548	.6263	.0392
12	.5485	.6263	.0389
13	.548	.6262	.0391
14	.548	.6261	.0391
15	.548	.6259	.0390
16	.548	.6258	.0389
17	.548	.6259	.0390
18	.548	.6258	.0389
19	.548	.6257	.0389
20	.548	.6258	.0389
21	.548	.6257	.0389
22	.548	.6259	.0390
23	.548	.6258	.0389
24	.548	.6259	.0390
25	.548	.6259	.0390
26	.548	.6261	.0391

B112-19 - Piece 5 (Cont'd)

	Avg. ID, Inches	Avg. OD, Inches	Tubewall, Inches
27	.548	.6269	.0390
28	.548	.6260	.0390
29	.548	.6258	.0389
30	.5485	.6258	.0387
31	.5485	.6258	.0387
32	.548	.6259	.0390
33	.548	.6259	.0390
34	.548	.6259	.0390
35	.5485	.6260	.0388
36	.5485	.6260	.0388
37	.5485	.6259	.0387
38	.548	.6261	.0391
39	.5485	.6265	.0390
40	.548	.6265	.0393
41	.5485	.6263	.0389
42	.548	.6263	.0392
43	.548	.6260	.0390
44	.548	.6268	.0394
45	.5495	.6259	.0382
46	.547	.6276	.0403
47	.545	.6262	.0406
48	.546	.6261	.0401
49	.547	.6260	.0395
50	.547	.6257	.0394
51	.546	.6257	.0399
52	.5465	.6254	.0395

APPENDIX D

Tube Sectioning Diagrams

B73-8

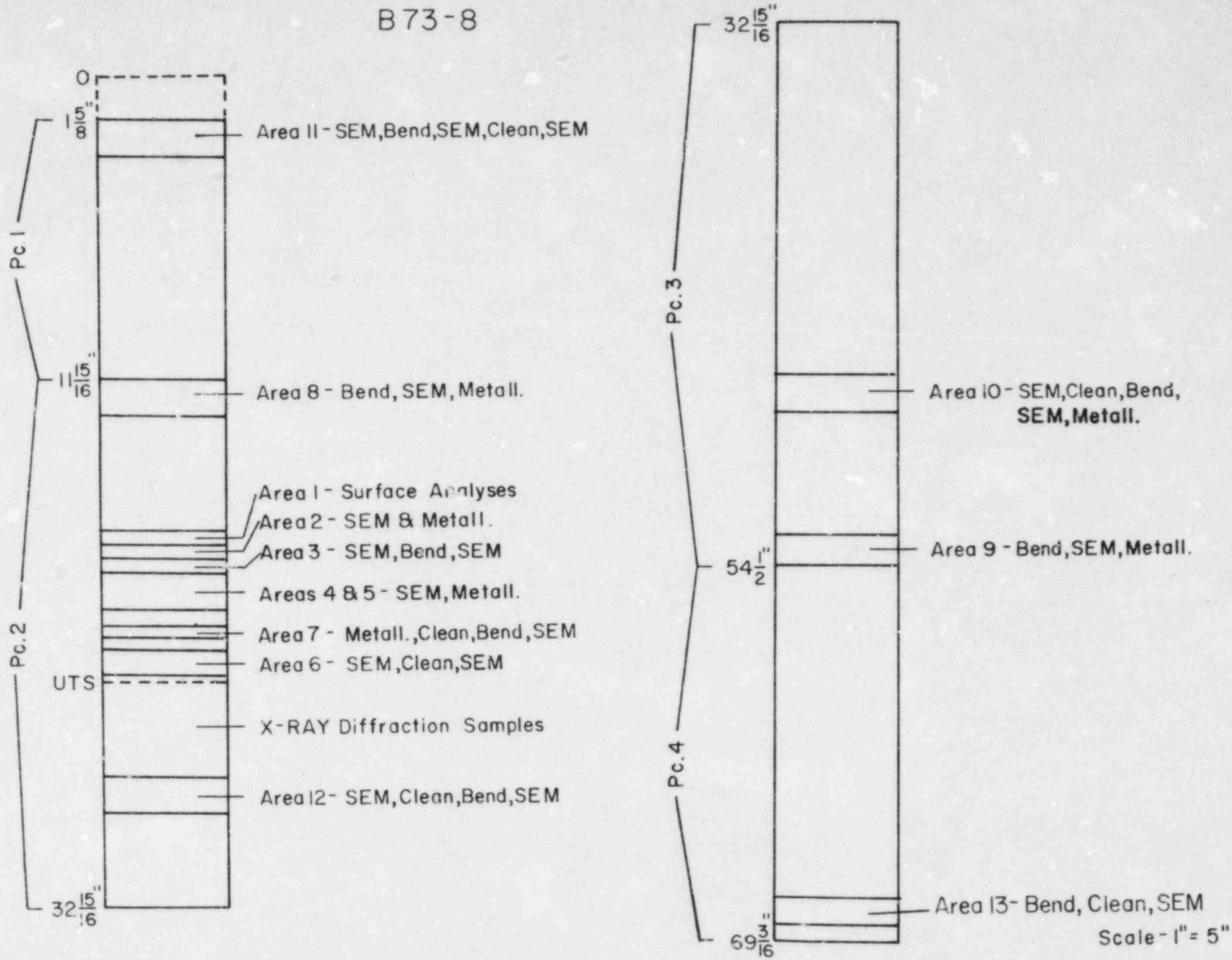
0
1 15/16"
11 15/16"
32 15/16"
Pc. 1
Pc. 2
Pc. 3
Pc. 4
UTS
54 1/2"
69 3/16"
Area 11 - SEM, Bend, SEM, Clean, SEM
Area 8 - Bend, SEM, Metall.
Area 1 - Surface Analyses
Area 2 - SEM & Metall.
Area 3 - SEM, Bend, SEM
Areas 4 & 5 - SEM, Metall.
Area 7 - Metall., Clean, Bend, SEM
Area 6 - SEM, Clean, SEM
X-RAY Diffraction Samples
Area 12 - SEM, Clean, Bend, SEM
Area 10 - SEM, Clean, Bend, SEM, Metall.
Area 9 - Bend, SEM, Metall.
Area 13 - Bend, Clean, SEM
Scale - 1" = 5"

B112-19

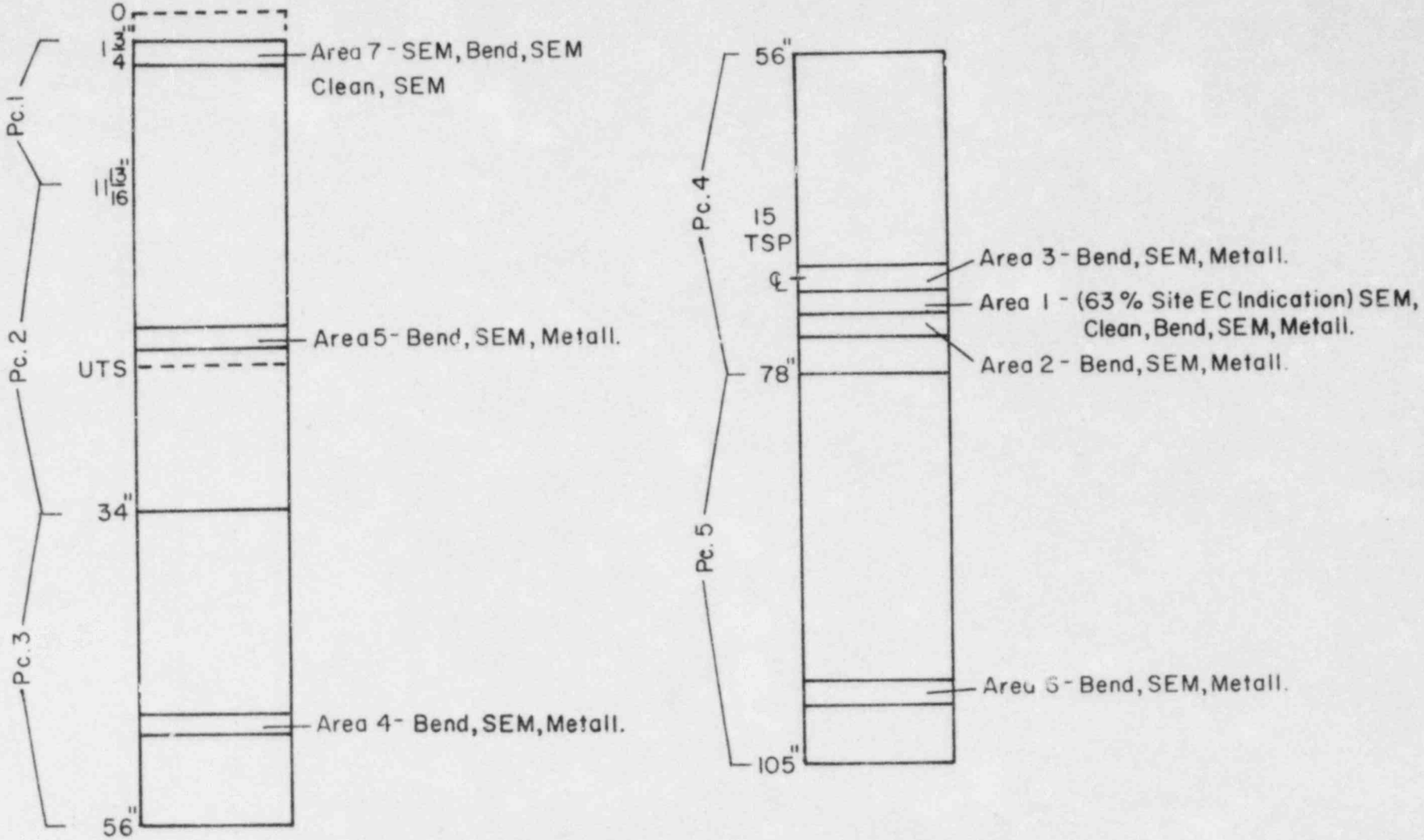

Scale - 1" = 10"

DISTRIBUTION

UPGD-OFR

Abell, GE
Boberg, RL
Bohn, LH
Chagnon, CW
Concklin, JR
Cuvelier, JF
Danley, TA
Gutzwiller, JE
Guza, DF
Hellman, SP
Koch, DW
Lee, DE
Library
Pearson, JF
Smith, JL
Snider, JH
Taylor, JH
Weatherford, LG

LRC

Bain, GM
Baty, DL
Davis, HH
Dietrich, MR
Engelder, TC
Hayner, GO
Library
Lynch, ED
Mayer, JT
McInteer, WA
Pavinich, WA

ARC

Ayres, PS
CIC (Library)(2)
Daniel, PL
Monter, JV
Pocock, FJ
Sarver, LW
Southards, WT
Theus, GJ